UNIVERSITÄTSKLINIKUM HAMBURG-EPPENDORF

Institut für Experimentelle Pharmakologie und Toxikologie

Direktor
Prof. Dr. med. Thomas Eschenhagen

Die Rolle der PDE4 für Inotropie und elektrische Stabilität im menschlichen Vorhof

Dissertation

Zur Erlangung des Grades eines PhD

an der Medizinischen Fakultät der Universität Hamburg

vorgelegt von:

Bernardo Dolce

aus Ivrea (TO), Italy

Hamburg, 2019

Date of Disputation: 16/03/2020

Accepted by the

Medical Faculty of the University of Hamburg on: <u>18/11/2019</u>

Published with permission of

Medical Faculty of the University of Hamburg.

Examining Board, Chair: <u>Dr. Torsten Christ</u>

Examination board, second reviewer: <u>Dr. Viacheslav Nikolaev</u>

Examination board, third reviewer: <u>Dr. Christian Meyer</u>

Table of Contents

1. Introduction

1.1 AF epidemiology

Atrial fibrillation (AF) is a complex and multifactorial disease and the most common sustained cardiac arrhythmia in humans. In the last 20 years, indeed, AF has become one of the most relevant public health problems and a significant cause of increasing health care costs in western countries. Some important studies on the epidemiology of AF carried out in developed countries and published between the end of the 20th century and the first years of the 21st century estimated that the prevalence of AF ranged between 0.5% and 1% of the general population (Go et al., 2001; Murphy et al., 2007). However, recently it has been shown that the prevalence of AF in the general adult population of Europe is more than double that reported just one decade earlier, ranging from 1.9% in Italy, Iceland, and England to 2.3% in Germany and 2.9% in Sweden (Figure 1) (Zoni Berisso et al., 2014).
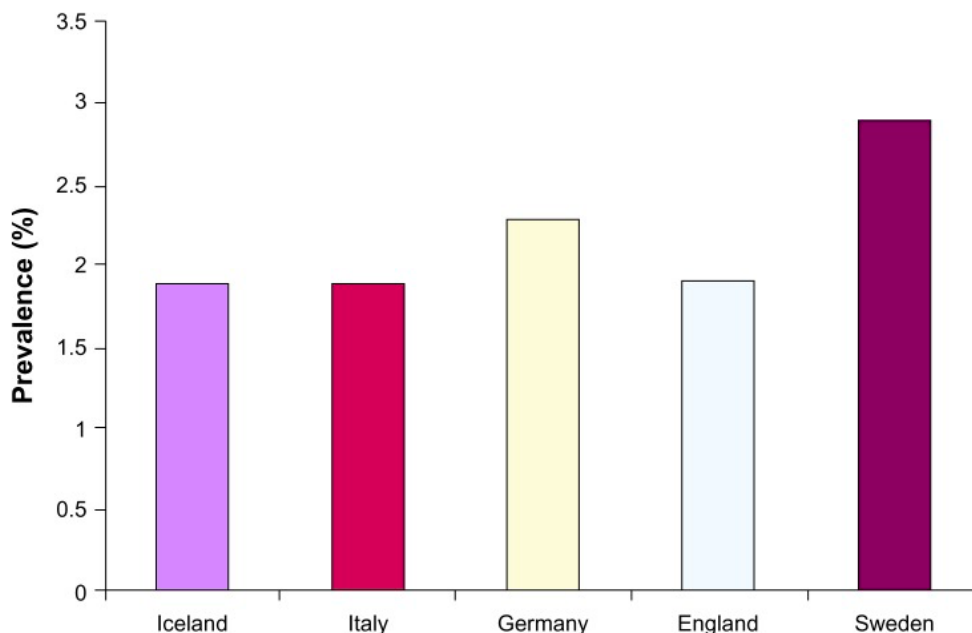
Figure 1: Prevalence of atrial fibrillation in European countries. (Zoni Berisso et al., 2014)

AF is a supraventricular arrhythmia that is characterized by rapid and irregular activation in the atria without discrete P waves on the surface electrocardiogram (ECG). AF can be easily diagnosed by ECG, or by intracardiac atrial electrogram recordings from pacemakers or defibrillators. An arrhythmia that has the ECG characteristics of AF and lasts sufficiently long for a 12-lead ECG to be recorded, or is otherwise documented to last for at least 30 seconds, should be considered to be an AF episode (Calkins et al., 2017). Although there are several classification systems for AF, for the present work, we have used in large part the classification system that was presented in the 2014 AHA/ACC/HRS Guideline for the Management of Patients with Atrial Fibrillation. Paroxysmal AF (paAF) is defined as AF that terminates spontaneously or with medical intervention within 7 days of onset; persistent AF (peAF) is defined as continuous AF that is sustained over 7 days (January et al., 2014).

AF is an exceedingly common age-related arrhythmia. Among people of European descent, the lifetime risk of developing AF after age 40 is 26% for men and 23% for women (Llyod-Jones et al., 2004). It is rare to develop AF before turn 50; and by age 80, approximately 10% of individuals are diagnosed with AF. The precise pathophysiological basis of this link between AF and age is not completely understood; however, age-related fibrosis certainly plays a key role (Benjamin et al., 1994). AF risk factors have also been shown to be of value in predicting progression of paroxysmal to persistent AF (de Vos et al., 2010). It is notable that many of the risk factors that have been associated with the development of AF also contribute to AF progression, recurrences of AF following ablation, and complications associated with AF (e.g., stroke).

1.2 Controversy: reentry and/or automaticity

Recent years have witnessed important advances in our understanding of the electrophysiological mechanisms underlying the development of a variety of cardiac arrhythmias (Figure 2).
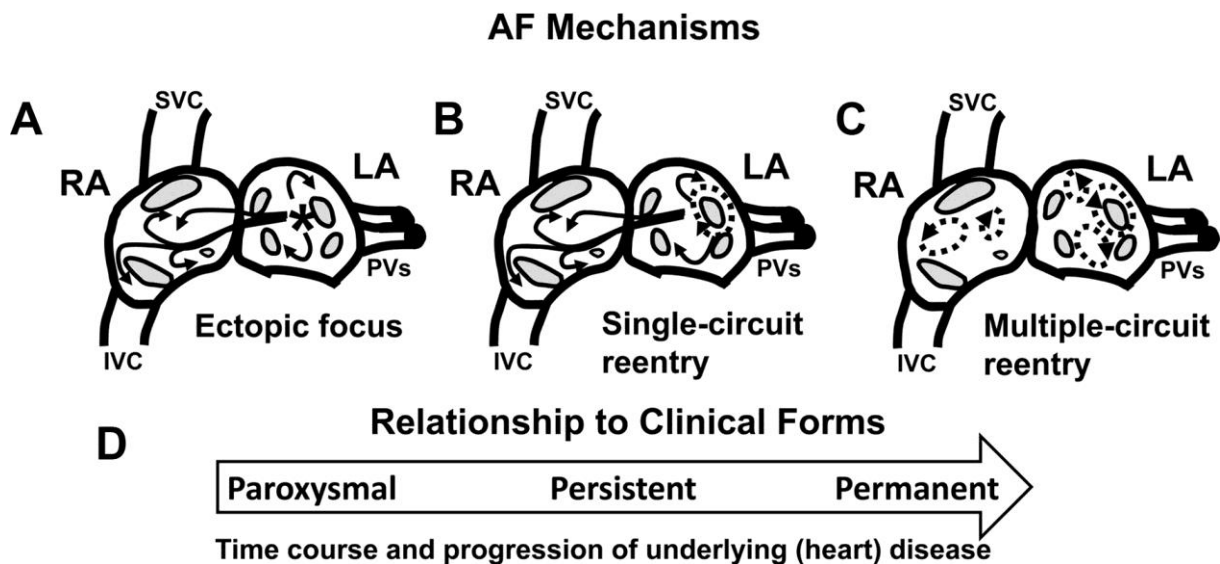
Figure 2: Principal atrial fibrillation–maintaining mechanisms
A, Local ectopic firing. **B,** Single-circuit reentry. **C,** Multiple-circuit reentry. **D,** Clinical AF forms and relation to mechanisms. Continuous arrows represent triggers and drivers. Dashed arrows represent functional and structural reentry circuits. Grey areas correspond to substrate undergoing triggers/drivers and reentry events. Paroxysmal forms show a high number of local triggers/drivers, particularly from pulmonary veins (PVs). As AF becomes more persistent and eventually permanent, reentry substrates predominate. RA indicates right atrium; SVC, superior vena cava; LA, left atrium; and IVC, inferior vena cava. (Iwasaki et al., 2011).

The mechanisms responsible for cardiac arrhythmias are generally divided into 2 major categories: (1) enhanced or abnormal impulse formation (i.e., ectopic firing) (Figure 3) and (2) conduction disturbances (i.e., reentry) (Figure 4) (Antzelevitch et al., 2011).

We show here three basic mechanisms underlying the remodeled impulse formation. The first is represented by an abnormal impulse or enhanced automaticity (Figure 3A), which is caused by changes

in the balance of repolarizing and depolarizing currents, e.g. a decrease of inward rectifier K^+ current (I_{K1}) and/or enhanced depolarizing currents. In normal human atrial myocytes (HAMs), the pacemaker current (I_f) is rather small, overwhelmed by much larger I_{K1}. The second mechanism is so called early afterdepolarization (EAD; Figure 3B). Episodes like this involve abnormal secondary cell membrane depolarizations during the repolarization phases. The main reason why early afterdepolarization occurs is AP duration (APD) prolongation, allowing L-type Ca^{2+} current ($I_{Ca,L}$) to recover from inactivation, leading to a further increase of depolarizing inward movement of Ca^{2+} ions. The third possible situation is called delayed afterdepolarization (DAD; Figure 3C). DADs are caused by abnormal diastolic release of Ca^{2+} from sarcoplasmic reticulum Ca^{2+} stores. Under physiological conditions, specialized Ca^{2+} channels in the membrane of the sarcoplasmic reticulum (called ryanodine receptors [RyRs]) release Ca^{2+} in response to transmembrane Ca^{2+} entry. RyRs are normally closed during diastole but can open if they are functionally defective or if the sarcoplasmic reticulum is Ca^{2+} overloaded. Ca^{2+} release depolarizes the membrane because 1 Ca^{2+} ion is exchanged against 3 extracellular Na^+ ions by the Na^+-Ca^{2+} exchanger, causing a net depolarizing inward positive-ion movement (called transient inward current [I_{ti}]) that underlies DADs (Iwasaki et al., 2011).
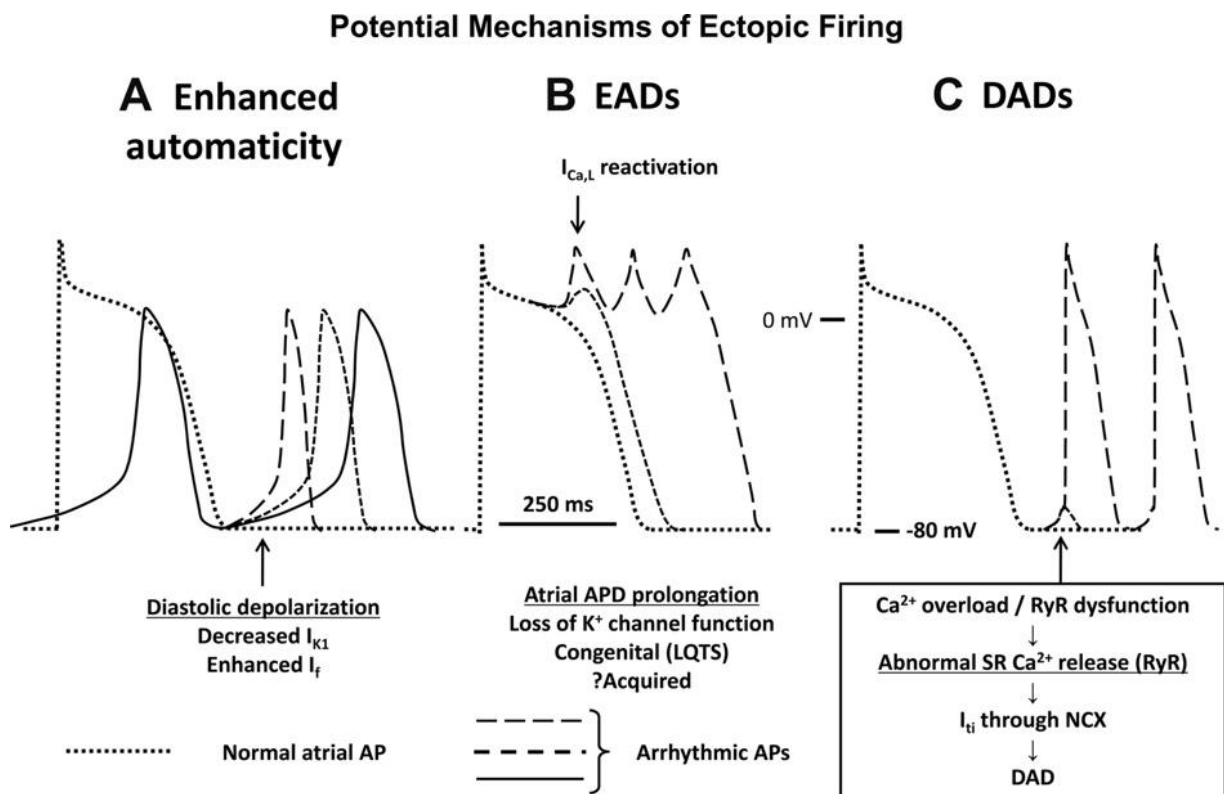
Figure 3: Mechanisms of atrial fibrillation–inducing ectopic firing
A, Enhanced automaticity. **B**, EADs. **C**, DADs. EAD indicates early afterdepolarizations; DAD, delayed afterdepolarizations; RyR, ryanodine receptor; NCX, Na^+-Ca^{2+} exchanger and AP, action potential. (Iwasaki et al., 2011).

Reentry can be conceptualized as either a leading circle (Figure 4A) or a spiral wave (Figure 4B). The maintenance of continuous activity in both models depends on atrial (substrate) properties, with an appropriate balance between refractory and excitability determinants. In the leading-circle model, reentry circuits spontaneously establish themselves in a circuit length (the wavelength [WL]; Figure 4C) given by the distance the impulse travels in 1 refractory period (RP), given by the following equation: WL=RP×CV, where CV is the conduction velocity (Allessie et al., 2001; Comtois et al., 2005). The shorter the wavelength is, the larger the number of simultaneous reentry circuits that the atria can accommodate is (Figure 4D); increasing wavelength reduces the number of possible circuits (Figure 4E).

Tissue Determinants of Reentry
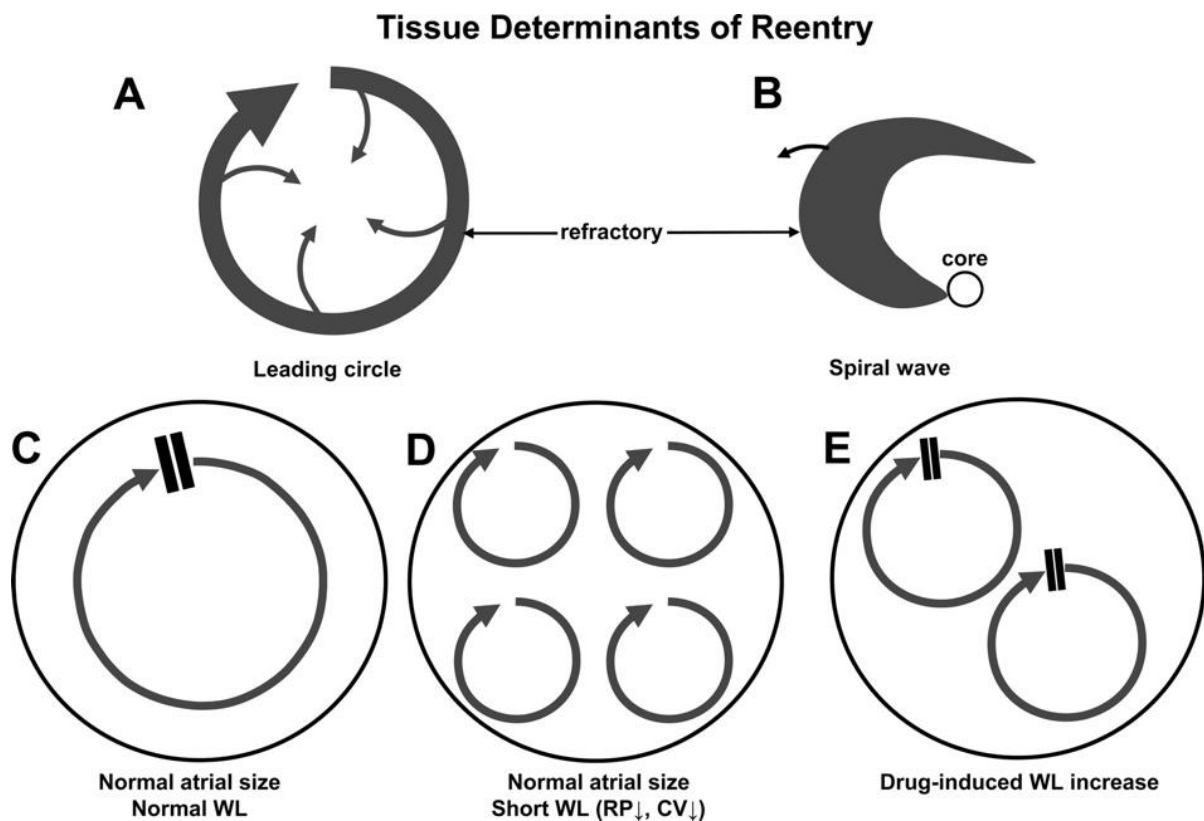
Figure 4: Conceptual models of reentry and implications for atrial fibrillation
A, Leading circle. **B,** Spiral-wave reentry. **C-E,** Role of wavelength (WL) in AF based on leading-circle model. **C,** In healthy atria, the number of reentrant waves that can be accommodated is small, and reentry easily ends. **D,** when wavelength is reduced, by decreasing the refractory period (RP) or conduction velocity (CV), reentrant circuits have a smaller size and more circles can exist; AF becomes unlikely to self-terminate. **E,** Drugs that increase wavelength reduce the number of circuits, allowing AF termination. (Iwasaki et al., 2011)**.**

In my thesis we worked with small individual trabeculae about 1 mm width and 10 mm long. Such small structures are not expected to generate re-entry, given their size. Therefore, arrhythmias results reported in this study can be interpreted as a surrogate for ectopic firing as underlying mechanisms in human atrium. We investigated the role of PKA/cAMP in inducing ectopic firing.

1.3 Present treatments not exhaustive

Currently, several AF treatments are available. Although there are important progresses in the treatment of AF, none of these treatments can be ensuring a complete eradication of the disease. Here below we give a general overview of current approaches to AF.

1.3.1 Restoration of sinus rhythm (SR)

In case of recent onset AF restoration of SR (conversion) is a realistic goal. The oldest method to stop AF and to restore SR is application of antiarrhythmic drugs. Alternatively, cardioversion can be reached by application of a DC shock (cardioversion shock) synchronized to the R wave. Both methods show a high success rate when used within a few days after AF occurrence.

1.3.2 Rhythm control therapy

There is a high recurrence rate of AF after initial successful conversion. Therefore, stabilization of SR (rhythm control therapy) is an important goal in AF treatment and generally assumed by antiarrhythmic drugs, e.g. flecainide, propafenon or amiodarone (despite this one should be used as last resort, since many side effects have been associated to the use of this drug). However, low success rate and substantial toxicity limits rhythm control by antiarrhythmic drugs. Another, increasingly used, way to prevent AF is catheter ablation (Arbelo et al., 2014). Catheter ablation is a minimally invasive procedure in which the cardiologist advances a flexible thin tube (catheter) through the blood vessels to the heart to ablate (destroy) atrial tissue involved in AF or AF conduction from the pulmonary veins to the atria. Catheter ablation appears to be more effective than antiarrhythmic drug therapy in maintaining sinus rhythm (Wynn et al., 2014). Nevertheless, the procedure is not without problems: it is reported in literature that 5-7 % of patients will suffer severe complications after catheter ablation of AF, and 2-3 % will experience life-threatening but usually manageable complications (Cappato et al., 2010; Dagres et al., 2009; Deneke et al., 2015).

1.3.3 Rate control therapy

Patients who cannot be converted to SR have a risk to develop inappropriate fast conduction of AF to the ventricles. Therefore, slowing of AV node (atrioventricular node) conduction (rate control) is needed. This can be achieved for acute or long-term rate control. For acute rate control, beta-blockers and diltiazem or verapamil are preferred over digoxin because of their rapid onset of action, effectiveness at high sympathetic tone and less toxicity (Segal et al., 2000; Schreck et al., 1997; Tisdale et al., 1998). Regarding long-term rate control, beta-blocker monotherapy is often the first-line rate-controlling agent largely based on observations of better acute heart rate control than digoxin (Kotecha et al., 2014). In addition to beta blockers there are non-dihydropyridine calcium channel blockers, mostly represented by verapamil or diltiazem, which provide reasonable rate control in AF patients (Ulimoen et al., 2013). However, they cannot be used in heart failure because of their negative inotropic effect in

patients with left ventricular ejection fraction (LVEF) < 40% (Goldstein et al., 1991; Ponikowski et al., 2016; Elkayam et al., 1998). Among the long-term rate control players we can also find digitalis. Digoxin and digitoxin are the cardiac glycosides most often used (Goldberger et al., 2014).

Despite the variety of choices and the possibility to do also combined therapies, the use of rate control agents is still under investigation. All available therapies indeed have potential for side effects. Nevertheless, rate control can be achieved also by atrioventricular node ablation with subsequent implantation of a pacemaker. It is a relatively simple procedure with a low complication rate and low long-term mortality risk (Queiroga et al., 2003; Lim et al., 2007). However, AV nodal ablation renders patients pacemaker-dependent for the rest of their lives, limiting AV nodal ablation and pacing to patients whose symptoms cannot be managed by rate-controlling medication or by reasonable rhythm control interventions.

1.3.4 Anticoagulation

The risk for stroke persists even after successful cardioversion. Therefore, one of the most important aim in the treatment of AF is anticoagulation. Vitamin K antagonists (VKAs) such as warfarin were the first anticoagulants used in AF patients. The use of VKAs is limited by the need for frequent monitoring and dose adjustments. They are still in use and reduce the risk of stroke by two-thirds and mortality by one-quarter compared with control (no therapy) (Hart et al., 2007). A suitable alternative for stroke prevention in AF is represented by the Non-vitamin K antagonist oral anticoagulants (NOACs) such as apixaban, dabigatran, edoxaban and rivaroxaban (Olesen et al., 2015). All NOACs have a predictable effect (onset and offset) without the need for regular anticoagulation monitoring.

1.4 Focus on relevant phases of AF

There is still a need to better understand atrial arrhythmias in order to provide a safer and more efficient treatments for future patients. In the next part we will address natural course of AF.

The mechanisms involved in the initiation of AF as well as the remodeling upon persistent AF are crucial points in the study of the disease. What does initiate AF and what can protect from it? How are structures and biological events remodeled by AF? Furthermore, the investigation on paroxysmal AF is considered important. Which role does paroxysmal AF play in the disease progression? Is it more similar to sinus rhythm or persistent AF?

The seminal observation by Haissaguerre et al. was that a focal source in the pulmonary veins can trigger AF, and ablation of this source can suppress recurrent AF (Haissaguerre et al., 1998). The mechanism of focal activity might involve both triggered activity and localized reentry, how described above in the present study. The consequence of persistent AF is a remodeling of the atria (structural and electrical remodeling). Activation of fibroblasts, enhanced connective tissue deposition, and fibrosis are the hallmarks of the process of structural remodeling (Anné et al., 2005; Chimenti et al., 2010; Nguyen et

al., 2009). Furthermore, structural remodeling results in electrical dissociation between muscle bundles and local conduction heterogeneities (Allessie et al., 2010), favoring re-entry and perpetuation of the arrhythmia (Spach et al., 1994).

Regarding electrical remodeling, AF induces a shortening of the atrial refractory period. Shortening of APD is largely due to downregulation of the Ca^{2+}-inward current (Van Wagoner et al., 1999; Christ et al., 2004). Contribution of K^+ currents is under debate (Dobrev et al., 2005; Schmidt et al., 2015). Structural heart disease, in contrast, tends to prolong the atrial refractory period, illustrating the heterogeneous nature of mechanisms that cause AF in different patients (Schotten et al., 2011). Hyperphosphorylation of various Ca^{2+}-handling proteins may contribute to enhanced spontaneous Ca^{2+} release events and triggered activity (Voigt et al., 2014; Voigt et al., 2012), thus causing ectopy and promoting AF. However, it should be noted that the concept of Ca^{2+}-handling instability has been challenged recently as the frequency of spontaneous Ca^{2+} release events was reduced in isolated trabeculae and cells from patients in peAF (Christ et al., 2014; Greiser et al., 2014).

A lot more has to be investigated on AF in order to elucidate the mechanism behind. In this thesis we focused indeed on the PKA/cAMP activation pathway and how it changes in cells and tissues isolated from patients in peAF and paAF.

1.5 Experimental evidences supporting a role of PKA/cAMP activation to induction of AF

1.5.1 G-protein coupled receptors

The research questions are related to the role of beta 1- and beta 2-adrenergic receptors (β_1- and by β_2-ARs) as well as 5-HT$_4$ receptors in AF. Therefore, in the present study we focused on G-coupled receptors transmitting effects of autonomous nervous system.

mRNA levels of β_1- and β_2-ARs are unchanged in AF (Grammer et al., 2001) (Figure 5) and it has been shown that in humans both β_1- and β_2-AR mediate atrial arrhythmias (Kaumann et al., 1993). Years later, Antony J. Workman suggested that AF is caused by β-ARs stimulation and that this involves increased $I_{Ca,L}$ and Ca^{2+}, rather than effects on action potential terminal repolarization or effective refractory period (ERP). As a matter of fact, the suppression of AF by β-blockers is likely to involve attenuation of such arrhythmic activity (Workmann et al., 2010). The scenario has still to be clarified.
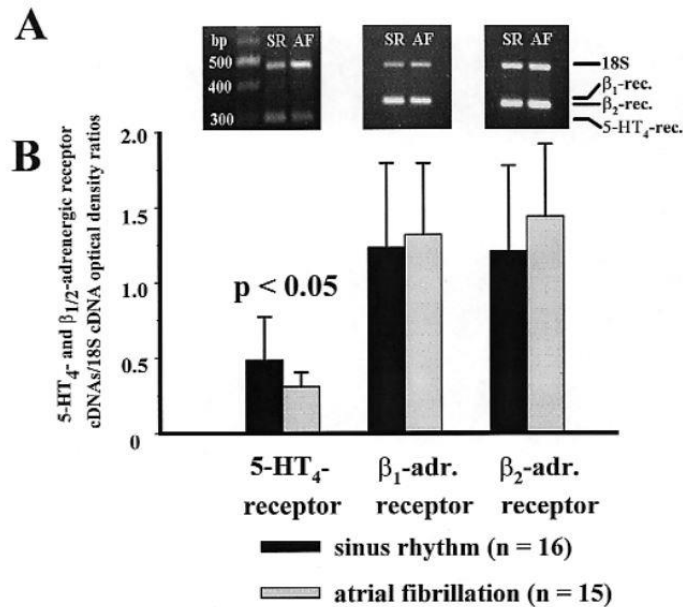
Figure 5: Comparison of 5-HT$_4$-receptor, β$_1$- and β$_2$-ARs mRNA expressions in human atrium myocytes

Comparison of 5-HT$_4$-receptor, β$_1$- and β$_2$-ARs mRNA expressions in right atrial appendages of patients in sinus rhythm and with persistent atrial fibrillation by semi quantitative RT-PCR. **A)** Agarose gel showing the 489 bp fragment of the 18S cDNA co-amplified with (i) the 311 bp fragment of the human 5-HT$_4$-receptor cDNA (left), (ii) with the 331 bp fragment of the β$_1$-AR cDNA (middle), and (iii) with the 329 bp fragment of the β$_2$-AR cDNA (right). The RT-PCR products of one typical patient of each group are shown. **B)** Histogram of the densitometric analysis of all patients. Error bars are standard deviations. (Grammer et al., 2001).

The density of 5-HT-receptors is lower than β$_1$- and by β$_2$-AR in human atrium and even lower in human ventricle (Kaumann et al., 2006). Nevertheless, several studies have been demonstrated that 5-HT can cause arrhythmias (Christ et al., 2014; Kaumann AJ, 2013; Kaumann AJ, 1994; Grammer et al., 2001). The 5-HT-evoked arrhythmias indeed are abolished by the selective inhibitor for 5-HT$_4$-R SB203186 at a concentration that does not affect catecholamines-evoked arrhythmias, indicating mediation through 5-HT$_4$-Rs (Kaumann AJ, 1994). In contrast to β$_1$- and by β$_2$-AR, 5-HT$_4$-receptor are affected by peAF as shown by reduced mRNA expression levels in right atrial appendages of patients in AF (Grammer et al., 2001) (Figure 5).

1.5.2 PDEs

Stimulation of many G-protein coupled receptors increases levels of cAMP (Berthet et al., 1957; Mika et al., 2013). The cyclic nucleotide phosphodiesterases (PDEs) comprise a group of enzymes that degrade the phosphodiester bond in the second messenger molecule cAMP (Figure 6) (Bender et al., 2006). PDEs are composed by 11 families and PDE3 and PDE4 contribute the most in rodent and human cardiomyocytes (Molina et al., 2012; Rochais et al., 2006).
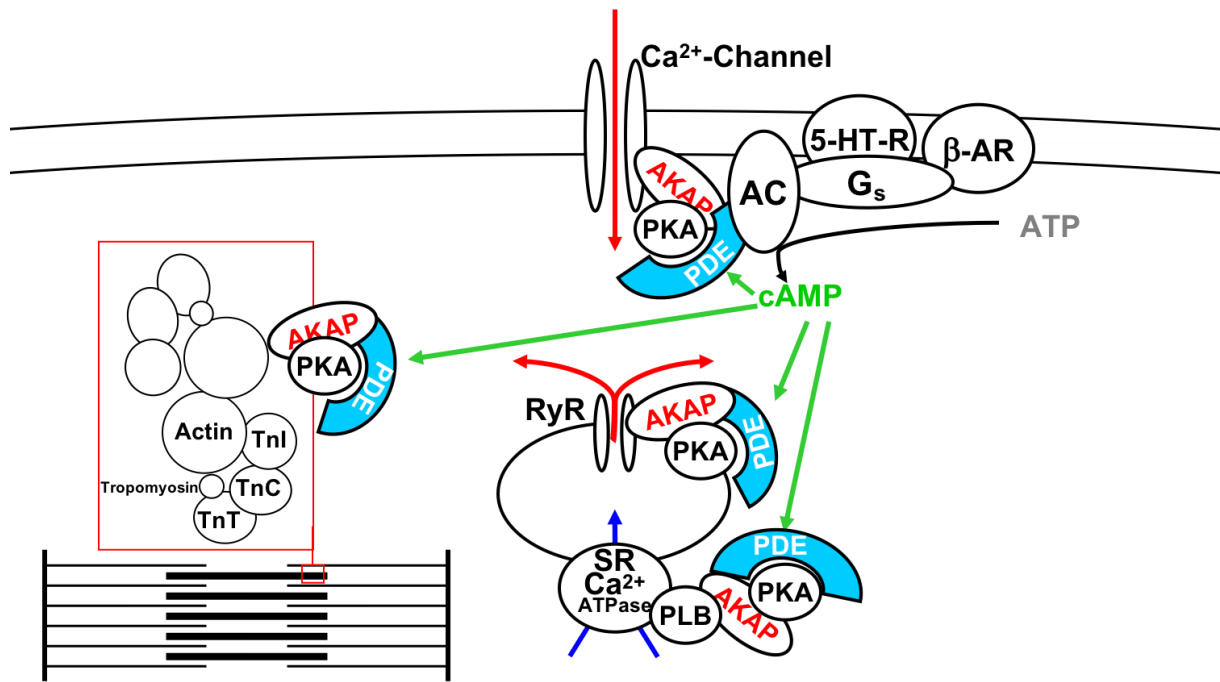
Figure 6: PDE isoforms and PDE-related macromolecular complexes in cardiac myocytes
Activation of G-protein coupled receptors increases cAMP concentration through adenylate cyclase activation. Consequently, protein kinase A (PKA) phosphorylates target proteins increasing contractile force, acceleration of relaxation, Ca^{2+}-influx trough Ca^{2+}-channels and Ca^{2+}-uptake/release from the SR. Activity of cAMP is regulated by PDEs which can degrade the phosphodiester bond in the second messenger molecule cAMP. AKAP: A kinase anchoring protein, PLB: phospholamban, RyR2: ryanodine receptor 2, TnI / TnT / TnC: troponin I / T / C; SR: sarcoplasmic reticulum.

Molina et al. demonstrated feasibility of monitoring cAMP in human atrial cardiomyocytes. Inhibition of PDE3 and PDE4 increased cAMP in isolated cells but also increased arrhythmias in human atrial trabeculae from patients in SR induced by β-AR stimulation. From lower total PDE and PDE4 activity in tissue homogenates from patients in peAF it was suspected that protection against arrhythmias by PDE4 is impaired in peAF. However, functional data for peAF and paAF are not given in that study (Molina et al., 2012). Berk et al. reported that inhibition of PDE3 and PDE4 increases also 5-HT evoked arrhythmias. However, 5-HT evoked arrhythmias were blunted in peAF and could no longer be provoked by inhibition of PDE3 and PDE4 (Berk et al., 2016).

1.6 Clinical evidences supporting a role of PKA/cAMP activation to induction of AF

Here we will present the clinical evidence for the involvement of norepinephrine (NE), epinephrine (Epi) and serotonin (5-HT) as well as the PDE3 and PDE4 inhibitors in AF.

1.6.1 Agonists

NE and post-operative AF

A study conducted on 131 patients showed an association between atrial fibrillation after coronary artery bypass grafting and sympathetic activation (Kalman et al., 1995). In this study, 50 % of patients developed AF and 36 % required treatment. Interestingly, plasma NE levels increased significantly in the immediate post-operative period. NE levels were significantly higher in patients developing AF (Figure 7).
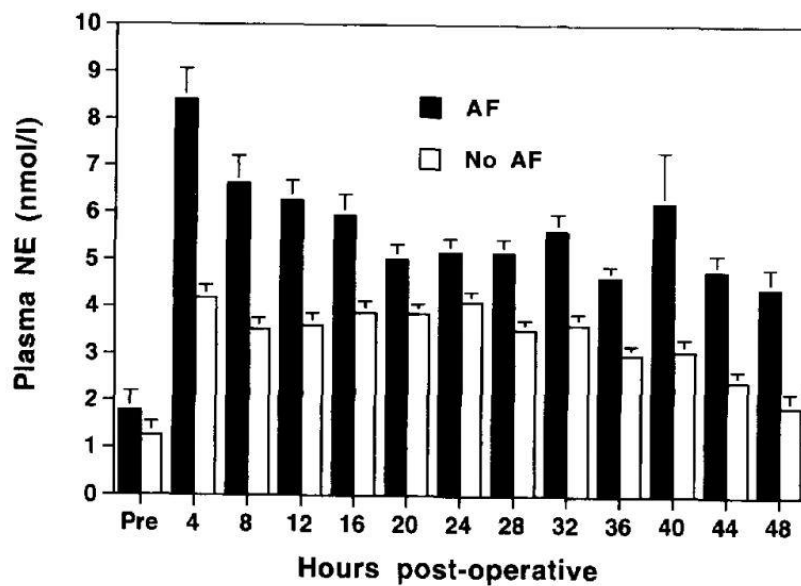
Figure 7: Increase in NE levels over time in SR and AF patients
Comparison of NE levels in patients in whom manifested AF and those whom did not incur in AF. At each postoperative sampling interval up to 48 hours there were significantly higher levels ($p < 0.001$) in those patients in whom AF developed. Each point represents the mean ± standard error. (Kalman et al., 1995).

Several years later, another study showed that even pre-operative NE tone is an important factor underlying post-operative AF (Anderson et al., 2017). In the morning of surgery, prior to administration of anesthesia, blood samples were obtained from 324 patients undergoing no emergent coronary artery bypass graft and/or aortic valve surgery with cardiopulmonary bypass. Levels of NE ($p = 0.0006$) in the 4th quartile were positively associated with post-operative AF, whereas dopamine (DA) ($p = 0.0034$) levels in the 4th quartile were inversely associated with post-operative AF (Figure 8).
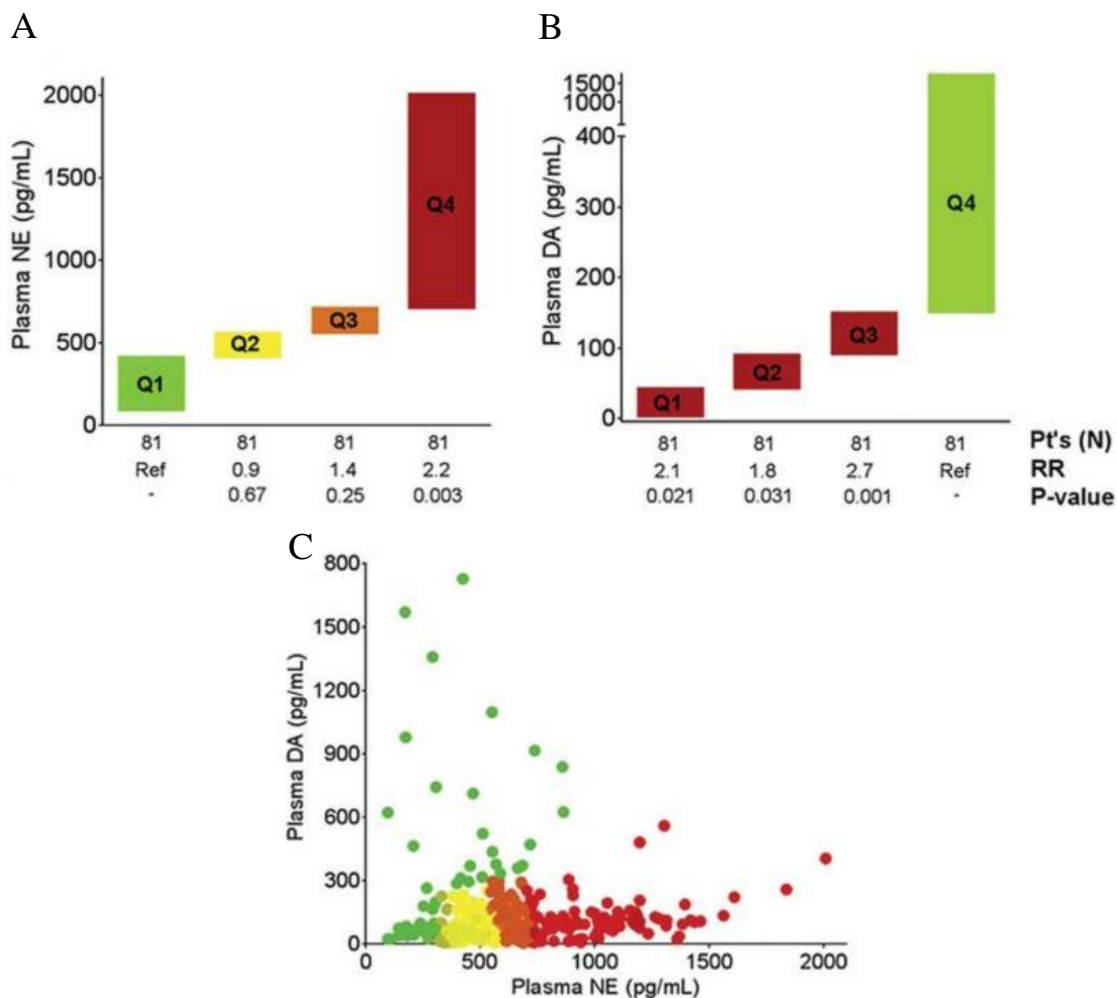
Figure 8: Quartiles of Plasma Catecholamines Stratified by Relative Risk for post-operative AF
The panels above show plasma concentrations of NE **(A)** and DA **(B)** grouped into quartiles (Q1 to Q4). RR for post-operative AF according to univariate analysis is shown numerically under each quartile. The Ref quartile is the lowest risk (Q1$_{NE}$ and Q4$_{DA}$), and the p value for each quartile relative to Ref is denoted underneath. Color shading corresponds to RR for post-operative AF, with green designating lowest risk, red designating highest risk, and yellow/orange intermediate. **(C)** The relationship between plasma DA and NE is shown, where each symbol is 1 individual patient. DA = dopamine; NE = norepinephrine; Ref = referent; RR = relative risk. (Anderson et al., 2017).

β₂-Agonists used in obstructive lung diseases

Agonists of β_2-AR are frequently used in obstructive lung diseases. Use of Epi in patients with obstructive airway diseases, such as bronchial asthma or chronic obstructive pulmonary diseases (COPD), increases the risk for adverse cardiovascular events (Salpeter et al., 2004). A typical single dose of a β_2-agonist caused an increase in heart rate of 9.12 beats/min (95% confident interval CI, 5.32 to 12.92) compared to placebo. The administration of a single dose also caused a reduction in potassium concentration by 0.36 mmol/L (95% CI, 0.18 to 0.54) compared to placebo.

The risk for AF by inhaled bronchodilators (β_2-AR agonists and anti-muscarinic antagonists) was summarized in a recent study (Lee CH et al., 2015). 3312 cases with tachyarrhythmia and 9732 matched controls were included in the analysis. Both long-acting muscarinic antagonists (LAMAs) and long-

acting inhaled β₂ agonists (LABAs) were associated with a small risk to develop AF. The authors expected that sympathetic system activation is most likely the mechanism responsible for the occurrence of tachyarrhythmia in patients treated with LAMAs and LABAs.

5-HT₄ and antidepressants

The evidence for 5-HT-based antidepressants to infer an increased risk of AF is conflicting. In a large Danish data set, antidepressant use was associated with a tripled risk of AF during the first month following antidepressant initiation (hazard ratio HR, 3.18; 95% CI, 2.98–3.39). On the surface, this finding seems alarming. However, in further analysis, this risk was found to attenuate during months 2–6 after antidepressant initiation (HR, 1.37; 95% CI, 1.31–1.44) and it further attenuated during months 6–12 after antidepressant initiation (HR, 1.11; 95% CI, 1.06–1.16) (Fenger-Groen et al., 2019). Contrarily, a study in UK did not show any relation between antidepressants and AF. Relative to past use of antidepressant drugs, neither current use (RR, 0.98; 95% CI, 0.86–1.12) nor recent use (RR, 1.02; 95% CI, 0.86–1.30) were associated with an increased risk of AF (Lapi et al., 2015).

1.6.2 PDEs-inhibitors

Milrinone and post-operative AF

The PDE3 inhibitor milrinone is associated with post-operative AF. A study compared the rate of AF in patients exposed to milrinone during mitral valve surgery with controls that were not. The use of milrinone was associated with a more than 2-fold higher risk for post-operative AF than control (Figure 9) (Fleming et al., 2008).
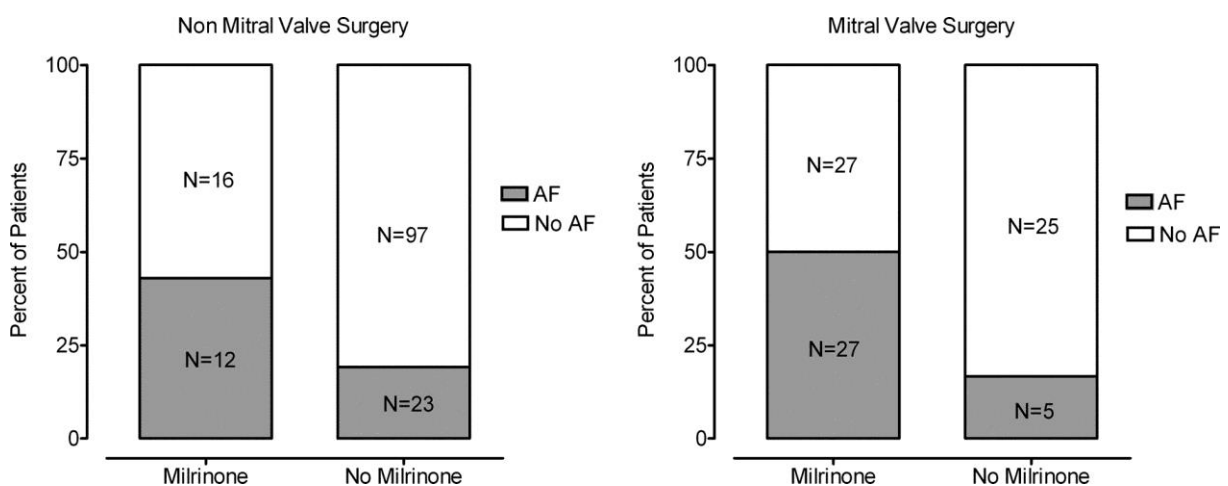
Figure 9: Rates of postoperative AF according to milrinone exposure stratified by mitral valve surgery
Two groups of patients were analyzed on the occurrence of post-operative AF. The graph on the left represents patients which are not undergoing mitral valve surgery (control), while the graph on the right reports patients undergoing mitral valve surgery. Each group was divided further in milrinone treatment and no-treatment. In grey is the percentage of patients showing AF and in white no AF. (Fleming et al., 2008).

Roflumilast and AF

Roflumilast, a potent PDE4 inhibitor, has been shown to improve lung function and reduce exacerbation rates in patients with chronic obstructive pulmonary disease (COPD) (Kelly Freeman et al., 2012). A study examining the efficacy and safety of roflumilast found that the variables depending on the use of roflumilast were mortality, adverse events (AE) and exacerbation rates. In a pool of 11257 patients (500 µg roflumilast = 5766; placebo = 5491), COPD-related AEs were significantly less frequent with roflumilast (5.8% *versus* 7.1%; $p =$ 0.008), but AF was more common than with placebo (0.4% *versus* 0.2%; $p = 0.02$) (Oba et al., 2013). The data argue for a certain role of PDE4 in protecting the heart from AF.

1.7 Research questions of this thesis

1.7.1 The PDE4 controversy: major player or little helper? Inotropy vs. arrhythmias

In human atrial trabeculae from patients with SR, inhibition of PDE3 shifted the concentration response curve (CRC) for the positive inotropic effect of NE and Epi via β_1- and by β_2-AR to the left (Christ et al., 2006) and increased the frequency of arrhythmias (Engel A., 2013). In contrast, inhibition of PDE4 did not shift the CRC for the positive inotropic effect of NE and Epi via β_1- and by β_2-AR (Christ et al., 2006) but increased arrhythmias (as seen with inhibition of PDE3). This discrepancy opens the question whether inhibition of PDEs can have divergent action on inotropy and electrical stability and on the overall physiological importance of PDE4 in human atrium. Since the discordance between arrhythmias induction and potentiation of positive inotropy by PDE4 could be due to incomplete inhibition of PDE4 it was the aim to investigate force and arrhythmias evoked by β_1- and by β_2-AR under more complete PDE4 inhibition. Same more appropriate inhibition of PDE4 was used to clarify the role of PDE4 in human paAF and peAF.

1.7.2 Control of cAMP by PDE in peAF: increased or decreased?

From the seminal work of Molina et al. it is known that total activity of PDE, measured as hydrolytic activity in tissue homogenates, is decreased in peAF. However, combined inhibition of PDE3 and PDE4 potentiate inotropic effects of 5-HT more in peAF than in SR, suggesting a larger control of 5-HT-evoked cAMP by PDE4 and PDE3 in peAF. Therefore, it was the aim of this study to estimate contribution of PDE3 and PDE4 to cAMP regulation in peAF under basal conditions and when cAMP delivery is increased. We have used interventions that generates increasing amount of cAMP (5HT-R activation< β-AR activation< direct adenylyl cyclase activation), since inotropy to 5-HT resulted blunted in peAF while NE, Epi and forskolin (FSK) responses were preserved. The aim of the study was to improve understanding of cAMP regulation to remodeling in different phases of AF (paAF and peAF).

2. Materials and Methods

2.1 Human samples

Atrial tissues were collected from patients undergoing cardiac surgery at the Department of Cardiovascular Surgery of the University Medical Center Hamburg-Eppendorf (UKE). The samples were obtained during open heart surgery when the top of the right atrial appendage was cut to allow insertion of a cannula (Figure 10). The cannulation is performed in order to drain systemic deoxygenated blood into the heart lung machine, taking over the function of the heart and lungs during surgery (El-Sherief et al., 2013).
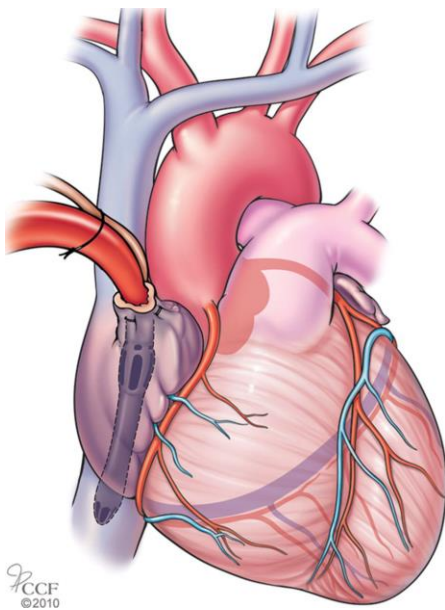
Figure 10: Cannulation of the right atrial appendage.
Drawing shows cavoatrial (two-stage) cannulation. It is performed by a single incision in the right atrial appendage or the lateral wall of the right atrium. The narrowed distal end of the cavoatrial cannula is threaded into the inferior vena cava and receives blood from the inferior vena cava, and the wider proximal portion of the cannula has side holes designed to rest within the right atrium, thus receiving blood from the superior vena cava and coronary sinus. (El-Sherief et al., 2013).

More in detail, the use of the heart lung machine (Figure 11), referring more precisely to cardiopulmonary bypass (CPB), allows the venous blood to flow from the body via a tube in the right atrium of the heart, or via two tubes in the major veins which converge in the heart. It is pumped through an oxygenator and a heat exchanger and returned via a plastic tube into the arterial system of the body, usually at the upper portion of the ascending aorta. CPB allows surgeons to operate on a non-beating heart in the setting of a bloodless field while maintaining adequate whole body tissue oxygenation and perfusion (Sarkar M. and Prabhu V., 2017).
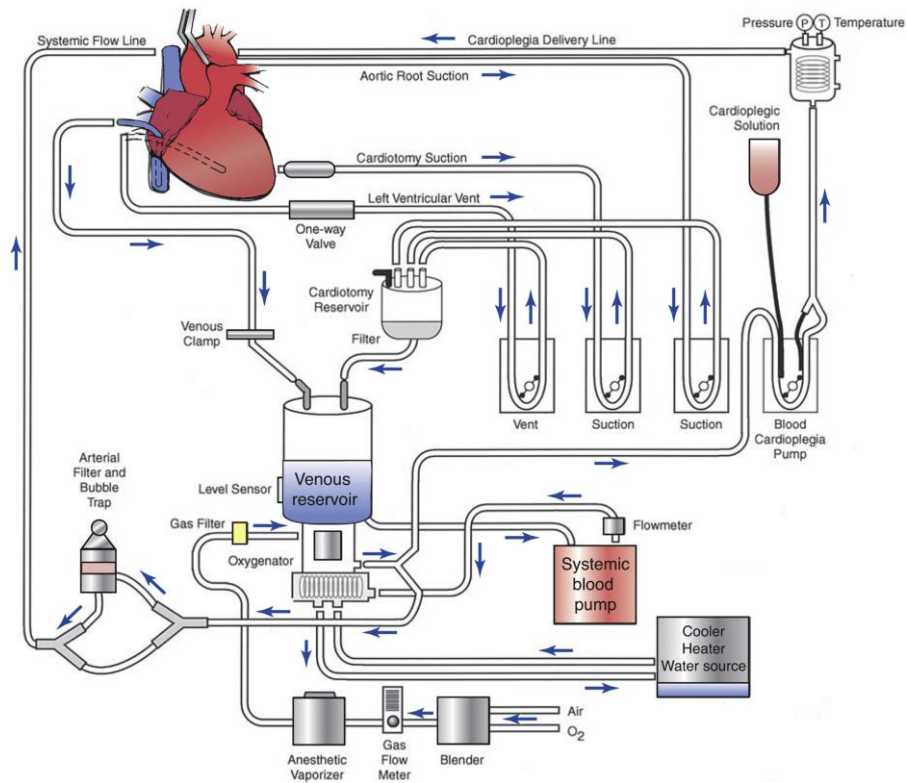
Figure 11: Heart–lung machine.
The main components are the venous reservoir, the oxygenator, and the systemic blood pump (in red). The vent and suction pumps drain from the field into the venous reservoir. (Sarkar M. and Prabhu V., 2017).

Therefore, due to this mandatory procedure and in order to cannulate the right atrial appendage, there is a need to open the right atrium. Many surgeons remove the tip of the right auricle of the heart (Figure 12), which was often collected by us. The size and weight of the tissues have usually a range respectively of ~ 2 cm^2 and ~ 0.3 g.
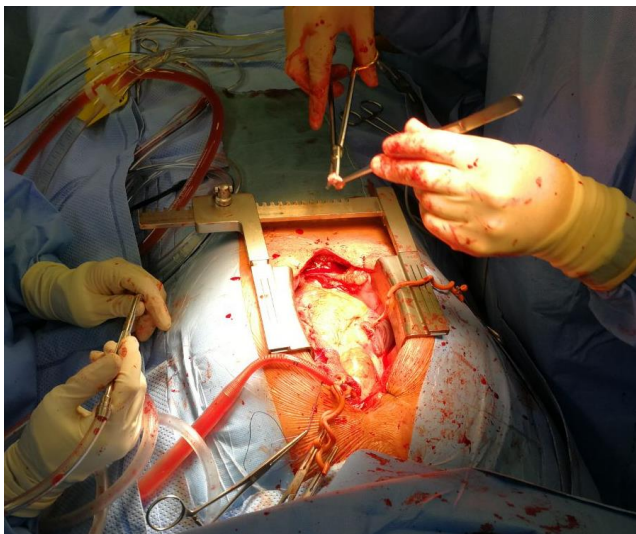
Figure 12: Open heart surgery.
Removal of the tip of the right atrial appendage by the surgeons.

Permission to use the tissue samples was obtained from each patient, and the study was approved by the Ethical Committee of our institution and conducted in accordance with the Declaration of Helsinki principles. Details regarding the clinical characteristics of the patients and their treatments are shown in Table 1.

Table 1: Clinical characteristics and treatments of the patients

	SR	paAF	peAF
Patients (n)	53	12	31
male (n)	48 (90.0 %)	10 (80.0 %)	24 (77.8 %)
female (n)	5 (10.0 %)	2 (20.0 %)	7 (22.2 %)
Age at surgery (years)	63.2	58.4	68.2
Indication for surgery			
Coronary artery disease (n)	31 (60.0 %)	10 (80.0 %)	8 (25.8 %)
Valvular heart disease (n)	11 (20.0 %)	2 (20.0 %)	17 (54.6 %)
Both (n)	11 (20.0 %)	0 (0.0 %)	3 (9.8 %)
Dilated cardiomyopathy	0 (0.0 %)	0 (0.0%)	3 (9.8 %)
Cardiovascular comorbidity			
Arterial hypertension (n)	21 (40.0 %)	7 (60.0 %)	14 (44.4 %)
Diabetes mellitus (n)	5 (10.0 %)	0 (0.0 %)	3 (11.1 %)
Hyperlipoproteinemia (n)	5 (10.0 %)	2 (20.0 %)	7 (22.2 %)
Echocardiography data			
LVEF (%)	55.4	52.5	54.2
Medication			
ACE inhibitors (n)	21 (40.0 %)	5 (40.0 %)	17 (55.5 %)
AT1 receptor antagonists (n)	0 (0.0 %)	0 (0.0 %)	0 (0.0 %)
Beta blockers (n)	16 (30.0 %)	10 (80.0 %)	17 (55.5 %)
Ca^{2+} channel blockers (n)	5 (10.0 %)	2 (20.0 %)	3 (11.1 %)
Diuretics (n)	11 (20.0 %)	0 (0.0 %)	7 (22.2 %)
Digitalis (n)	0 (0.0 %)	0 (0.0 %)	0 (0.0 %)
Nitrates (n)	0 (0.0 %)	0 (0.0 %)	0 (0.0 %)

2.2 Protein expression analysis

2.2.1 Western blot

For analysis of protein levels, homogenized tissues were dissolved in 100 µL TPER Tissue Protein Extraction Reagent (ThermoScientific, Dreieich, Germany) with complete Mini EDTA-free protease inhibitor cocktail (Roche Diagnostics, Mannheim, Germany). 1x laemmli buffer was added to the sample lysate. Subsequently, the samples were heated for 5 min at 95 °C and then loaded on a SDS-PAGE gel. Proteins were separated by 12% acrylamide/bisacrylamide (29:1, BioRad, Feldkirchen, Germany) in electrophoresis gels and thereafter transferred onto nitrocellulose (NC) or polyvinylidene fluoride (PVDF) membranes (0.45 µm). Membranes were washed with TBS-Tween 0.1% and blocked in 5% skim milk powder. Primary antibodies obtained from Dr. Marco Conti (University of California, San Francisco, USA) and Dr. Chen Yan (University of Rochester School of Medicine and Dentistry, New York, USA) (Table 2) were incubated overnight at 4°C in TBS-Tween 0.1%, secondary antibodies (Table 2) for 1 h at room temperature (RT) in 5% skim milk powder/TBS-Tween 0.1% with gentle shaking. Visualization was performed with the Clarity Western ECL Substrate (BioRad, Feldkirchen, Germany) on the ChemiDoc imaging system (BioRad, Feldkirchen, Germany). Finally, the band analysis tool of ImageLab (Bio-Rad Laboratories, Feldkirchen, Germany) was used to quantify protein bands of the blots. Each protein band was normalized to the protein elf4E. Protein analysis was performed with the help of Anna Steenpass (Institute of Experimental Pharmacology and Toxicology, UKE, Hamburg).

Table 2: Antibodies

Primary antibodies	Secondary antibodies
PDE3A (1:1000) – Chen Yan	Anti-rabbit (1:10000)
PDE4B (1:1000) – Marco Conti	Anti-rabbit (1:10000)
PDE4D (1:1000) – Marco Conti	Anti-rabbit (1:10000)

2.2.2 Immunofluorescence

For the immunofluorescence staining, HAMs were fixed in formaldehyde for a period of 20 minutes followed by permeabilization in blocking solution (1x PBS, milk powder 3% (w/v), Triton X-100). Subsequently HAMs were incubated in antibody solution (TBS 0.05 mol/L pH 7.4, 1% BSA, 0.5% Triton X-100) with primary antibodies overnight (Table 2). After three wash steps in PBS, primary antibodies were detected with secondary antibodies conjugated to fluorophores (Table 2) and nuclei were stained with DAPI (1:1000, Sigma Aldrich, Darmstadt, Germany) for two h at RT. Finally, stained HAMs were rinsed 2-3 times in PBS and embedded in Fluoromount-G (SouthernBiotech, Eching,

Germany) in concave microscope slides (Carl Roth, Karsruhe, Germany). All immunofluorescence images were captured using the laser scanning microscope Zeiss LSM 800.

2.3 Cells isolation

Tissues from atrial appendages were transferred from the operating theater to the laboratory in small tubes filled with Custodiol® (Dr. Franz Köhler Chemie GmbH, Bensheim, Germany) (Table 3) as quick as possible, typically within 10 minutes (Figure 13). Custodiol® was developed to flush organs prior to removal from the donor and to perfuse explanted donor organs afterwards. It is used for transplantation of kidneys, liver, pancreas and heart. The solution has lower K^+ content (9 mmol/l) than other cardioplegia solution, which avoid the toxic effect of high-K^+ concentration. Furthermore, in Custodiol® buffering is provided by a high concentration of an amino acid agents, histidine/histidine hydrochloride, the amino acid tryptophan a-ketoglutarate, and the osmotic agent mannitol. The histidine/histidine hydrochloride buffering system provides normal osmolarity and enhances the solution's buffering capacity during the ischemic-induced acidosis. With the exception of mannitol, all constituents are normally found in the body. Therefore, it is also indicated to preserve biopsies such heart appendages during transportation.

Atrial cardiomyocytes were isolated by enzymatic digestion as previously described (Molina et al., 2012). More in details, as first step, fat and connective tissue were removed and then the sample was chopped into small pieces ~ 1 mm^2 size (Figure 14) using either scissors or blades. Afterwards the pieces of tissue were incubated at 36°C for 30 minutes in a Ca^{2+} free solution containing 0.5 mg/ml collagenase (Worthington type 1, 240 U/mg; Columbus, United States), 0.5 mg/ml proteinase (Sigma type XXIV, 11 U/mg; St. Louis, Missouri, USA) and 2% bovine serum albumin (BSA; Sigma, St. Louis, Missouri, USA).
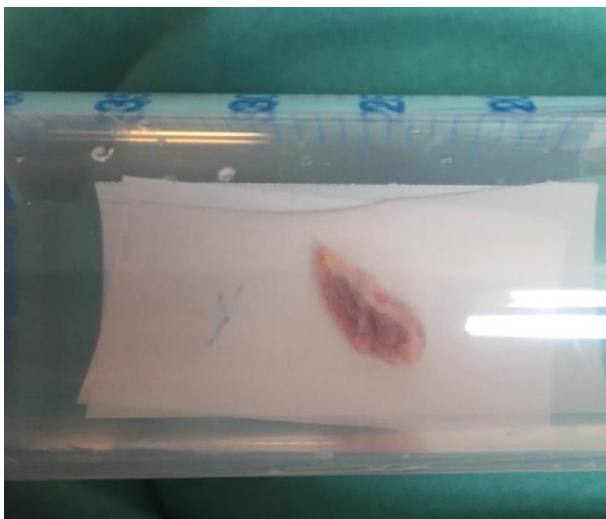
Figure 13: Right atrial appendage
Right atrial appendage´s transportation in a Custodiol® filled tube from the operating theater to the isolation lab.
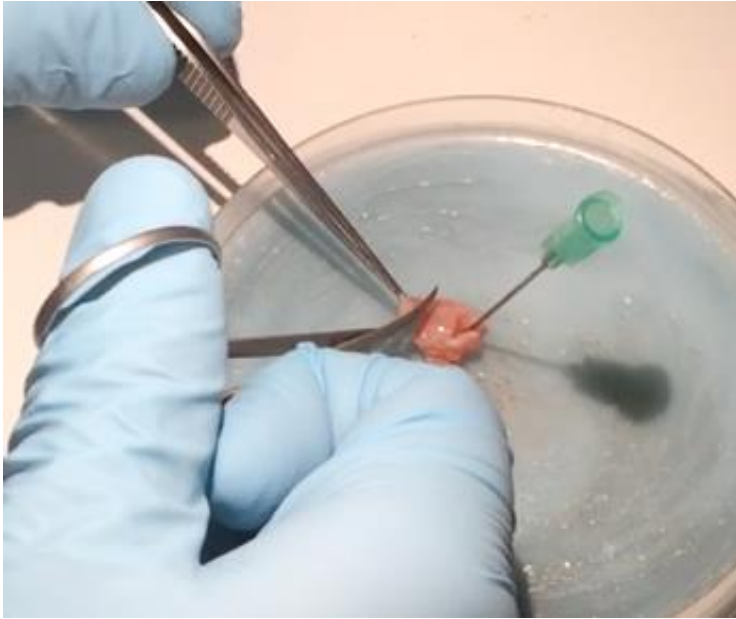
Figure 14: Cutting of the right atrial appendage in small pieces
Chopping of the right atrial appendage in small pieces performed with the help of scissors and tweezers. The procedure requires the use of a dish already coated with silicone, in order to allow needles to fix the tissue on the bottom.

The exact composition of Ca^{2+} free solution is reported in Table 4. Different types of collagenases have been tested and the type 1 revealed to be the most efficient in getting human cells preserving the criteria previously defined: minimized cell damage, cell yield should be high and the ionic environment during disassociation should be normal (Cavanaugh DJ et al., 1963). Subtilisin Carlsberg (Protease XXIV, former Protease VII, Sigma-Aldrich, Darmstadt, Germany), instead, is obtained from *Bacillus licheniformis*. As for trypsin, also subtilisin Carlsberg is a serine endoprotease with pH-optimum of 7.5. It appears to play effectively his role of less specific protease, digesting hydrolytically the collagen fragments previously treated with collagenase. After 30 min, the tissue was picked by tweezers from the enzymatic solution and transfer to a Ca^{2+}-free solution containing 2 µM blebbistatin (Sigma, St. Louis, Missouri, USA) and 5% BSA to stop digestion. The tissue pieces left were agitated with a Pasteur pipette in order to mechanically isolate cells from it. The use of blebbistatin ensured us to inhibit myosin II and thereby contracture of the myocytes (Kovács et al., 2004), in order to increase the probability of obtain quiescent cardiomyocytes at the end of the isolation. The remaining tissue was digested again for 3×15 min in a fresh Ca^{2+} free solution containing 0.4 mg/ml of the mentioned above collagenase and 2% BSA. After the three steps of 15 minutes, all the isolation solutions collected were centrifuged. Finally, cells were separated from the supernatants by gentle centrifugation (500 rpm for 5 minutes). Freshly isolated cells were suspended in minimal essential medium (MEM: M 4780; Sigma, St. Louis, Missouri, USA), 2.5% fetal bovine serum (FBS, Invitrogen, Cergy-Pontoise, France), 1% penicillin-streptomycin, 2% HEPES (pH 7.6) and 2 µM blebbistatin.

Due to the presence of calcium, the application of it directly on cell pellets required a particular procedure. Indeed, as mentioned above, cells were isolated in the absence of Ca^{2+} while the MEM just

described contained Ca^{2+}. The sudden rise of Ca^{2+} can increase risk of losing many cells since they will start to contract very hardly (Bers DM, 2008). For this reason, we performed interspersed application of MEM (~ 200 µL of ~ 1 ml of final volume) containing Ca^{2+} every 10 minutes break, avoiding a shock for the cells.

In line with previous studies (Voigt et al., 2015), we found that tissue of ~ 0.3 g will get a cells yield of ~ 30 cells/10 µL (Figure 15A). Considering a final volume of ~ 1 ml, after isolation we usually counted ~ 30000 cells in total, a number high enough for us to perform our experiments. The use of a bigger tissue would require a higher volume for the isolation solutions, since the presence of too many cells aggregated on a petri dish does not favor the survival rate. Therefore, for our experiments we believe we found a good compromise between number of cells and resources.

In Figure 15B is showed a typical freshly isolated cardiomyocyte. Only cardiomyocytes with their typical elongated shape, with clear cross-striation and with preserved cell membrane, were used for experiments.
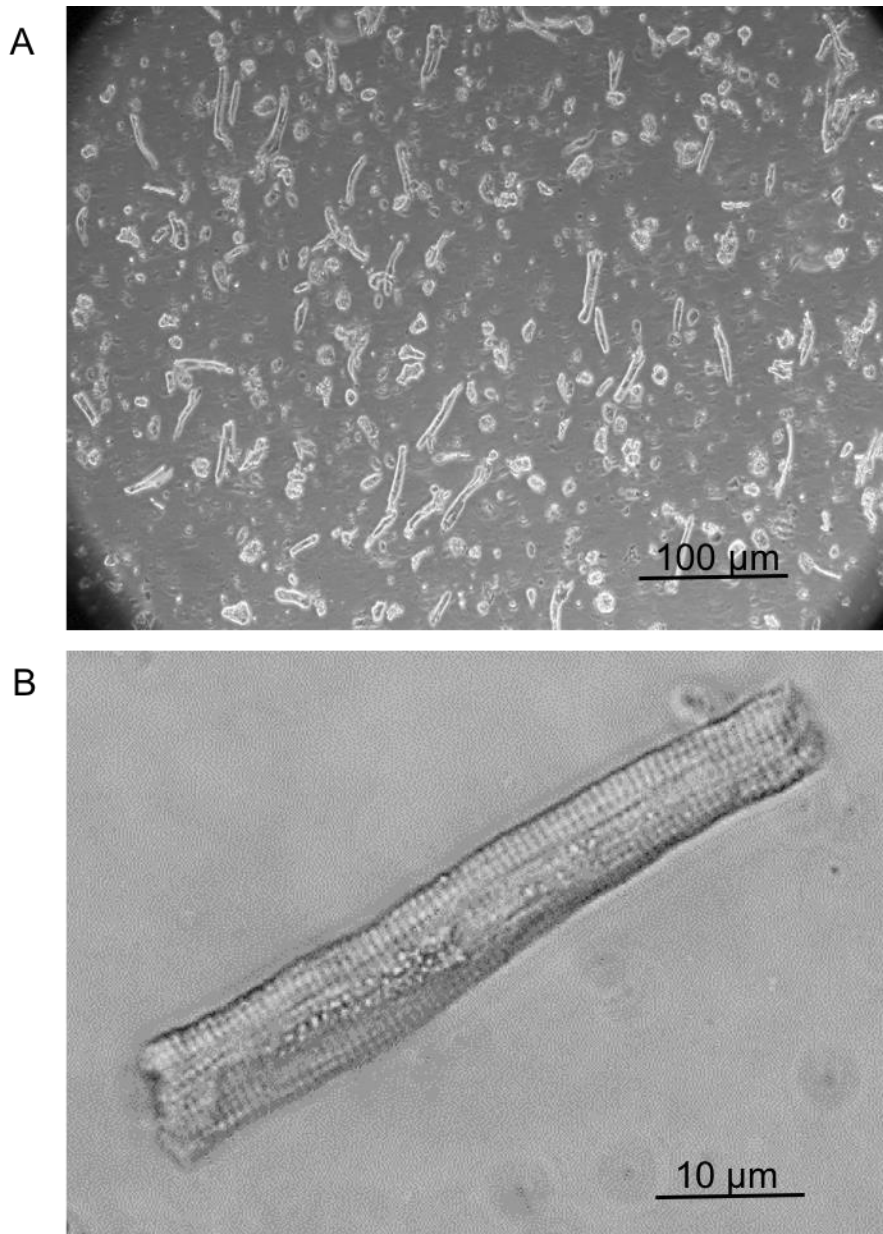
Figure 15: Representative fresh isolated human atrium cardiomyocytes
(A) Overview of isolated cardiomyocytes from human right atrial appendage at low magnification. Average of cells yield: 30 cells/10µl. **(B)** Representative isolated cardiomyocyte from human right atrial appendage at high magnification. The cells shows intact cross striation and a smooth cell membrane.

Table 3: Cardioplegia solution Custodiol®: composition

Compounds	Concentration in mM
KCl	9
NaCl	15
$C_5H_5KO_5$	1
$MgCl_2$	4
Histidine hydrochloride - H2O	18
Histidine	180
Tryptophan	2
Mannitol	30
$CaCl_2 – 2 H_2O$	0,015

Table 4: Ca^{2+} free Solution: composition

Compounds	Concentration in M
KCl	1
NaCl	2
KH2PO4	0,1
MgSO4	0,1
Taurin	0,25
MOPS	5
Glucose	20
NaOH	1 N

2.4 Whole-cell recording of $I_{Ca,L}$

After the cell isolation, while part of the cells was plated and then transfected for FRET experiments (Förster resonance energy transfer), some other were instead directly suspended in a solution use mostly for patch clamp (Table 5). Currents were measured in a small perfusion chamber placed on the stage of an inverse microscope. A system for rapid solution changes, named Octaflow, allowed application of drugs in the close vicinity of the cells (Cell Micro Controls, Virginia Beach, VA; ALA Scientific Instruments, LongIsland, NY, USA). After moving few drops of the solution containing the suspended cells to the chamber, the experiments were performed then with Na^+-free superfusion solution at pH 7.4 (adjusted with CsOH) (Table 6). The pipette solution (Table 7) included also calculated free Ca^{2+} concentration of ~ 60 nM (computer program EQCAL, Biosoft, Cambridge, UK), pH=7.2 (adjusted with

CsOH). Current amplitude was determined as the difference between peak inward current and current at the end of the depolarizing step. $I_{Ca,L}$ was measured at 37°C with standard voltage-clamp technique + (Axopatch 200, Axon Instruments, Foster City, CA, USA), ISO2 software was used for data acquisition and analysis (MFK, Niedernhausen, Germany) as described (Christ T et al., 2004). Heat-polished pipettes were pulled from borosilicate filamented glass (Hilgenberg, Malsfeld, Germany). Tip resistances were 3-5 MΩ, seal resistances were 3-6 GΩ. Membrane capacitance (CM) was calculated from steady-state current during depolarizing ramp pulses (1 Vs -1) from -40 mV to -35 mV. Five minutes after establishing the whole-cell configuration (Figure 16) $I_{Ca,L}$ was measured during a test pulse from a holding potential of -80 mV at +10 mV.
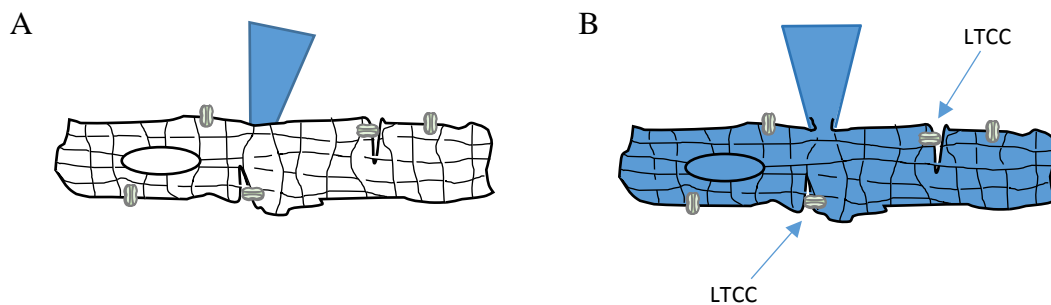
Figure 16: Draft of two patched cardiomyocytes
In the picture are shown myocytes having ion channels (in particular the LTCC located in the T-tubules). Cell-attached patch **(A)**. For this method, the pipette is sealed onto the cell membrane in order to obtain a gigaseal. In the meanwhile, it can ensure that the cell membrane remains intact. This allows the recording of the ion channel/s currents contained in the patch of membrane sealed by the pipette. Whole cell recording **(B)** of a human atrial cardiomyocyte. Whole-cell recordings involve recording currents through multiple channels simultaneously, over the membrane of the entire cell. The electrode is left in place on the cell, as in cell-attached recordings, but more suction is applied to rupture the membrane patch, thus providing access from the interior of the pipette to the intracellular space of the cell.

Table 5: Patch clamp storage solution: composition

Compounds	Concentration (mM)
KOH	90
L-glutamic acid	70
Taurin	15
KCl	30
KH_2PO_4	10
$MgCl_2$	0.5
HEPES	10
Glucose	11
EGTA	0.5

Table 6: Na⁺-free superfusion solution: composition

Compounds	Concentration (mM)
Tetraethylammonium chloride	120
CsCl	10
CaCl	22
MgCl₂	21
HEPES	10
Glucose	20

Table 7: Pipette solution: composition

Compounds	Concentration (mM)
Cs methanesulfonate	90
CsCl	20
CaCl	23
Tris-GTP	0.4
HEPES	10
Mg-ATP	4
EGTA	10

2.5 Atrial trabeculae isolation. Inotropic and arrhythmic effects. Experimental design

After transporting of the right atrial appendage to the laboratory (Figure 13), a maximum of eight trabeculae were dissected. Preparation was done at room temperature in modified Tyrode's solution (Table 8). The solution was maintained at pH 7.4 by bubbling with a mixture of 95% CO_2 and 5% O_2. More in detail, the trabeculae preparation started with an incision at the lateral wall in order to open the tissue and get access to the trabeculae (Figure 17). The edges of the tissue were fixed by pins to a petri dish coated with silicon. Using tweezers and surgical scissors, trabeculae were cut, strictly avoiding damaging the central part of the muscle.
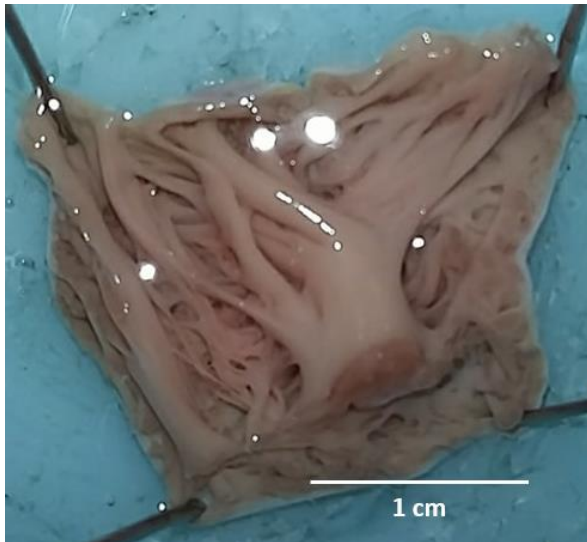
Figure 17: Trabeculae from the right atrial appendage of a human heart
The picture shows preparation of trabeculae starting from a human right atrial appendage. The operator proceeds fixing the tissue at the silicon coated dish and opening it cutting with scissors. Once the intact muscles, as known as trabeculae, are exposed they can be cut again by surgical scissors.

The optimum was to remove each trabecula from the two extremes where they are connected to the wall, in order to preserve the anatomical structure of the trabecula. Once the trabeculae were dissected, they were mounted in pairs, attached to a system to measure isometric force, containing above solution at 37°C and stretched as described (Gille E at al., 1985) (Figure 18 and 18B). They were knotted from one extreme with a thread and clamped from the other to the contraction system. The other side of the thread was attached to a metallic hook (Figure 18C). Trabeculae were stimulated at 1 Hz each and incubated with 5 µM phenoxybenzamine for 90 min to irreversibly block α-adrenoceptors as well as neuronal and extraneuronal uptake of catecholamines (Gille E at al., 1985). Phenoxybenzamine, as well as all the other compounds were applied through a tube filled with Tyrode solution (Figure 18D). We investigated the effects of NE, mediated through β_1-adrenoceptors, in the presence of 50 nM ICI 118,551 to block β_2-adrenoceptors and the effects of EPI, mediated through β_2-adrenoceptors, in the presence of 300 nM CGP 20712A to block β_1-adrenoceptors (Hall J et al., 1990). Both kind of experiments were made in the presence and absence of PDE4 inhibitor, rolipram. Contractile force was recorded with 400 data points/sec using Chart Pro for Windows version 5.51 analysis program (ADI Instruments, Castle Hill, Australia). A single cumulative concentration effect curve for the agonist was determined. Every additional contraction besides the 1 Hz rhythm was considered arrhythmic.

Table 8: Modified Tyrode´s solution composition

Compounds	Concentration (mM)
KCl	5.4
NaCl	126.7
$MgCl_2$	1.05
$CaCl_2$	1.8
EDTA	0.04
NaH_2PO_4	0.42
Glucose	5
Ascorbic acid	0.2
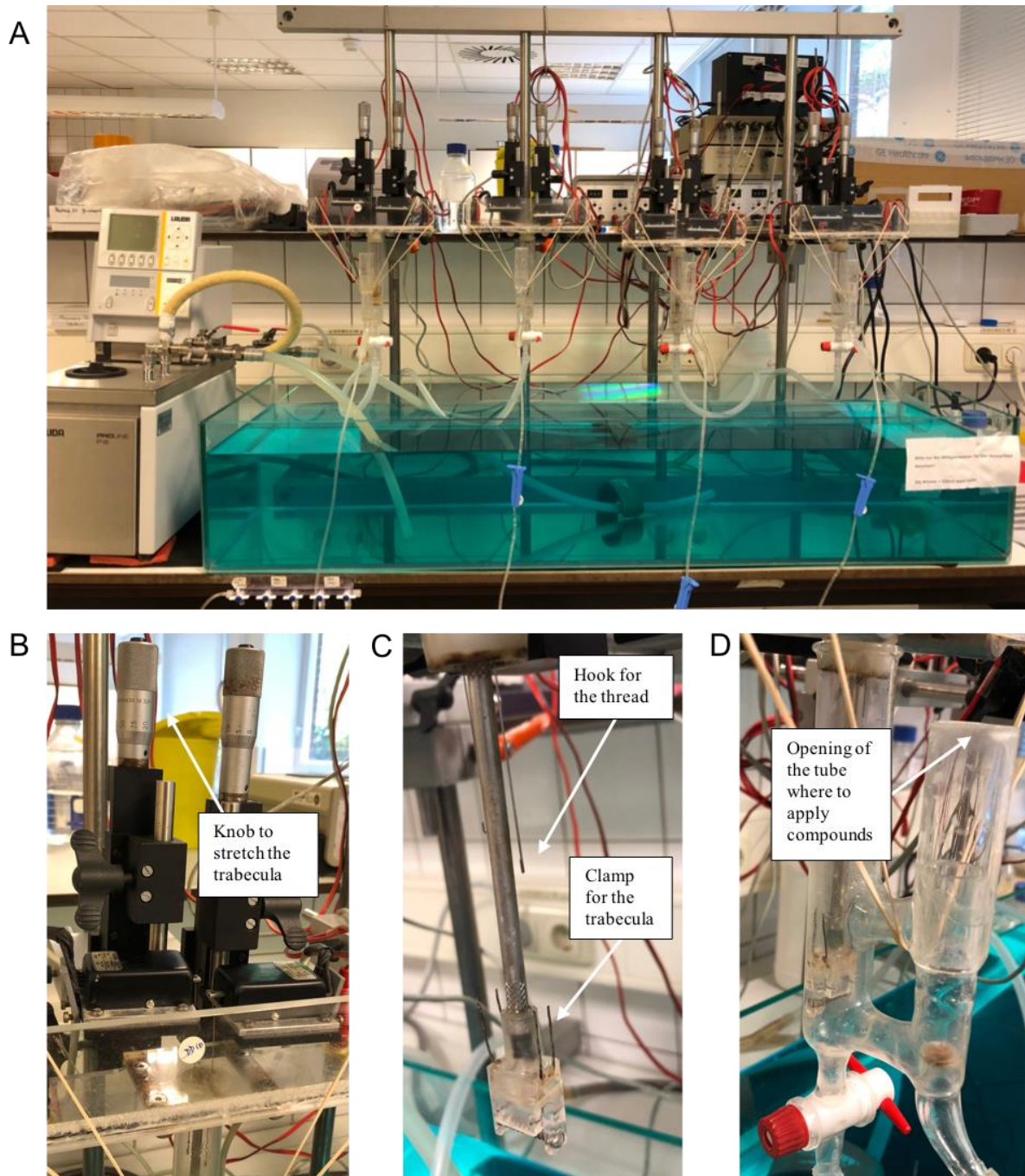
Figure 18: Setup to measure isometric force

System to measure isometric force of trabeculae composed by SWEMA 4-45 strain gauge transducers with an organ bath capable to maintain physiological temperature at 37º C. **(A)** Overview of the system showing four apparatus. Each apparatus can clamp and stretch two different trabeculae for a maximum of eight. **(B)** The knobs used by the operator to stretch the muscles. **(C)** Apparatus contained within the tube. From one side is represented the hook where to attach the thread. The tread is then linked around one of the two extremes of the trabecula. The other side of the trabecula is clamped as shown. **(D)** The tube keeps the trabeculae always perfused and from the opening on the top, compounds can be applied. Two trabeculae each tube can be measured and they are subjected to same conditions.

2.6 Infection and culture of human atrial myocytes

After suspension in medium, cells were plated on 29 mm dia (diameter) culture glass bottom dishes (Laminin L2020, Sigma, St. Louis, Missouri, USA). In order to perform FRET experiments cells needed to be infect with adenovirus encoding for a biosensor, which will be describe later. The process takes usually around 48 h and, differently from patch clamp experiments, the preparation of cells for FRET experiments requires them to be attached at the bottom of the dish. In order to determine the most efficient way to have cells attached, we decided to test two different concentration of laminin, 2 µg/mL and 0,02 µg/mL and fibronectin (5 µg/mL) in cells freshly isolated. We checked them 2 h after the replacement of MEM. The best solution appeared to be undiluted laminin showing an average of 27 cells attached per 10 mm dia, which was significantly higher than the other two conditions (Figure 19). After 2 h, which was the time needed for the cells to attach, the medium was replaced by 2 ml per dish of FBS-free MEM (Gibco/Invitrogen, Cergy-Pontoise, France) containing adenovirus encoding Epac1-camps (MOI=200 pfu/cell) (Börner S et al., 2011). To express this biosensor in cardiomyocytes, indeed, adenoviruses and adeno-associated viruses are highly effective tools (Mironov et al., 2009; Leroy J et al., 2008; Nikolaev VO et al., 2010)
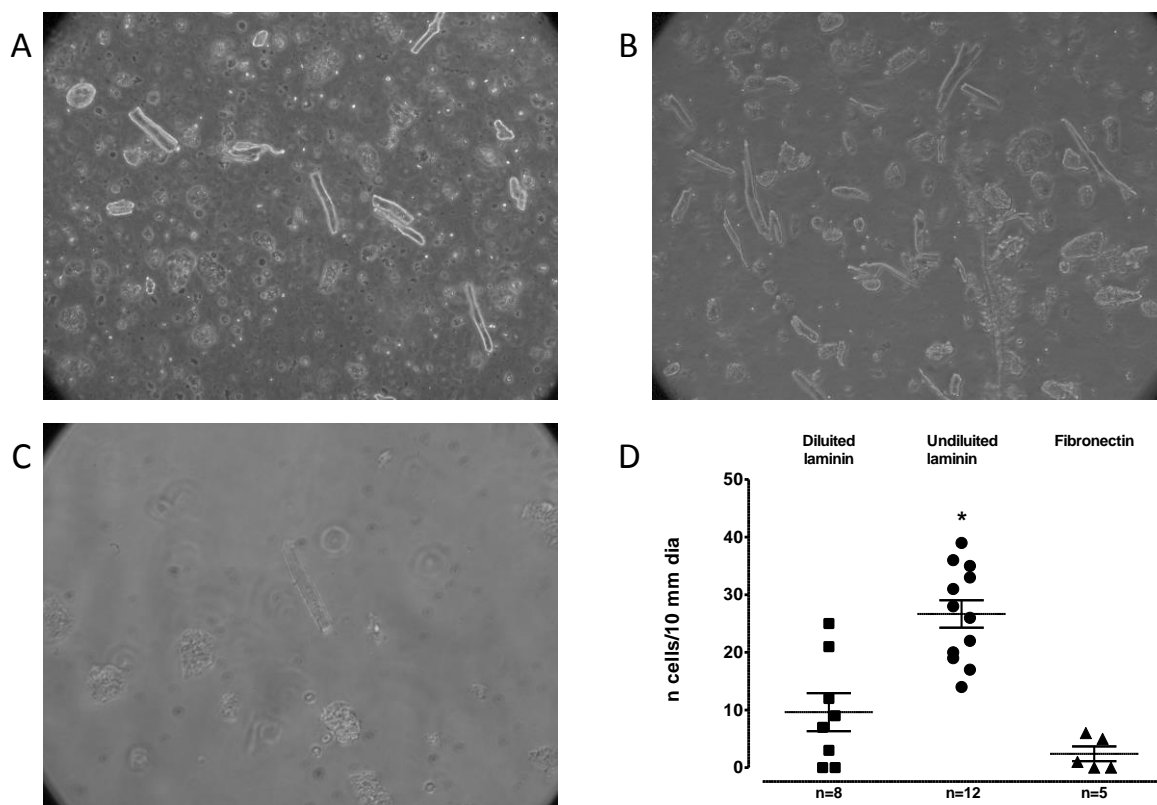
Figure 19: Effect of different coating on number of cells attached
Results after plating cells with **(A)** 0,02 µg/mL laminin; **(B)** 2 µg/mL laminin and **(C)** 5 µg/mL fibronectin. **(D)** Summary of the testing of diluted laminin (0,02 µg/mL), undiluted laminin (2 µg/mL) and fibronectin on cells attachment. Mean values ± SEM are indicated by the lines. n = number of dishes. *p < 0.05 *vs.* diluted laminin and fibronectin (one-way ANOVA; followed by Kruskal-Wallis test, based on myocytes).

Fluorescence resonance energy transfer (FRET) measurements in this study were performed on myocytes 48 h after infection, which is considered a time long enough for the virus to infect the cells (Molina et al., 2012; Nikolaev VO et al., 2004). All experiments were performed at room temperature. Only cells that were striated, rod-shaped myocytes after transfection were used for experiments (Figure 15).

2.7 Live cell imaging of intracellular cAMP

Traditional biochemical methods, as measuring of cAMP in homogenized tissue, do not allow insights into second messenger dynamics at the level of a single cell as well as in shorter space and time, since biochemical methods needs to destroy cells. Furthermore time of course of effect is hard to calculate. Therefore new techniques based on fluorescent microscopy have recently been developed, showing the ability to follow biochemical events and signaling molecules in living cells and tissues (Börner S et al., 2011). These new approaches are based indeed on FRET, Förster resonance energy transfer or Fluorescence resonance energy transfer (FRET setup shown in Figure 20) a phenomenon described in 1946 by the scientist Theodor Förster as a mechanism of non-radiative transfer of energy (Förster T., 2012).
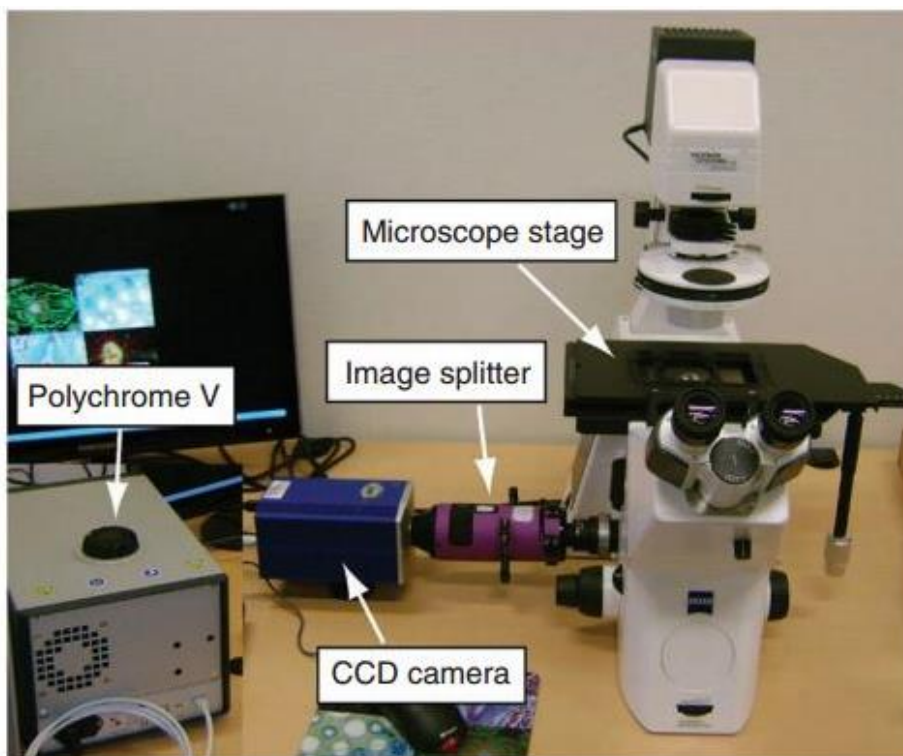
Figure 20: Equipment setup for FRET imaging
Layout of the experimental setup used for FRET imaging. Microscope stage is the place where the dish, with cells attached and cultured, is located. The microscope is also equipped with a monochromator excitation light Polychrome V and an image splitter for emission light. CCD camera allows recording of CFP (cyan fluorescent protein) and YFP (yellow fluorescent protein) emissions. (Börner S et al., 2011).

Researchers could use this method, later on, to measure the space between fluorescent molecules in different biological environments. The transfer of energy occurs between a pair of two different fluorophores connected to one or two protein molecules. This leads to a change in distance of the fluorophores. It can be used indeed to report protein-protein interactions or conformational changes. As matter of fact, this principle can be applied by using biosensors, such the one mentioned in the previous chapter and used for our experiments, capable of visualizing various cellular processes and second messengers in intact cells (Zhang J. et al., 2002; Miyawaki A. et al., 2003; Lohse MJ et al., 2008). The sensor we used is known as Epac1-camps and is based on one of the cAMP effectors called Epac. Epac is encoded by the RAPGEF3 gene and expressed in human heart (Rooij J. et al., 1998). It is a protein that possess a physiological cAMP binding site. Binding of cAMP to Epac induces a conformational change that liberates the catalytic domain of Epac from intrasubunit allosteric inhibition (Rehmann H. et al., 2003). Dipilato research group suggested that sandwiching such Epac-based responsive elements between a FRET pair of fluorophores would allow the detection of cAMP and Epac activation by changes in FRET. Therefore, they generated a number of chimeric proteins by fusing the N terminus of various Epac truncations to enhanced cyan fluorescent protein (ECFP) and the C terminus to citrine, an improved version of yellow fluorescent protein (YFP) (Figure 21) (Dipilato et al., 2004). Among all of them, the construct which gave the most accurate relation between FRET signal and cAMP increase was the so called ICUE1 (indicator of cAMP using Epac 1). The structural difference with the others was that they made the sandwich between ECFP and citrine with the full-length epac1. Therefore, this is the biosensor which we used for our experiments. The scheme and mechanism are illustrated in figure 22.
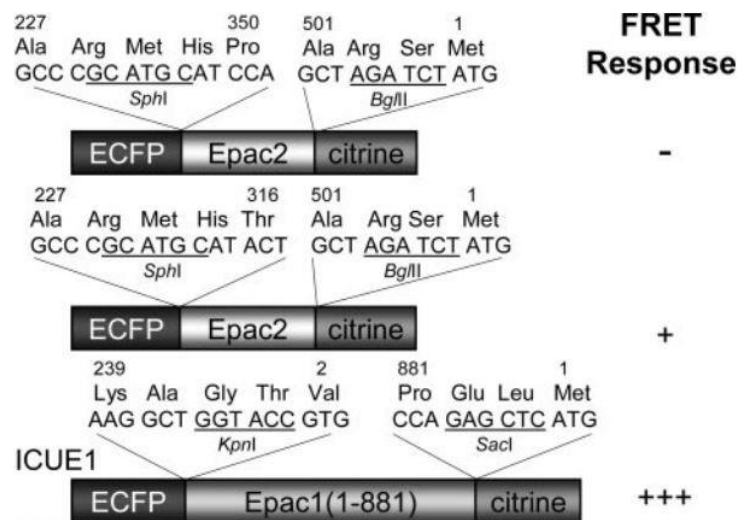
Figure 21: Domain structure and comparison of FRET responses for Epac-based cAMP reporters
Domain structure and comparison of FRET responses for Epac-based cAMP reporters. Sandwiched between ECFP and citrine are truncated forms of Epac2. The construct that generated the biggest FRET response was designated as ICUE1. Picture modified from Dipilato et al. (Dipilato et al., 2004).

A

B
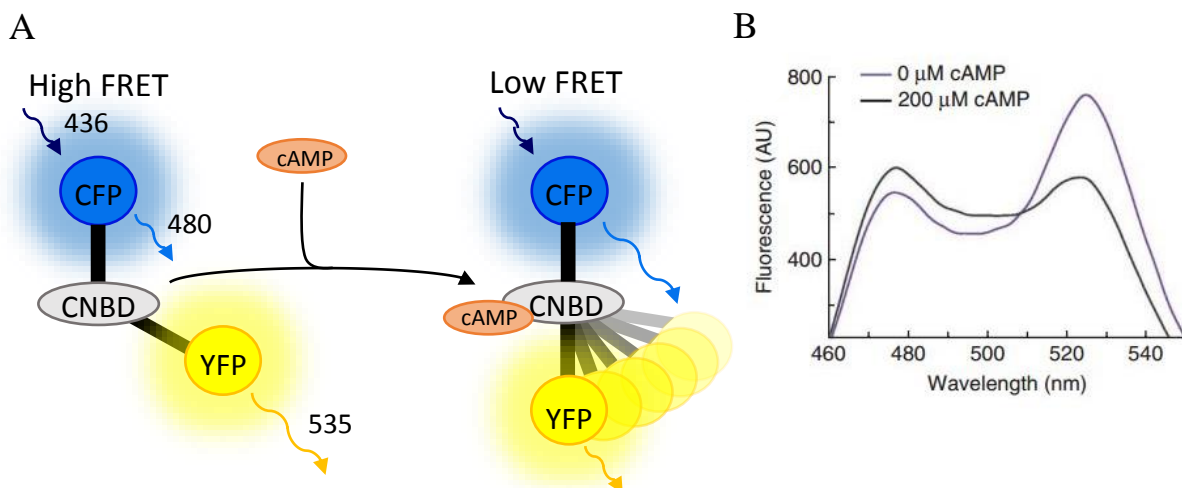
Figure 22: Scheme and graph of Epac1-camps/cAMP interaction
(A) Epac-based cAMP sensors (camps) are comprised of a single cyclic nucleotide binding domains (CNBD) fused between CFP and YFP. cAMP induces a conformational change leading to an increase in distance between the fluorophores, which is measured as a decrease in FRET. **(B)** The graph shows how at the wavelength of 480nM there is no difference between fluorescence intensity in the presence or in the absence of cAMP. Instead, at 535 nM, in the presence cAMP, the signal is lower than the one in the absence of cAMP. Modified from Nikolaev VO et al. (Nikolaev VO et al., 2006).

FRET measurements were performed on myocytes 48 h after transfection with the cAMP-based sensor Epac1-camps (Nikolaev VO et al., 2004). Cytosolic cAMP was measured in a total of 208 isolated HAMs. FRET imaging of intracellular cAMP typical procedure is described below. As a first step, we took a laminin-coated culture glass bottom dish, with adherent cells, out of the cell-culture incubator. We removed gently the medium and carefully added around 400 µl of the so-called FRET buffer, in

order to cover the all central part of the surface of the dish. FRET buffer is a K^+-Ringer solution adjusted to pH 7.4 with NaOH (Table 9). For our experiments we used an inverted fluorescent microscope (Leica DMI3000 B), equipped with a beam-splitter Dual-View DV2 with a 505dcxr dichroic mirror and a CMOS Camera (QIMAGING optiMOS, Surrey, Canada). After applying oil-immersion on the high magnification objective (63x), the dish was placed on the FRET microscope stage and using transmitted light we searched for a suitable cell (*xy* axes for stage movement). The selected cell was defined at the membrane level, cross striated and not contracting. Application of D480/30m and D535/40m emission filters (Photometrics) was necessary to visualize Epac-1camps transfection. Afterwards, we switched on the fluorescent light. Cells suitable for cAMP imaging should have sufficiently high expression of the sensor, as judged by fluorescence intensity and the operator should avoid the use of too-dim cells. In figure 23 it is shown two days-cultured cardiomyocytes with a high expression of the biosensor. Moreover, long-term illumination (within few minutes) of the cells with fluorescent light had to be avoided, as it may cause bleaching (so called photobleaching). After identifying the proper cell, immediately the fluorescent light was switched off. Using the 'Configure Acquisition' button, we adjusted the exposure time such that it was sufficient to record images with a good signal-to-noise ratio (usually 5 ms) and, using the 'Set Time-lapse' option, we selected how many images per time were acquired. In our case, images in CFP and YFP emission channels were captured every 5 s. Once setting these parameters, the region of interest was drawn over the cell with the region drawing tool ('Regions' button); after we opened a log file and selected the 'save images' option in the 'Experiment Control Panel'. Right after, we started the imaging protocol by pressing the 'Acquire' button.
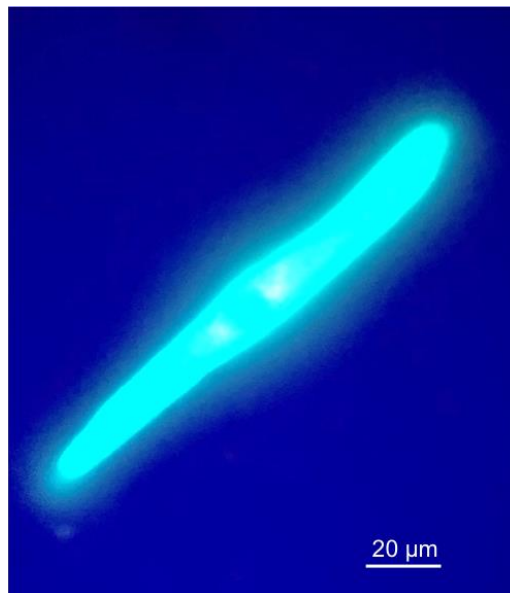
Figure 23: Representative human atrium myocytes after 48 hours of culture and transfected with the cytosolic cAMP sensor Epac1-camps

Table 9: FRET Buffer: composition

Compounds	Concentration (mM)
KCl	5.4
NaCl	121.6
MgCl$_2$	1.8
CaCl$_2$	1.8
NaHCO$_3$	4
NaH$_2$PO$_4$	0.8
Glucose	5
HEPES	10
Sodium pyruvate	5

After an initial equilibration period, of around 60 seconds, in which the FRET signal became stable, various different drugs could be applied to the bath solution during the recording, by accurately pipetting them into the dish. For example, to record changes in cAMP levels over time, cells can be stimulated with an agonist, which evoke increases in cAMP; cells can be subsequently treated with another compound, which might provoke a further increase of the FRET signal (Figure 24). We always waited for the FRET ratio to reach a stable baseline or a plateau before applying any ligand. After running the protocol and finishing an experiment, we saved the log file and removed the dish from the microscope. Signals were analyzed offline by the software Micro-Manager 1.4.5 together with ImageJ (Sprenger JU et al., 2012). Excel and GraphPad Prism were used to calculate the corrected FRET ratio and for statistical analysis. All experiments were performed at room temperature.
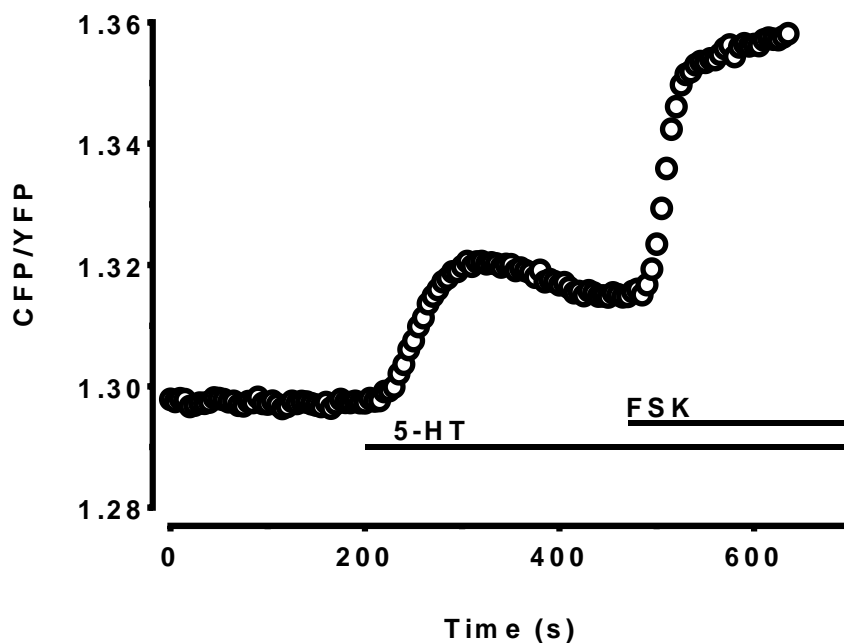
Figure 24: Time course of changes of the corrected CFP/YFP ratio
The cell was exposed first to 100 µM 5-HT and then, after reaching maximum effect, to 10 µM FSK.

2.8 Drugs

5-Hydroxytryptamine HCl (5-HT), norepinephrine (NE), epinephrine (Epi), forskolin (FSK), rolipram (Rol), cilostamide (Cil), ICI118.551, CGP20712A and phenoxybenzamine were purchased from Sigma Chemicals (Poole Dorse, UK).

2.8.1 5-Hydroxytryptamine (5-HT)
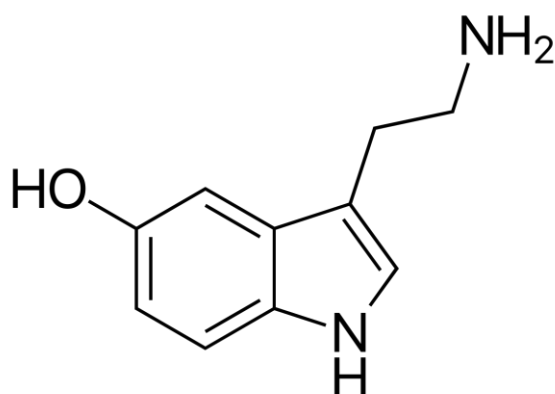
Figure 25: Chemical structure of 5-hydroxytryptamine

Serotonin or 5-hydroxytryptamine (5-HT) is a monoamine neurotransmitter (Figure 25). Biochemically, the indoleamine molecule derives from the amino acid tryptophan, via the (rate-limiting) hydroxylation of the 5 position on the ring (forming the intermediate 5-hydroxytryptophan), and then decarboxylation to produce serotonin (Gonzales FD et al., 2011). Serotonin is primarily found in the enteric nervous

system located in the gastrointestinal tract (GI tract). Anyhow, it is also known that 5-HT increases contractile force, cAMP, the activity of PKA and hastens relaxation through 5-HT$_4$ receptors in human trabeculae from right and left atrium (Kaumann et al., 1990; Sanders L. et al., 1995; Sanders L. and Kaumann AJ, 1992). 5-HT directly interacts with 5-HT receptors. In this work the drug has been used in maximum rather high concentration of 100 µM, in order to verify the maximum concentration response after application.

2.8.2 Norepinephrine (NE)
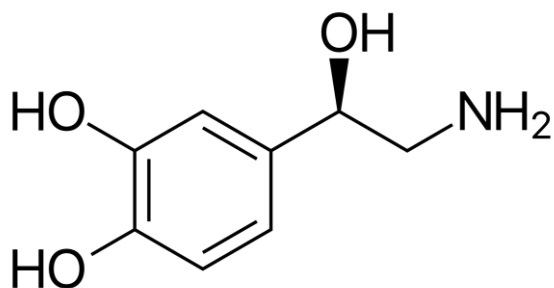
Figure 26: Chemical structure of norepinephrine

Norepinephrine (NE), also called noradrenaline (NA) or noradrenalin, is an organic chemical in the catecholamine family that functions in the brain and body as a hormone and neurotransmitter (Figure 26). Norepinephrine is active in the brain as well as extremely involved in the cardiovascular system: it increases heart rate and blood pressure. Norepinephrine is synthesized from the amino acid tyrosine by a series of enzymatic steps in the adrenal medulla and postganglionic neurons of the sympathetic nervous system. While the conversion of tyrosine to dopamine occurs predominantly in the cytoplasm, the conversion of dopamine to norepinephrine by dopamine β-monooxygenase occurs predominantly inside neurotransmitter vesicles. Norepinephrine is released from internal nerve endings and it has a particularly high affinity for α1, β$_1$- and β$_3$-AR. For β$_2$-AR, the affinity is significantly lower. In our experiments, interactions of norepinephrine with α-AR were excluded by the previous treatment with phenoxybenzamine. As already described, there is no β$_3$-AR-mediated effect on the human atrium under physiological conditions (Christ et al., 2011). From binding studies on recombinant human β-AR, it is known that binding to β$_2$-AR takes place (Hoffmann et al., 2004). Therefore, the β$_2$-AR-selective antagonist ICI 118,551 was used in the experiments. In the present project, norepinephrine was used in increasing concentration starting from 1 nM up to 100 µM.

2.8.3 Epinephrine (Epi)
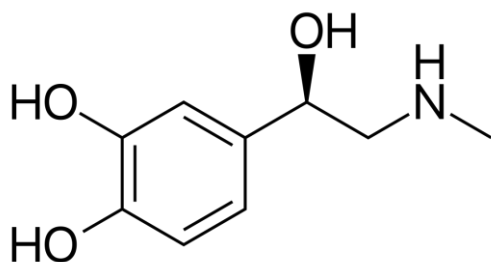
Figure 27: Chemical structure of epinephrine

Epinephrine, also known as adrenaline, is a hormone and neurotransmitter (Figure 27). Epinephrine is normally produced by both the adrenal glands and certain neurons. It plays an important role in the fight-or-flight response by increasing blood flow to muscles, output of the heart, pupil dilation response, and blood sugar level. The mechanism behind those events is the binding to alpha and beta receptors. From binding studies on recombinant human β-AR it is known that adrenaline, in contrast to norepinephrine, has comparable affinities to β_1- and β_2-AR (Hoffmann et al., 2004). Therefore, the β_1-AR selective antagonist CGP 20712A was used in the experiments to achieve an increase in force exclusively by activation of the β_2-AR. As for Norepinephrine, also Epi was used in increasing concentration starting from 1 nM up to 100 µM.

2.8.4 Forskolin (FSK)
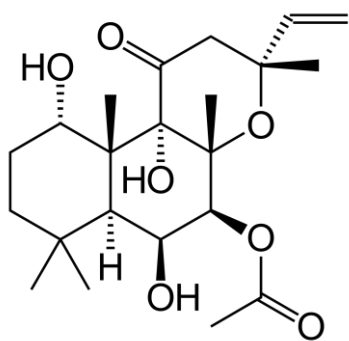
Figure 28: Chemical structure of forskolin

Forskolin (coleonol) (Figure 28) is a labdane diterpene that is produced by the Indian Coleus plant (*Plectranthus barbatus*) (Figure 29). Forskolin (FSK) activates the enzyme adenylyl cyclase and increases intracellular levels of cAMP. In the present work FSK was used as internal control at the concentration of 10 µM. In particular for FRET experiments, it allowed the cells to reach saturation of cAMP.

Figure 29: *Plectranthus barbatus*
Plectranthus barbatus, also known by the synonym *Coleus forskohlii* and vernacular names forskohlii and Indian coleus, is a tropical perennial plant related to the typical coleus species. It produces forskolin, an extract useful for pharmaceutical preparations and research in cell biology.

2.8.5 Rolipram (Rol)
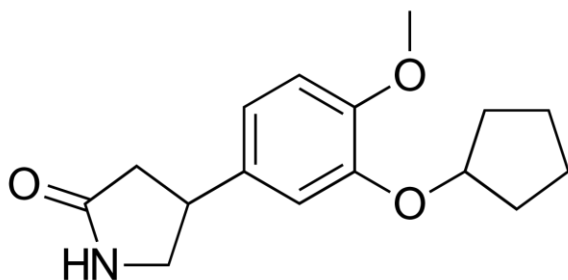
Figure 30: Chemical structure of rolipram

Rolipram is a selective phosphodiesterase-4 inhibitor discovered and developed by Schering AG (Berlin, Germany) as a potential antidepressant drug in the early 1990s (Figure 30). PDE4 hydrolyzes cyclic adenosine monophosphate (cAMP) to inactive adenosine monophosphate (AMP). Inhibition of PDE4 blocks hydrolysis of cAMP, thereby increasing levels of cAMP within cells. 1 µM has been found to inhibit about 50% of PDE4 (Berk et al., 2016) while 10 µM about 90%.

2.8.6 Cilostamide (Cil)
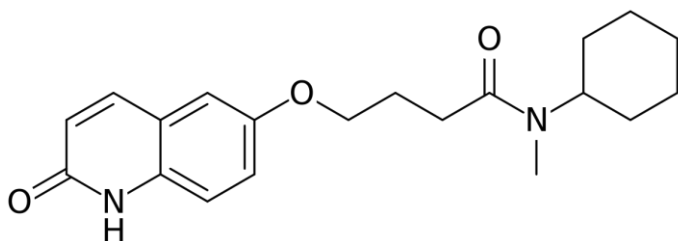
Figure 31: Chemical structure of cilostamide

Cilostamide or N-cyclohexyl-N-methyl-4-(1,2-dihydro-2-oxo-6-quinolyloxy)-butyramide is a relatively selective inhibitor of PDE3 (Figure 31). To avoid inhibition of PDE4, cilostamide was used at the concentration limited to 300 nM in our experiments. This results in inhibition of PDE3 of about 86% while only <0.4% of PDE4 are inhibited (Beavo JA, 1995; Sudo et al., 2000; Vargas et al., 2006).

2.8.7 ICI 118,551
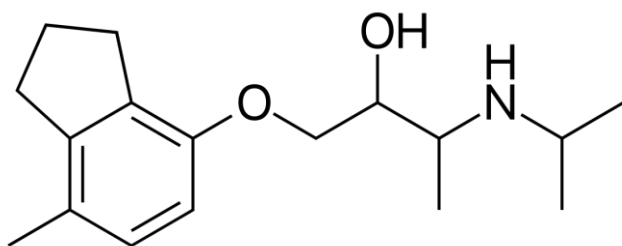
Figure 32: Chemical structure of ICI 118,551

ICI-118,551 is a selective β_2-AR antagonist (Figure 32). ICI-118,551 binds to the β_2 subtype with at least 100 times greater affinity than β_1 or β_3, the two other known subtypes of the beta adrenoceptors. We used ICI-118,551 in experiments with norepinephrine at a concentration of 50 nM to form a β_1-AR-selective experimental condition (Bilski AJ et al., 1983; Kaumann AJ and Molenaar P, 1997). In a study, it was proved how the EC_{50} of the inhibition of [^{125}I] ICYP, which is an antagonist of β-ARs, was reached at lower concentration of ICI-118,551 for β_2-AR compared to β_1- (Chakir K et al., 2003) (Figure 33). In conclusion we found the use of this compound suitable to selectively stimulate β_1-AR.
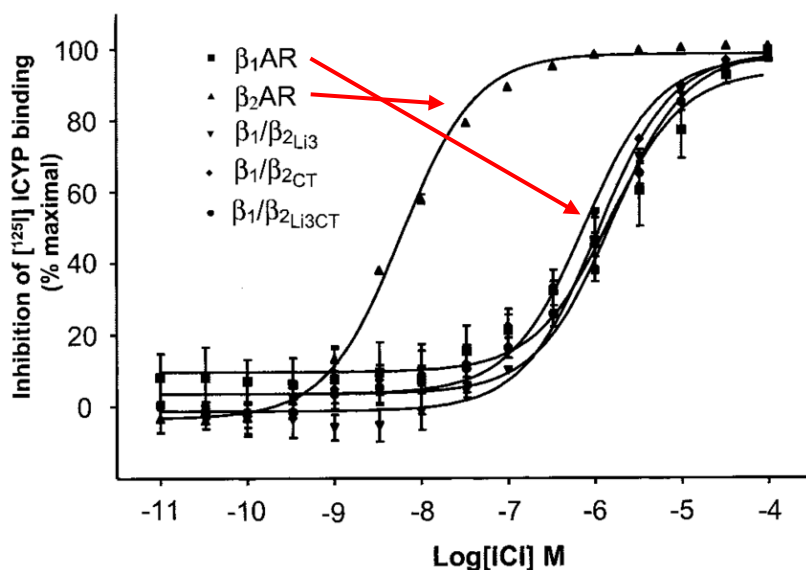
Figure 33: Percentage of inhibition of [^{125}I] ICYP binding to beta adrenoceptors

The experiments were conducted in the presence of increasing concentration of ICI-118,551 in membranes from double knockout (DKO) mice cardiac myocytes. Cells were infected with adenoviruses encoding either β_1- and β_2-AR or one of the β_1/β_2-AR chimeras. In the three chimeras the third intracellular loop ($\beta_1/\beta_{2\text{-Li3}}$) or the carboxyl terminus ($\beta_1/\beta_{2\text{-CT}}$) or both domains ($\beta_1/\beta_{2\text{-Li3CT}}$) of β_1-AR are replaced by the corresponding parts of the β_2-AR. Modified from Chakir K et al. (Chakir K et al., 2003).

2.8.8 CGP 20712A
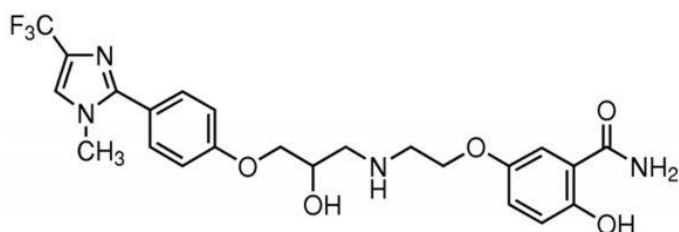
Figure 34: Chemical structure of CGP 20712A

CGP 20712A is a selective β_1-AR blocker with a K_i-value-β_1AR of 4.7 nM and 4.0 μM for β_2-AR, respectively (Hoffmann et al., 2004) (Figure 34). We used the compound in a concentration of 300 nM in the experiments with adrenalin to form a β_2-AR-selective experimental condition (Dooley DJ et al., 1986; Kaumann AJ et al., 1989). In the same study mentioned in the paragraph before, it was proved how the EC$_{50}$ of the inhibition of [^{125}I] ICYP was reached at lower concentration of CGP 20712A for β_1-AR compared to β_2 (Chakir K et al., 2003) (Figure 35). Therefore, we found the use of this compound suitable to selectively stimulate β_2-AR.
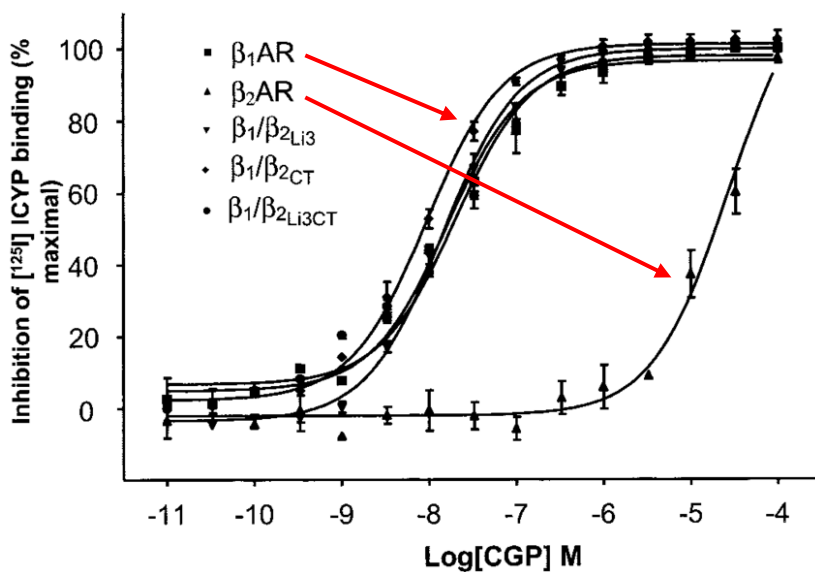
Figure 35: Inhibition of [^{125}I] ICYP binding to beta adrenoceptors in percent

The experiments were conducted in the presence of increasing concentration of CGP 20712A in membranes from double knockout (DKO) mice cardiac myocytes. Cells were infected with adenoviruses encoding either β₁- and β₂-AR or one of the β₁/β₂-AR chimeras. In the three chimeras the third intracellular loop (β₁/β₂-Li₃) or the carboxyl terminus (β₁/β₂-CT) or both domains (β₁/β₂-Li₃CT) of β₁-AR are replaced by the corresponding parts of the β₂-AR. Modified from Chakir K et al. (Chakir K et al., 2003).

2.8.9 Phenoxybenzamine
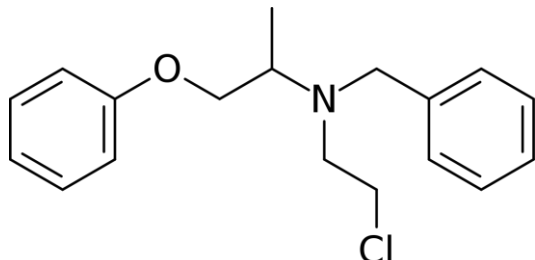
Figure 36: Chemical structure of phenoxybenzamine

Phenoxybenzamine is an irreversible, non-selective α-AR antagonist (Figure 36) and it can be clinically used to lower the blood pressure. As a result of α₁-AR block, the vasoconstricting action of norepinephrine is prevented while blocking of presynaptic α₂-AR leads to increased norepinephrine release, emptying of the intracellular norepinephrine reservoir and blocking of reuptake. After administration of phenoxybenzamine there is a huge increase in force due to the positive inotropic effect of NE released from intramyocardial nerve endings by the electrical stimulation (Mo et al., 2017).

2.9 Statistic

Values are expressed as mean ± SEM. Statistical significance was evaluated using a Student's t-test and ANOVA was used for comparison of multiple effects. Differences were considered statistically significant when $p < 0.05$. Data obtained by FRET experiments as well as clinical data of patients linked to FRET experiments were also analysed by an univariable and multivariable model realized by the

statistician Dr. Geelhoed Bastiaan (Department of General and Interventional Cardiology, University Heart Center, Hamburg, Germany).

3. Results

The data presented regarding cAMP measurement under stimulation of 5-HT receptor (Chapter 3.4.6) were recently elaborated as a paper and submitted to the journal "Europace" in July 2019. Title: "Impact of phosphodiesterases PDE3 and PDE4 on 5-hydroxytryptamine receptor-mediated increase of cAMP in atrial fibrillation". List of authors: Bernardo Dolce, Torsten Christ, Yalin Yildirim, Hermann Reichenspurner, Thomas Eschenhagen, Viacheslav Nikolaev, Alberto J Kaumann, Cristina E Molina.

3.1 Expression and localization of PDE3 and 4 in human atrial myocytes

In previous studies, only PDE3 protein expression was tested in human cardiomyocytes isolated from patients in SR and peAF (Rozmaritsa et al., 2014). The results did not show significant differences between them. Regarding immunohistochemistry with PDE3 and PDE4 antibodies instead, only data about SR are available from the work of Molina at al (Molina et al., 2012).

Therefore we decided to test PDE3A, PDE4B and PDE4D isoform expression and localization by Western blot and immunofluorescence in HAMs isolated not only from patients in SR but also from peAF. PDE3A and PDE4B were detected at the Z-line of atrial myocytes, at the level of the sarcomere-protein α-actinin (Figure 37A and Figure 39A). PDE4D instead appeared expressed homogenously in the cytoplasm (Figure 38A). Western blots revealed a differential expression among the three isoenzymes. While PDE3A and PDE4D did not show significant differences between samples isolated from patients in SR and peAF (Figure 37B,C and Figure 38B,C), PDE4B was almost two times higher expressed in peAF than in SR (Figure 39B,C). Quantification of proteins bands was performed by normalization to protein eIF4E and their respective control.
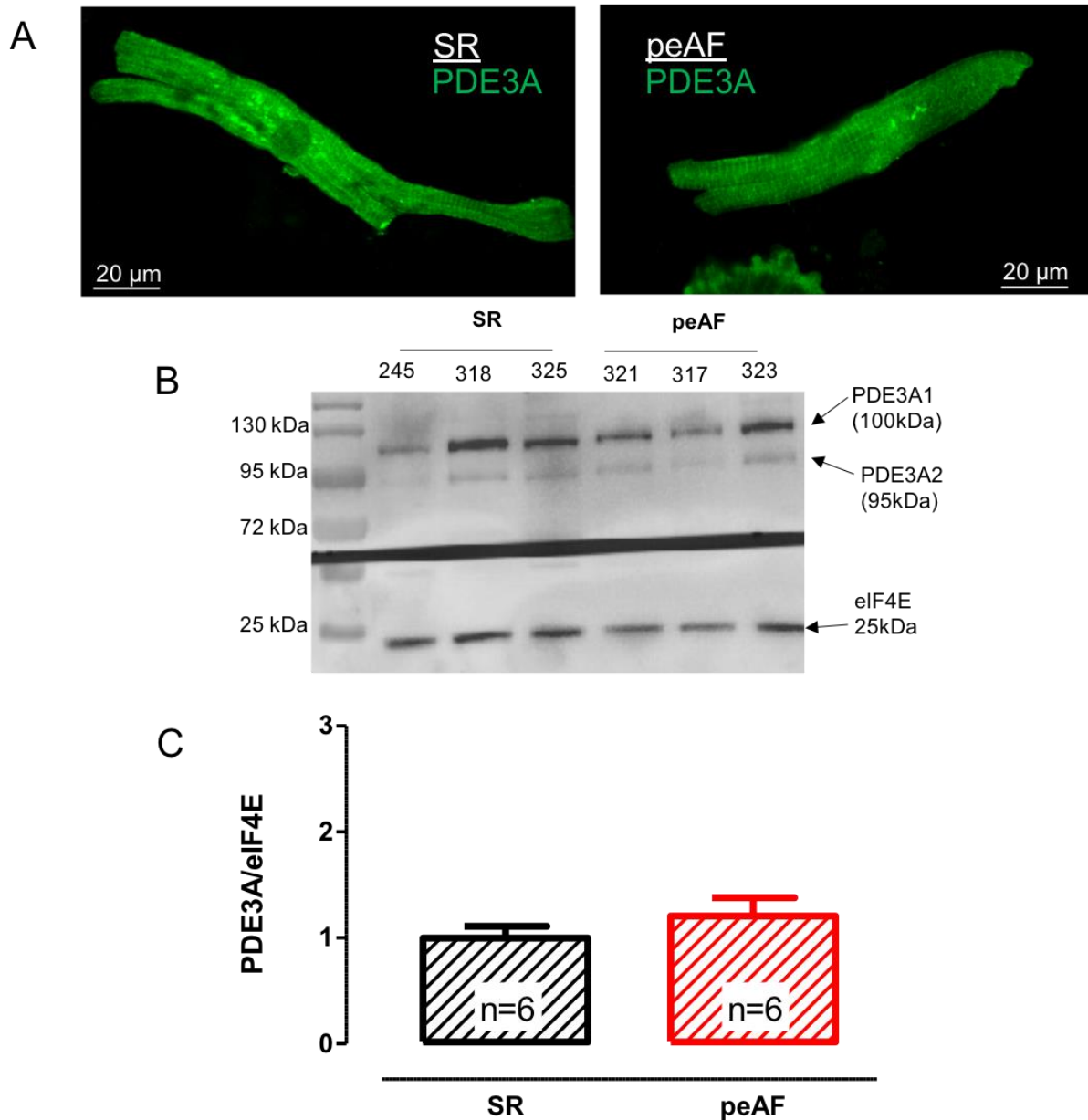
Figure 37: PDE3A expression tested with immunofluorescence and WB

Immunofluorescence staining of PDE3A (green) in 2 HAMs isolated from patients in SR and peAF. Cells were stained with an antibody against PDE3A. The specificity of the antibody was tested on PDE3A-KO mice (Zuo et al., 2018). **(A)**. Representative blot of cardiac tissues isolated from 3 patients with SR and 3 patients with peAF. Prominent bands were detected at 100 kDa (PDE3A1) and 95 kDa (PDE3A2). Numbers on top refer to patient´s code **(B)**. Protein levels of PDE3A in RA samples of 6 patients in SR and 6 patients in peAF were detected by western blot and normalized to elf4E. Unpaired t-test; no significant difference between the two groups. Data are mean ± SEM **(C)**.
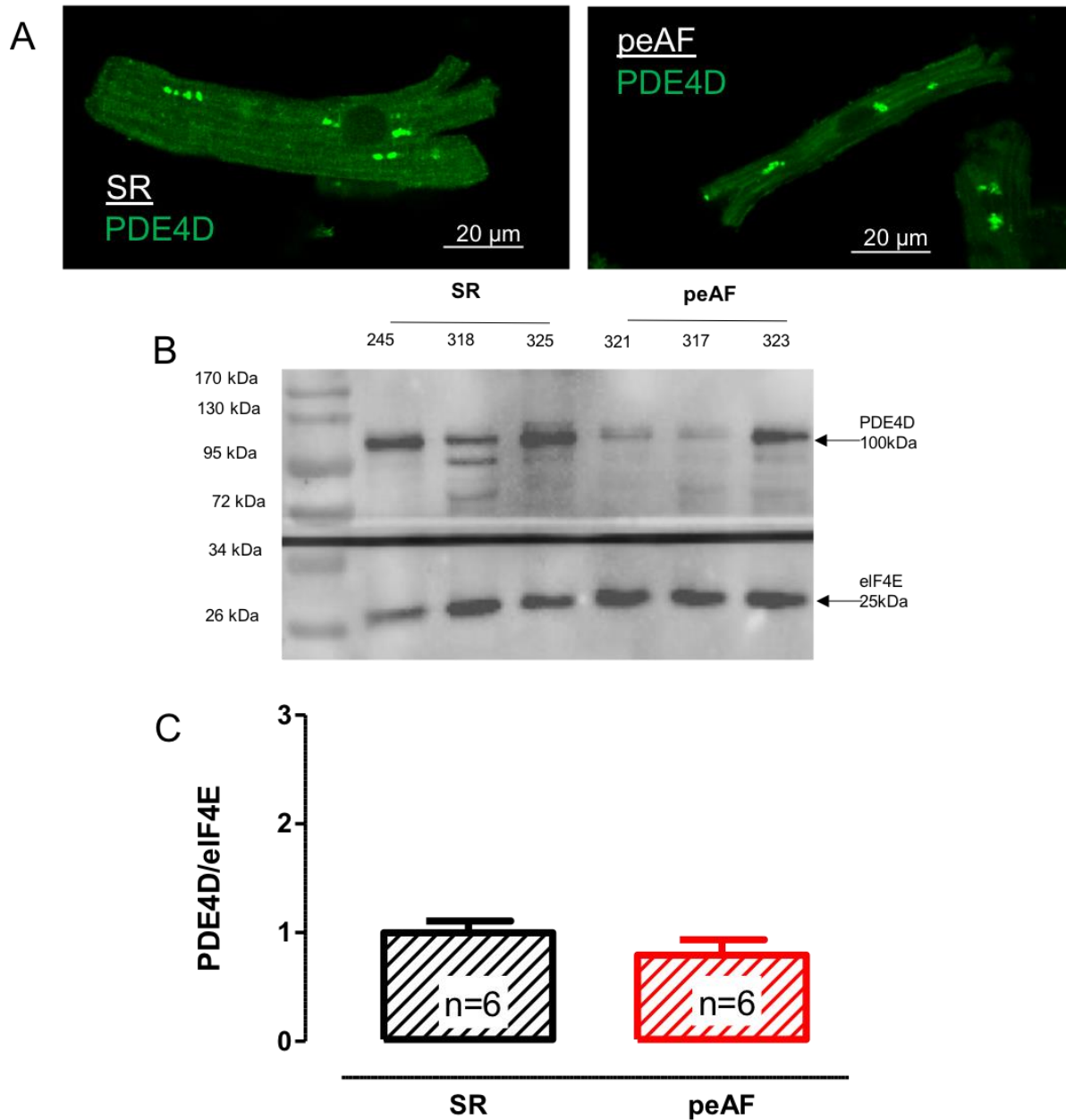
Figure 38: PDE4D expression tested with immunofluorescence and WB
Immunofluorescence staining of PDE4D (green) in 2 HAMs isolated from patients in SR and peAF. Cells were stained with anti-PDE4D specific antibody. The specificity of the antibody was tested on KO mice (Kraft A., 2019) **(A)**. Representative blot of cardiac tissues isolated from 3 patients with SR and 3 patients with peAF. Prominent bands were detected around 100 kDa. Numbers on top refer to patient´s code. Detected extra bands are putative PDE4D isoforms. **(B)**. Protein levels of PDE4D of 6 patients in SR and 6 patients in peAF were detected by western blot and normalized to elf4E. Unpaired t-test; no significant difference between the two groups. Data are mean ± SEM **(C)**.
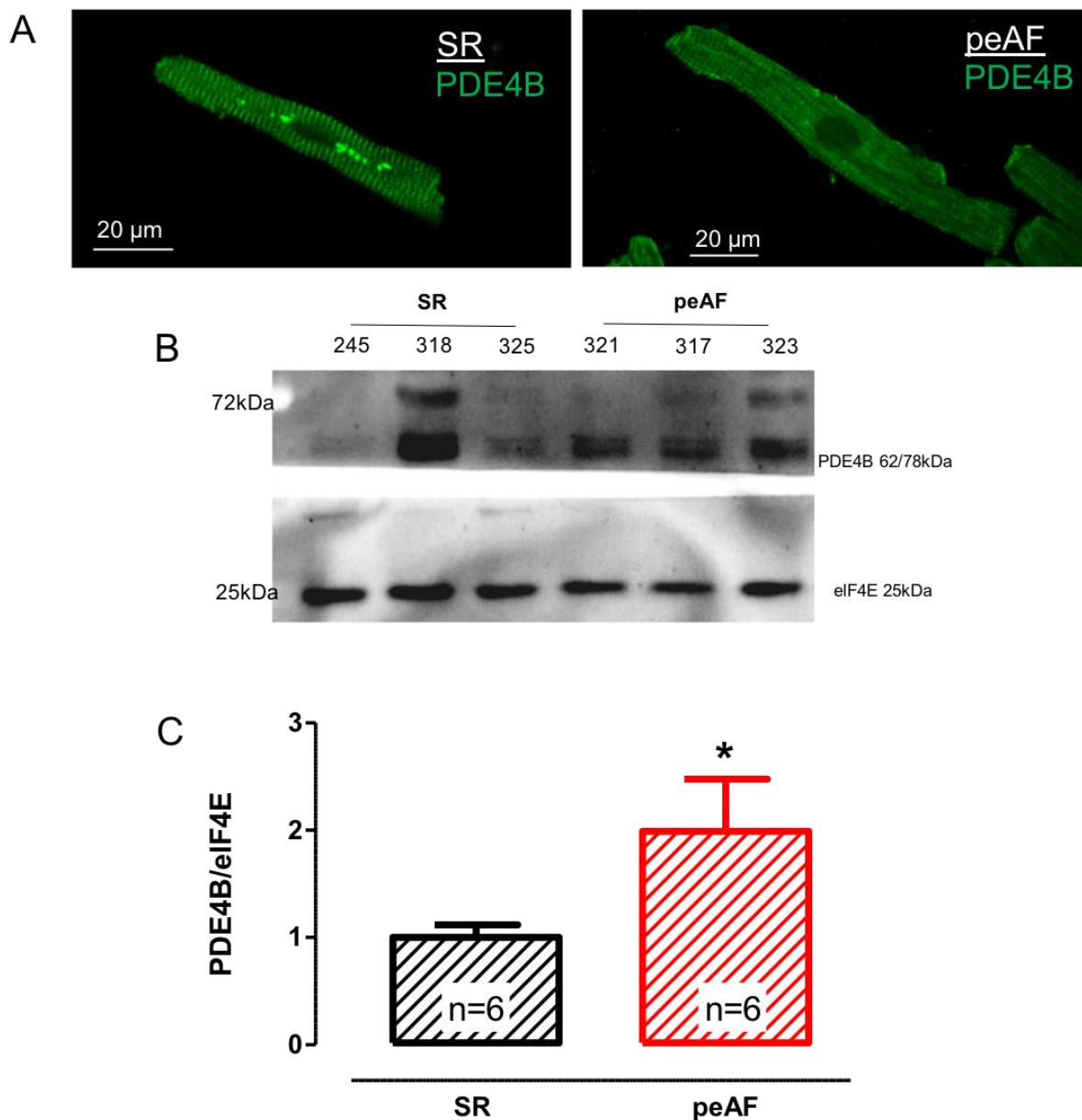
Figure 39: PDE4B expression tested with immunofluorescence and WB
Immunofluorescence staining of PDE4B (green) in 2 HAMs isolated from patients in SR and peAF. Cells were stained with anti-PDE4B specific antibody. The specificity of the antibody was tested on KO mice (Kraft A., 2019) **(A)**. Representative blot of cardiac tissues isolated from 3 patients with SR and 3 patients with peAF. Prominent bands were detected in the range of 62-78 kDa. Numbers on top refer to patient´s code. Detected extra bands are putative PDE4B isoforms **(B)**. Protein levels of PDE4B of 6 patients in SR and 6 patients in peAF were detected by western blot and normalized to elf4E. Unpaired t-test; *p < 0.05 vs SR. Data are mean ± SEM **(C)**.

3.2 Effects of PDE4 inhibition on $I_{Ca,L}$

Increase in cAMP by PDE4 inhibition should boost the activity of the excitation-contraction coupling (ECC) elements controlled by cAMP. Therefore, in the next step of the project we aimed to elucidate the correlation between arrhythmias and $I_{Ca,L}$ role controlled by PDE4 inhibition. For that purpose we

measured $I_{Ca,L}$ in isolated human atrial cardiomyocytes from patients in SR and peAF (Figure 40 and 41). The experiments were performed either in the absence or presence of the PDE4 inhibitor rolipram (10 μM), and under stimulation of β_1-AR or β_2-AR. To investigate whether rolipram potentiates effects of β-AR stimulation we used a single submaximal concentration of NE or Epi (1 μM concentration), expected to exert only 50% of the maximal effect (Christ et al., 2014).

3.2.1 Effects of PDE4 inhibition on $I_{Ca,L}$ in SR

In this set of experiments, we investigated whether rolipram 10 μM increases $I_{Ca,L}$. To inhibit PDE4 we used 10 μM rolipram. Cells were exposed to rolipram and then in the continuous presence of rolipram to 1μM NE or Epi. TMC without rolipram were used for comparison.
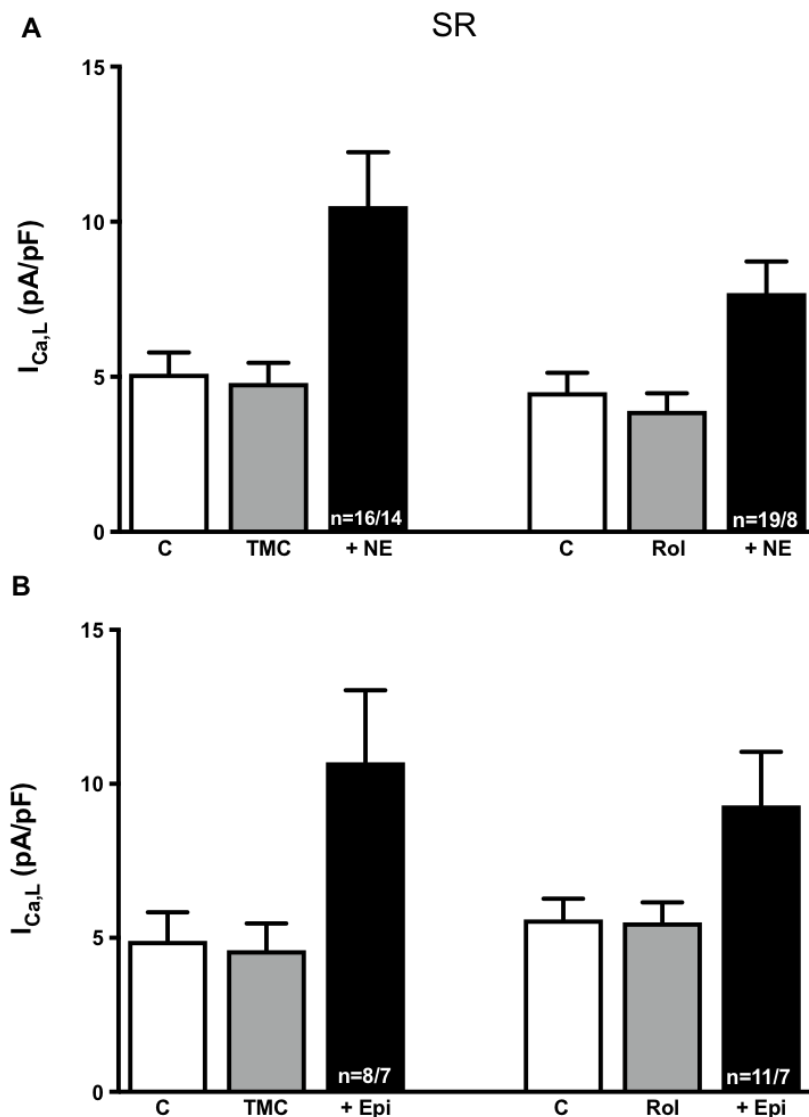
Figure 40: Effects of rolipram 10 μM on basal and β-AR stimulation-activated $I_{Ca,L}$ in SR
(A) Effects of 1 μM NE on $I_{Ca,L}$ in SR, in the absence and presence of 10 μM rolipram. (B) Effects of 1 μM Epi on $I_{Ca,L}$ in SR, in the absence and presence of 10 μM rolipram. C stands for "control" while TMC for "time matched control". Data are mean ± SEM from the number of patients (n=myocytes/patients) shown in the bar. *$P < 0.05$ vs TMC or Rol. One-way ANOVA followed by Kruskal-Wallis test.

Inhibition of PDE4 by rolipram 10 µM did not increase $I_{Ca,L}$ neither in the absence nor in the presence of NE or Epi in SR (Figure 40).

3.2.2 Effects of PDE4 inhibition on $I_{Ca,L}$ in peAF

$I_{Ca,L}$ in peAF is smaller than in SR, not only under basal (drug-free) conditions but also when cAMP/PKA is maximally activated by β-AR stimulation or direct activation of adenylyl cyclase with FSK. In order to investigate whether low $I_{Ca,L}$ amplitudes in peAF may result from PDE4 activity we have measured both basal and $I_{Ca,L}$ β-AR stimulation-activated current in the presence of 10 µM rolipram.
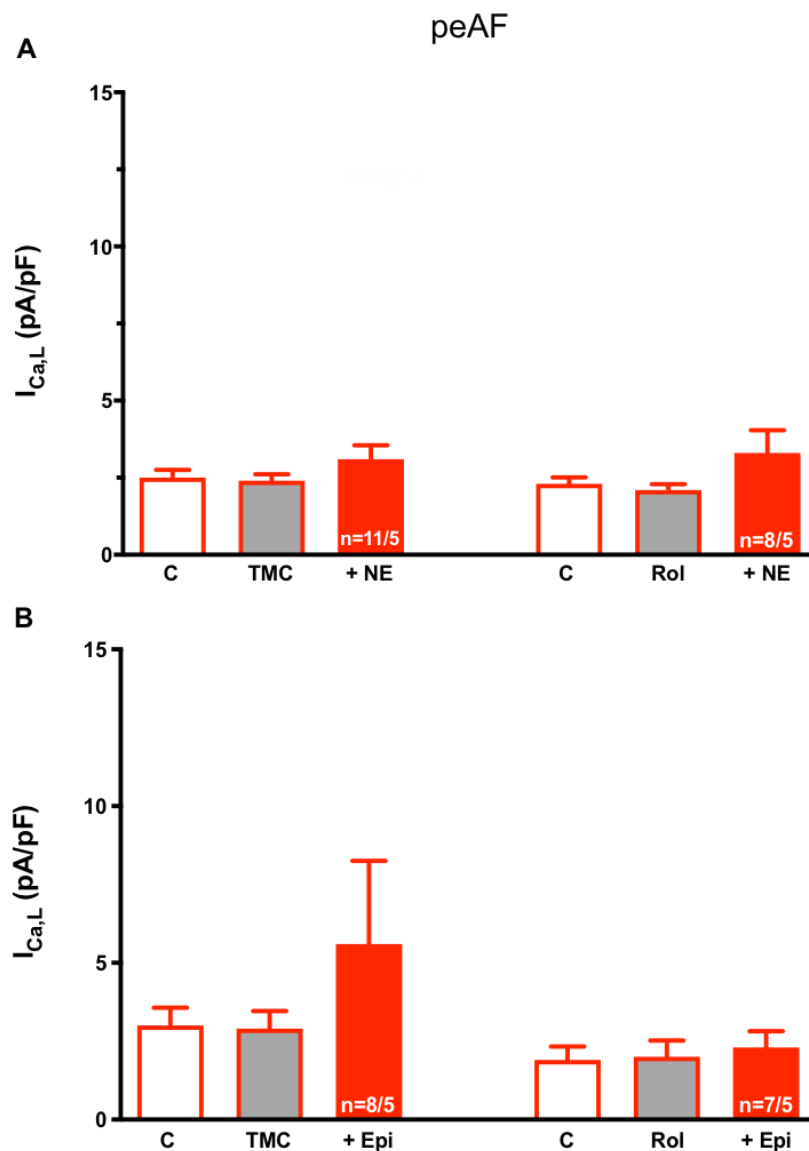
Figure 41: Effects of rolipram 10 µM on basal and β-AR stimulation-activated $I_{Ca,L}$ in peAF
(A) Effects of 1 µM NE on $I_{Ca,L}$ in peAF, in the presence and absence of 10 µM rolipram. **(B)** Effects of 1 µM Epi on $I_{Ca,L}$ in peAF, in the presence and absence of 10 µM rolipram. C stands for "control" while TMC for "time matched control". Data are mean ± SEM from the number of patients (n=myocytes/patients) shown in the bar. *P < 0.05 vs TMC or rol. One-way ANOVA followed by Kruskal-Wallis test.

Also in peAF, inhibition of PDE4 by rolipram 10 µM did not increase $I_{Ca,L}$ neither in the absence nor in the presence of NE or Epi (Figure 41). These findings argue against relevant contribution of PDE4 to the decreased in $I_{Ca,L}$ in peAF.

3.3 Effect of PDE4-inhibition on force and arrhythmias in human atrium

In an earlier report, inhibition of PDE4 did not increase sensitivity of $β_1$- and $β_2$-AR to increase force in human atrium (Christ et al., 2006). Molina et al., reported an increase in catecholamine-evoked arrhythmias by PDE4 inhibition with rolipram. However, data about inotropic potencies were not given. In contrast to inhibition of PDE4, inhibition of PDE3 potentiates both inotropy and arrhythmias evoked by serotonin (Berk et al., 2016). In order to clarify whether inhibition of a PDE isoenzyme can facilitate arrhythmias without sensitizing for catecholamine-evoked inotropy we decided to investigate effects of PDE4 inhibition more in detail. Importantly, we decided to use different levels of inhibition by PDE4. Results in the paper of Molina were obtained with 0.1 µM rolipram. Christ et al. had used 1 µM rolipram. From both concentrations there is less than 50% inhibition of PDE4. In addition, we wanted to focus also on peAF and paAF, since data for both conditions were not present in the papers mentioned above. First, we tested effects of 10 µM rolipram, which should give about 90 % inhibition of PDE4, on force and arrhythmias in human right atrium from patients in sinus rhythm, paroxysmal atrial fibrillation and persistent atrial fibrillation. For activation of $β_1$- and $β_2$-AR we used increasing concentrations of NE and Epi in the presence of the respective $β_2$- and $β_1$-AR antagonist.

3.3.1 Effect of PDE4 inhibition on basal force

First, we measured the effect of 10 µM rolipram on basal force. Tissues were exposed to 10 µM rolipram after complete change of bath solution and an equilibrium period. After stabilization, force declined spontaneously over time during 30 min (Figure 42A). Although the absolute values of force (in mN) were considerably smaller in trabeculae from patients in peAF vs. paAF and SR, the relative decline (when expressed as % of control) did not differ between peAF vs. paAF and SR (Figure 42B-D). Force declined in the presence of 10 µM rolipram too, however to a lesser extent than the respective TMC. After correction for the time-dependent decline in force, rolipram similarly increased basal force in all three groups, consistent with a similar regulation of basal force by PDE4 in the three groups (Figure 42B-D).
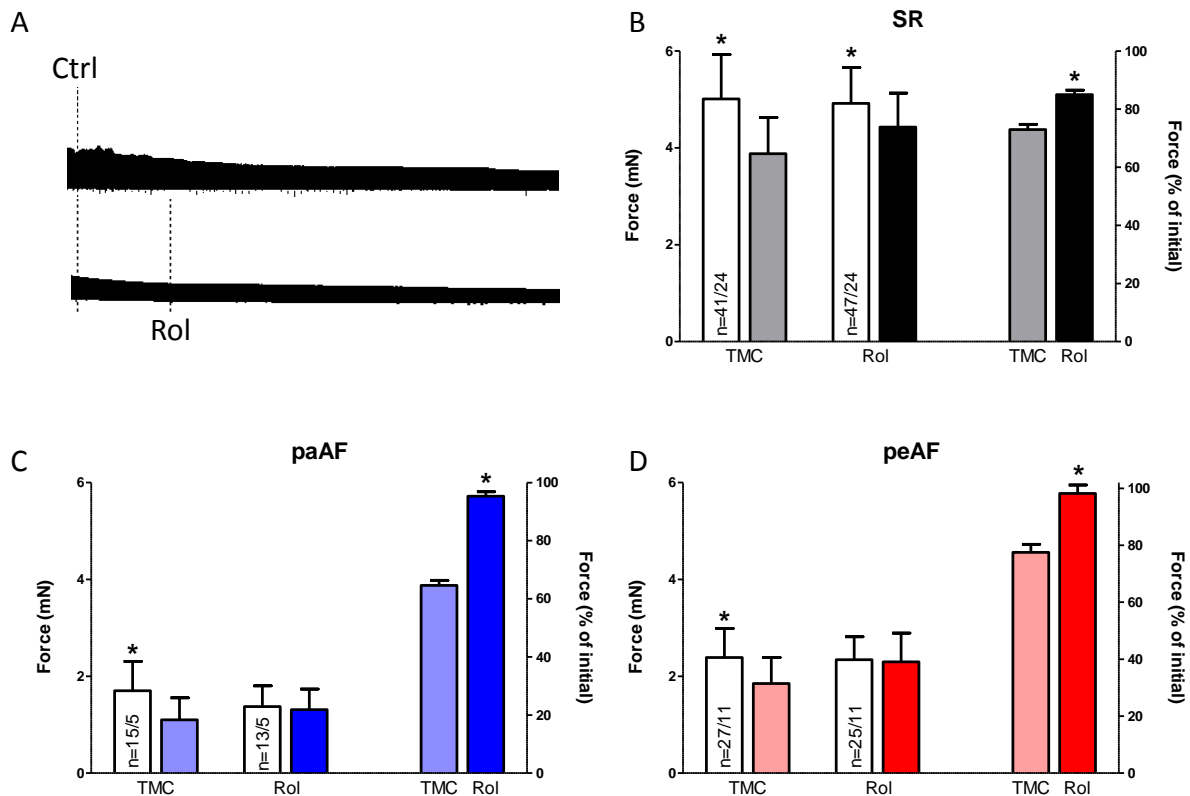
Figure 42: Effects of 10 μM rolipram on basal force of trabeculae from patients with SR, paAF and peAF

A: The panel represents original tracing from two trabeculae of a patient with SR. The up one is in control and the one below in the presence of 10μM rolipram. **B-D**: show summary of results with rolipram 10 μM. The four left-hand bars in each panel are absolute data of force (mM). The initial value of bars 1 and 3 were taken at a time immediately before the administration of the PDEi. The data of bars 2 and 4 were obtained at the end of the incubation with the PDEi. Columns 5 and 6 show the % change of force between TMC (bar 2) and initial (bar 1) and PDEi (bar 4) and initial (bar 3) respectively. n = number of trabeculae/number of patients. *p < 0.05 *vs* TMC or Rol. Data are mean values ± SEM

3.3.2 Effects of 10 μM rolipram on β_1-AR mediated inotropy

Concentrations of NE higher than 10 nM started to increase force of contraction in human atrial trabeculae. Effects were maximal at concentrations higher than 10 μM (Figure 43). The EC_{50} as a measure of sensitivity tended to be smaller in peAF but not in paAF (Figure 43C,D). Again, maximum force in the presence of 100 μM NE tended to be smaller in peAF but not in paAF (Figure 43C, D and Figure 44). Plotting individual data points revealed a large data scatter. More importantly neither the sensitivity to NE (expressed as-$logEC_{50}$) nor maximum force were increased by 10 μM rolipram in SR (Table 10). However, it should be noted that both basal and maximum force was not smaller in peAF than in SR. This is in strong contrast to earlier work (Christ et al., 2014). The reason remains unclear. The unchanged sensitivity for NE argues against a relevant contribution of PDE4 to regulation of catecholamine-evoked inotropy both in SR and AF (Table 10).
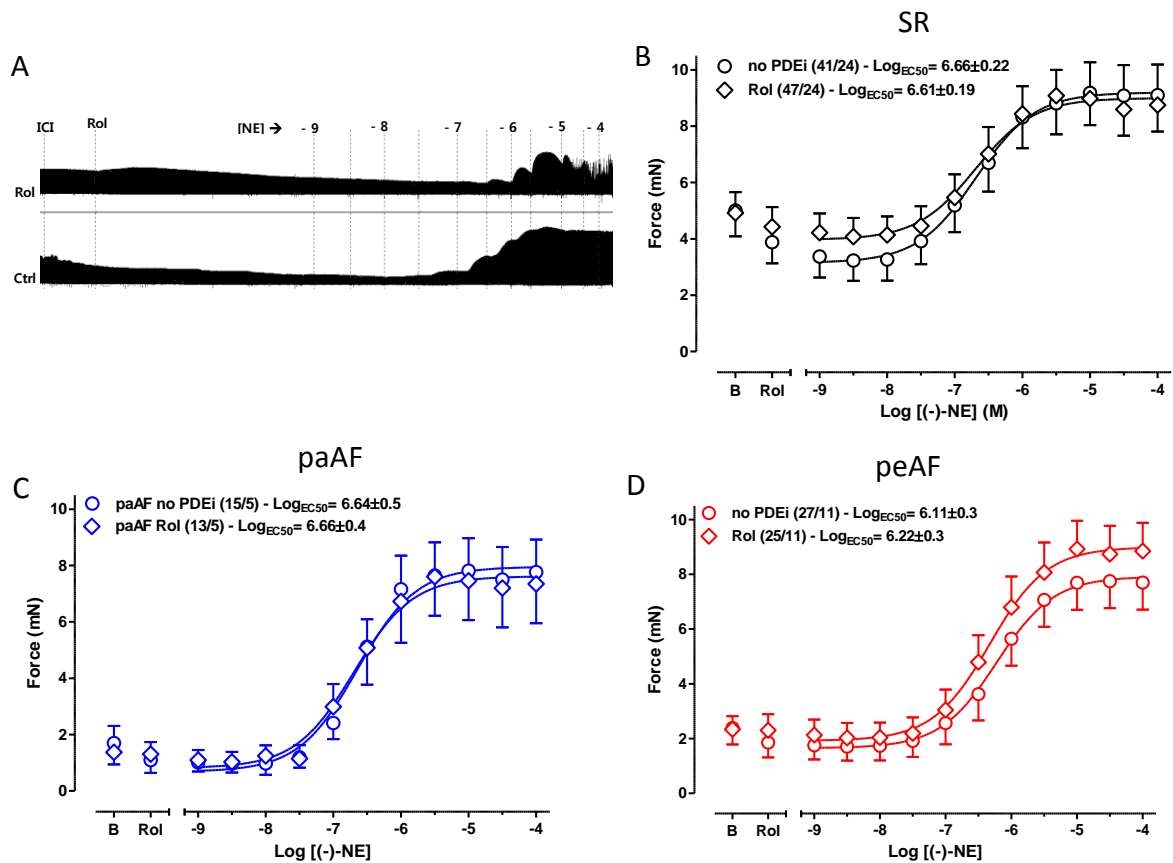
Figure 43: Impact of the inotropic effects of NE by rolipram 10 µM in trabeculae from patients with SR, paAF and peAF

Panel **A** shows a representative experiment of trabeculae initially treated with 50 nM ICI118,551. A trabecula of a patient in SR in the presence of 10 µM rolipram (top tracings) and a trabecula in control condition (bottom tracings) were measured and a concentration-effect curve was determined. Panels shown in **B-D** represent cumulative concentration-effect curve of NE in the absence and presence of rolipram 10 µM, obtained from paired trabeculae from patients in SR, paAF and peAF. Mean values of –LogEC$_{50}$ ± SEM in the absence and presence of the PDEi were referring to patients and were compared with paired t-tests. n = number of trabeculae/number of patients.
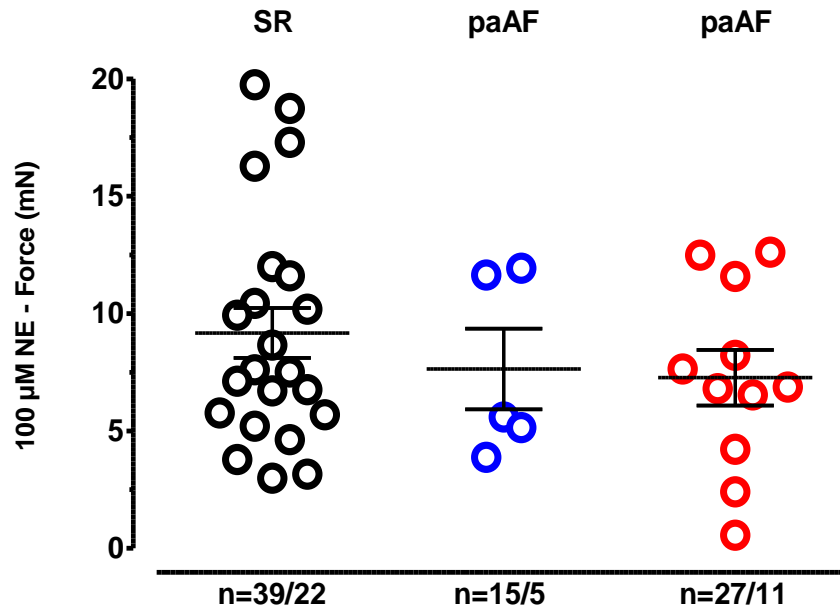
Fig. 44: Maximum force in the presence of 100 µM NE in SR, paAF and peAF

Force values in the presence of 100 µM NE (every data point represents mean values calculated for an individual patient) and mean values ± SEM for SR, paAF and peAF. n = number of trabeculae/number of patients. There was no significant difference among the three groups. One-way ANOVA followed by Kruskal-Wallis test.

Table 10: NE induced contractile potencies (-log EC 50 M) and maximum response force

	Control		10 µM rolipram	
	EC_{50}	Max_{force}	EC_{50}	Max_{force}
SR	6.66 ± 0.2 (41/24)	9.10 mN (41/24)	6.61 ± 0.2 (47/24)	8.90 mN (47/24)
paAF	6.64 ± 0.5 (15/5)	7.70 mN (15/5)	6.66 ± 0.5 (13/5)	7.40 mN (13/5)
peAF	6.11 ± 0.3 (27/11)	7.65 mN (27/11)	6.22 ± 0.3 (25/11)	9.00 mN (25/11)

n/N indicates number of trabeculae/number of patients

3.3.3 Effects of 10 µM rolipram on β_1-AR mediated arrhythmia

Stimulation of β-AR is able to induce arrhythmias in isolated human atrial trabeculae. We studied whether inhibition of PDE4 would increase arrhythmias while sensitivity to NE to increase force was unchanged. For that purpose, we reanalyzed all the experiments we did with NE and 10 µM rolipram. Inotropic and arrhythmic actions of NE behaved differently. While every trabecula responded to NE with an increase in force, only some of them developed arrhythmias. Arrhythmias always started at a concentration giving already inotropic actions. Uncoordinated contractions during arrhythmias decreased force drastically. If arrhythmias started at low concentration of NE, construction of complete concentration-response curve for NE inotropy was impossible. Importantly, NE-induced arrhythmias in

the absence of rolipram were rare in trabeculae from patients in peAF but also paAF (Figure 45A-D). Inhibition of PDE4 by 10 µM rolipram alone did not increase arrhythmias in the absence of NE neither in SR, nor in peAF and paAF, but potentiated NE-induced arrhythmias in SR and paAF (Figure 45B,C). In the presence of rolipram, the incidence of NE-induced arrhythmias in paAF was not different from SR. In contrast, we never saw NE-induced arrhythmias in peAF, neither in the absence or presence of 10 µM rolipram (Figure 45D) (Table 11).
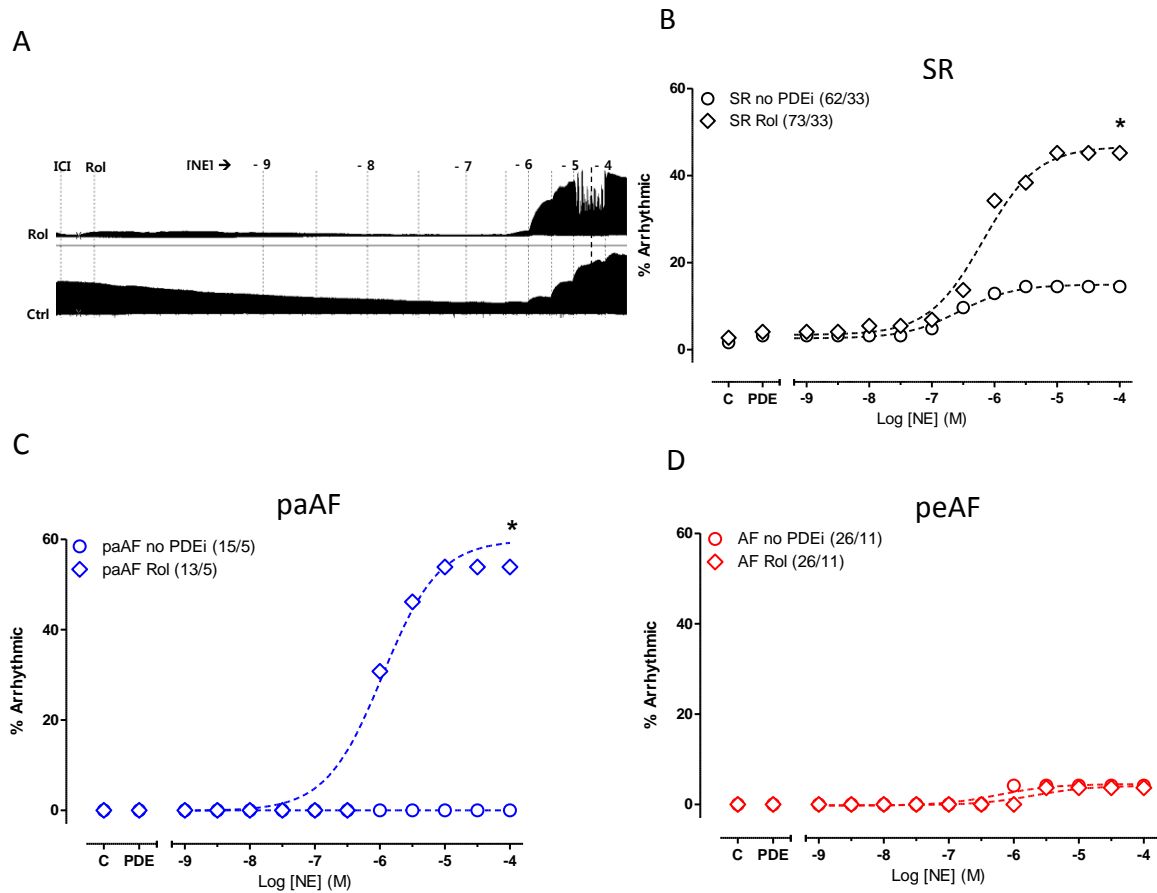
Figure 45: Impact of NE-mediated arrhythmias by 10 µM rolipram in trabeculae from patients with SR, paAF and peAF

Panel **A** shows a representative experiment of trabeculae initially treated with 50 nM ICI118,551. A trabecula of a patient in SR in the presence of 10 µM rolipram (top tracings) and a trabecula in control condition (bottom tracings) were measured and number of episodes of arrhythmias were determined. Top tracings show episodes of arrhythmias at high concentration of catecholamine. The influence of rolipram 10 µM on the incidence of arrhythmias evoked by 100 µM NE is shown in panels **B-D**. Data are mean ± SEM from the number of patients. N = number of trabeculae/number of patients. *p<0.05 *vs* control of each group (Paired t-tests).

Table 11: NE induced increase in incidence of arrhythmias in %

	Control	**10 μM rolipram**
SR	14 % (62/33)	45 % (73/33)
paAF	0 % (15/5)	54 % (13/5)
peAF	4 % (26/11)	4 % (26/11)

n/N indicates number of trabeculae/number of patients

3.3.4 Effects of 0.1 μM rolipram on β₁-AR mediated arrhythmia in SR

In order to confirm results of Molina et al. (2012) we decided to perform experiments on trabeculae isolated from patients in SR and stimulate them with increasing concentration of NE (from 1 nM up to 100 μM) in the presence of 50 nM ICI118,551. The experiments were performed in controls and in the presence of 0.1 μM rolipram. Despite not reaching statistical significance, a tendency was noted towards a larger increase in percentage of arrhythmias in the presence of rolipram than in trabeculae non treated (Figure 46).

Figure 46: Impact of NE-mediated arrhythmias by 0.1 μM rolipram in trabeculae from patients with SR

Influence of rolipram (0.1 μM) on the incidence of arrhythmias evoked by increasing concentration of NE (from 1 nM up to 100 μM) in the presence of 50 nM ICI118,551. Data are mean ± SEM from the number of patients. n = number of trabeculae/number of patients. *p<0.05 *vs* control of each group (Paired t-tests).

3.3.5 Effects of 10 µM rolipram on β_2-AR mediated inotropy

We could not get enough samples from patients in paAF to replicate experiments with Epi. Therefore, we focused on experiments with Epi on SR and peAF. As for NE, concentrations of Epi higher than 10 nM started to increase force of contraction in all human atrial trabeculae. Effects of Epi were already at the top of the curve around the concentration of 10 µM (Figure 47). Maximum force in the presence of 100 µM Epi tended to be smaller in peAF than in SR (Figure 47B, C and Figure 48). The EC_{50} as a measure of sensitivity was equal between peAF and SR (Figure 47B, C). Plotting individual data points revealed a large data scatter. More importantly, 10 µM rolipram did not increase the sensitivity to Epi or its maximal effect on force, neither in SR nor in peAF (Table 12).
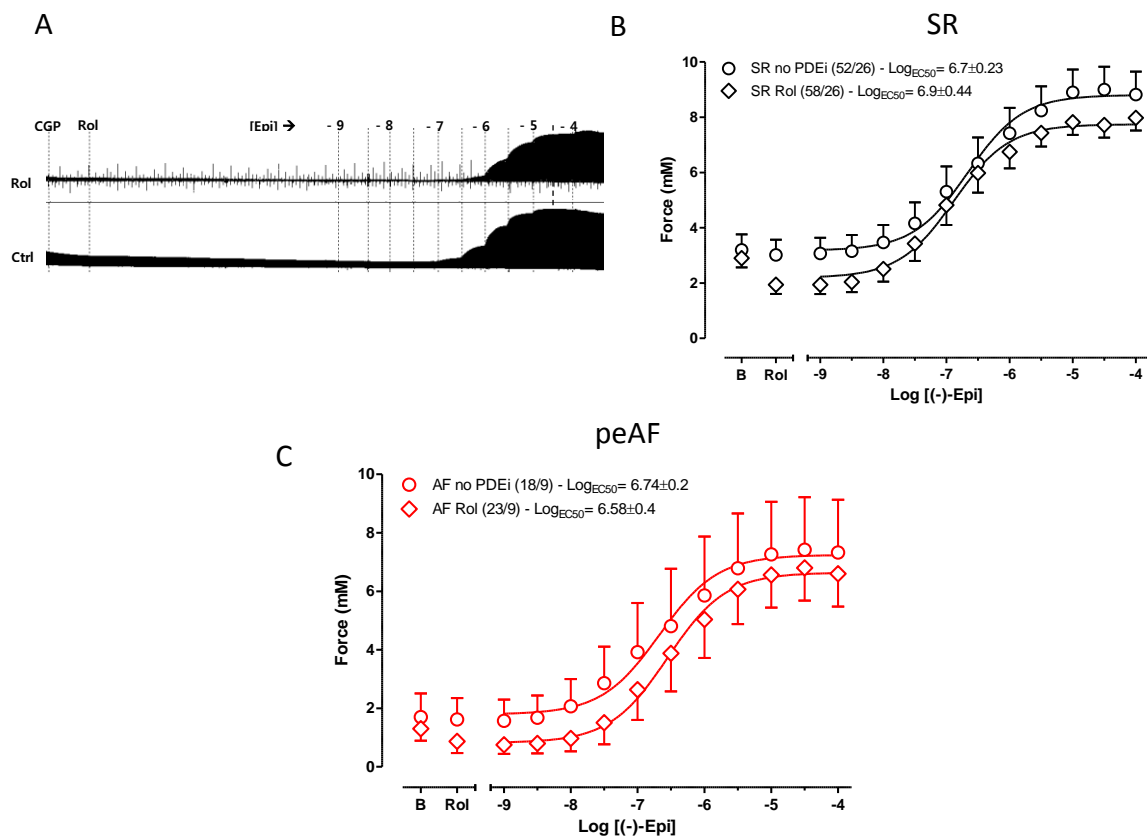
Figure 47: Impact of the inotropic effects of Epi by rolipram 10 µM in trabeculae from patients with SR and peAF

Panel **A** shows a representative recording of trabeculae initially treated with 300 nM CGP20712A. A trabecula of a patient in SR in the presence of 10 µM rolipram (top tracings) and a trabecula in control condition (bottom tracings) were measured and a concentration-effect curve was determined. Panels shown in **B**-**C** represent cumulative concentration-effect curve of Epi in the absence and presence of rolipram 10 µM, obtained from paired trabeculae from patients in SR and peAF. Mean values of −LogEC$_{50}$ data ± SEM in the absence and presence of the PDEi were referring to patients and were compared with paired t-tests. n = number of trabeculae/number of patients.
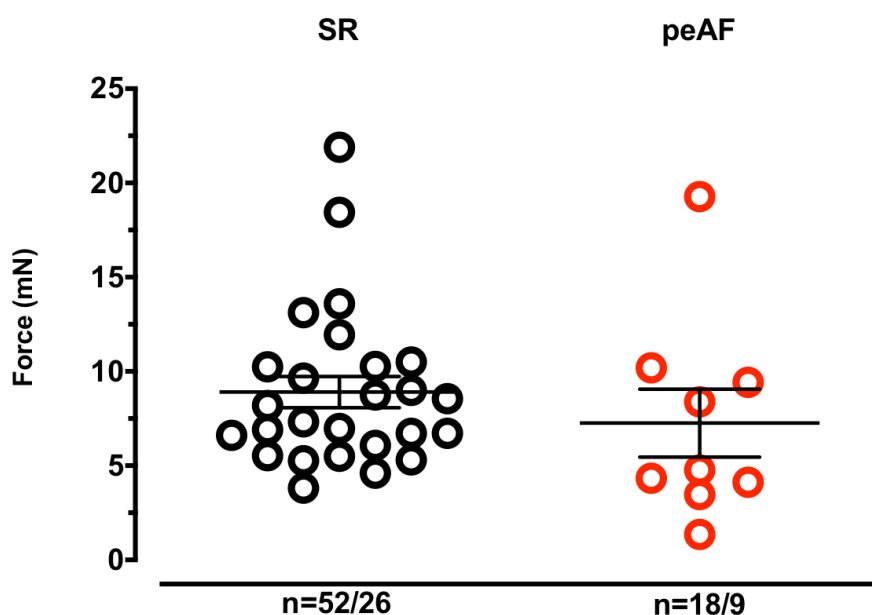
Figure 48: Maximum force in the presence of 100 µM Epi in SR, paAF and peAF

Force values in the presence of 100 µM Epi (every data point represents mean values calculated for an individual patient) and mean values ± SEM for SR and peAF. n = number of trabeculae/number of patients. No significant difference was detected between the two groups. One-way ANOVA followed by Kruskal-Wallis test.

Table 12: Epi-induced contractile potencies (-log EC 50 M) and maximum response force

	Control		10 µM rolipram	
	EC_{50}	Max_{force}	EC_{50}	Max_{force}
SR	6.70 ± 0.2 (52/26)	8.82 mN (52/26)	6.90 ± 0.4 (52/28)	7.98 mN (52/28)
peAF	6.74 ± 0.2 (18/9)	7.33 mN (18/9)	6.58 ± 0.4 (23/9)	6.60 mN (23/9)

n/N indicates number of trabeculae/number of patients

3.3.6 Effects of 10 µM rolipram on β_2-AR mediated arrhythmia

Also for β_2-AR, we investigated whether inhibition of PDE4 would affect arrhythmias, taking in account that sensitivity to Epi did not show significant change. For that purpose, we used the same data from the experiments we did with Epi and 10 µM rolipram to measure the incidence of arrhythmias. Once again, as for NE, inotropic and arrhythmic actions of Epi behaved differently. While every trabecula responded to Epi with an increase in force only some of them developed arrhythmias. Importantly, Epi-induced arrhythmias in the absence of rolipram were absent in trabeculae from patients in peAF (Figure 49). Inhibition of PDE4 by 10 µM rolipram alone did not increase arrhythmias in the absence of Epi, neither in SR nor in peAF, but it potentiated Epi-induced arrhythmias in SR (Figure 49B). Also in peAF we saw an Epi-induced increase in the incidence of arrhythmias, but the extent was less than 1/3 of the arrhythmias obtained in trabeculae coming from patients in SR (Figure 49B, C; Table 13).
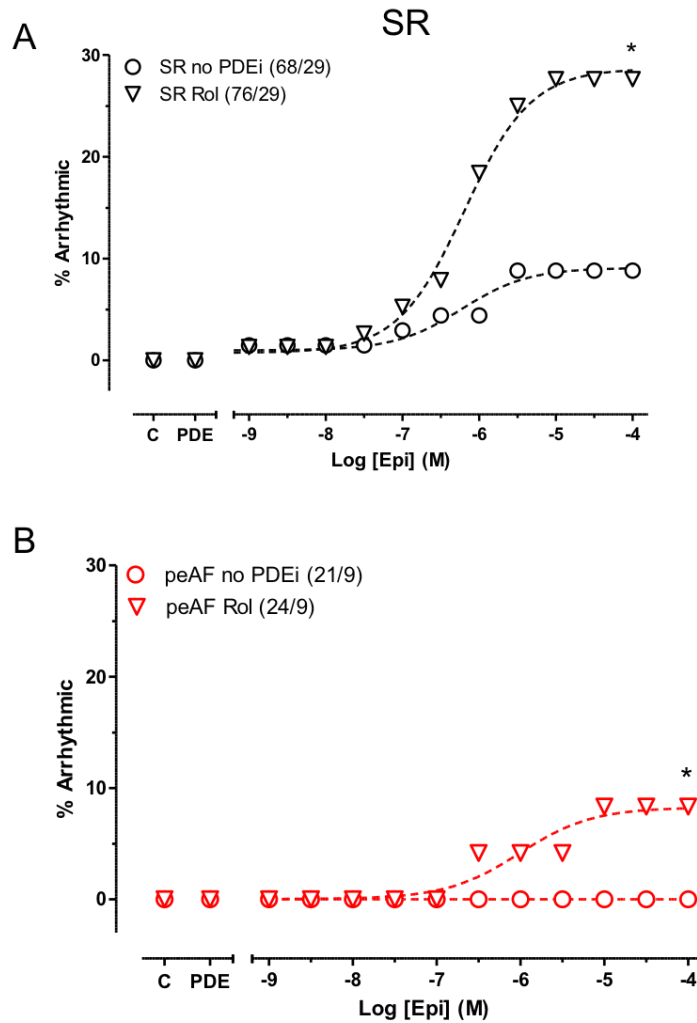
Figure 49: Impact of Epi-mediated arrhythmias by rolipram 10 µM in trabeculae from patients with SR and peAF

Every experiment was initially treated with 300 nM CGP20712A. A trabecula of a patient in SR in the presence of 10 µM rolipram and a trabecula in control condition were measured and number of episodes of arrhythmias were determined. The influence of rolipram 10 µM on the incidence of arrhythmias evoked by 100 µM Epi is shown in panels **A** and **B**. Data are mean ± SEM from the number of patients. n = number of trabeculae/number of patients. *p<0.05 *vs* control of each group (Paired t-tests).

Table 13: Epi induced increase in incidence of arrhythmias in %

	Control	**10 µM rolipram**
SR	9 % (68/29)	28 % (76/29)
peAF	0 % (21/9)	8 % (24/9)

3.3.7 Effects of 0.1 µM rolipram on β₂-AR mediated arrhythmia in SR

Here we reported experiments on trabeculae isolated from patients in SR and stimulate them with increasing concentration of Epi (from 1 nM up to 100 µM) in the presence of 300 nM CGP20712A. The

experiments were performed in the absence and presence of 0.1 μM rolipram, in order to confirm Molina et al. (2012) results. Once again, we could see a tendency to a larger increase in percentage of arrhythmias in the presence of rolipram (Figure 50).
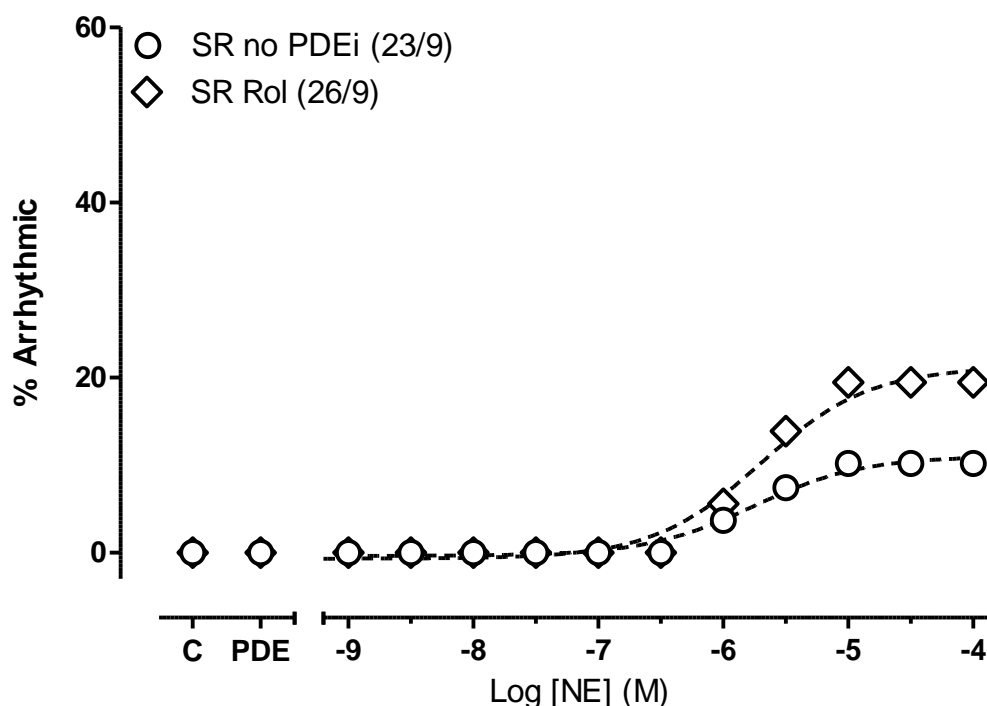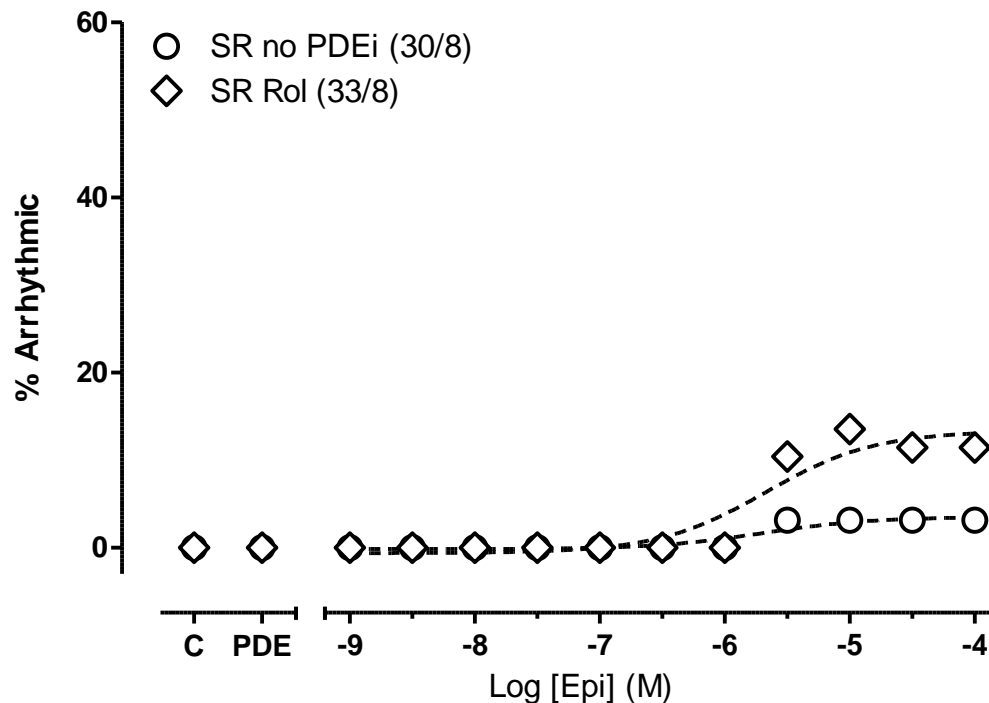

Figure 50: Impact of Epi-mediated arrhythmias by rolipram 0.1 μM in trabeculae from patients with SR

Influence of 0.1 μM rolipram on the incidence of arrhythmias evoked by increasing concentration of Epi (from 1 nM up to 100 μM) in the presence of 300 nM CGP20712A. Data are mean ± SEM from the number of patients. n = number of trabeculae/number of patients. *$p<0.05$ *vs* control of each group (Paired t-tests).

3.4 Effect of combined inhibition of PDE3 and PDE4 on cAMP

In human atrial cardiomyocytes from patients in SR PDE3 and PDE4 regulate basal as well as β-AR stimulation-induced cAMP. Enzymatic activity of PDE tended to be smaller in AF (Molina et al., 2012). However, effects of PDE on cAMP in AF are not known. From a reduced hydrolytic activity of PDE in AF we would expect more arrhythmias in AF. However, arrhythmias induced by catecholamines and 5-HT are markedly reduced in AF (Christ et al., 2014). We therefore investigated whether hydrolysis of cAMP by PDE3 and PDE4 is changed in AF. First we aimed to investigate effects of inhibition of PED3 and PDE4 on basal unstimulated cAMP.

Therefore, at this point of the project we wanted to investigate whether the data obtained measuring force and incidence of arrhythmias were a product of changes in cAMP regulation. Furthermore, we decided to study cAMP behave in 5-HT pathway as well, since previous studies showed a reduced inotropic effect upon 5-HT stimulation in trabeculae from patients in peAF (Berk et al., 2016). Hence it

was our interest, to investigate whether the reduced inotropic response in peAF was due to variations in cAMP concentration.

3.4.1 Day to day variability of cAMP measurements

Before we illustrate the results about PDE3 and PDE4 effect on GPCR-cAMP evoked (G-protein coupled receptor-cAMP evoked), we dedicate two sub-chapter on stability of the isolation protocol and FRET system on our experimental data.

Infection of HAM was recently established in Hamburg. In order to investigate whether a "learning curve" has affected data scattering we plotted results for cAMP increase as a function of time (experimental days). We choose FSK effects as an internal control. Despite we witnessed a large data scattering, we did not see a correlation between our experimental FSK data and a possible learning curve over time (days) (Figure 51).
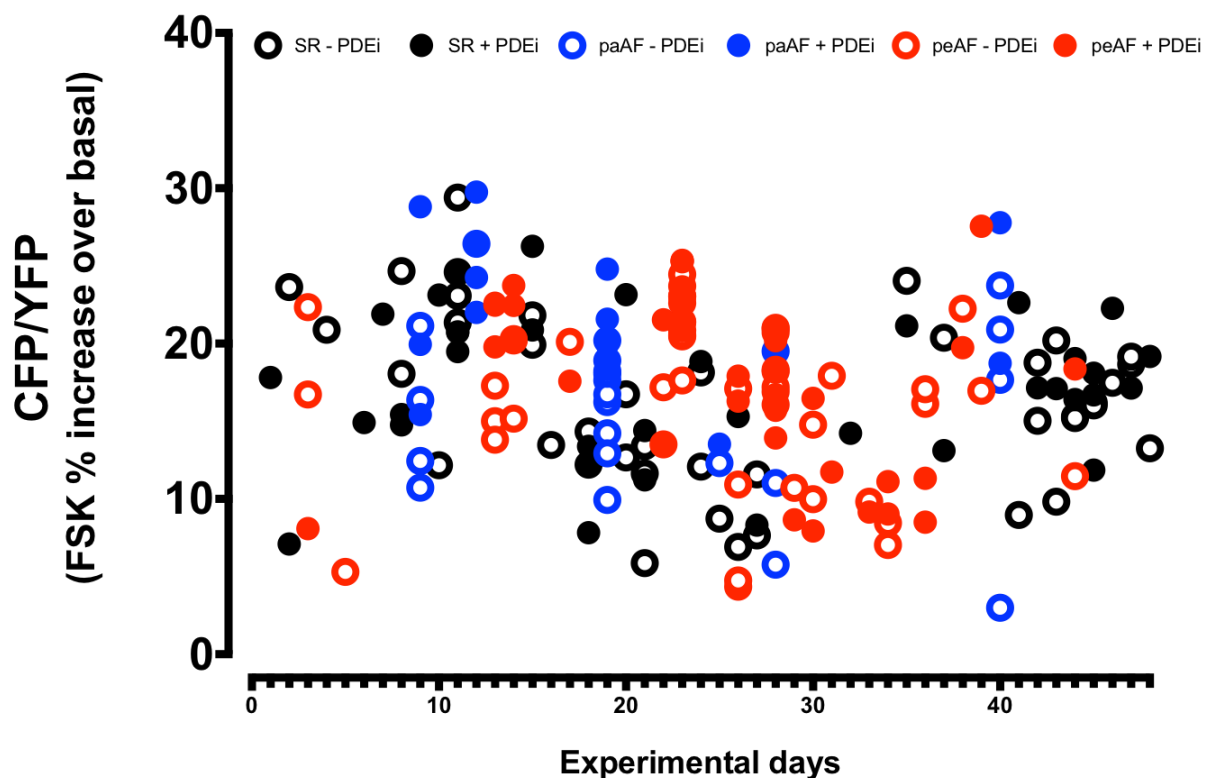
Figure 51: Variation of FSK responses over days of isolation
Data for cAMP increase by 10 µM FSK of 208 myocytes are shown in the presence and in the absence of PDE3 inhibitor cilostamide 300 nM together with PDE4 inhibitor rolipram 1 µM in cells previously exposed to 5-HT, NE and Epi. Data for SR are given in (black), paAF (blue) and peAF (red). Every circle represents one cell. Empty circles are cells in the absence of PDEi while filled ones in the presence of PDEi.

3.4.2 FSK as an internal control

Same increase in cAMP by a specific intervention (stimulation of GPCR or inhibition of PDE) does not necessarily means same contribution to cAMP regulation. Maximum ranges of cAMP dynamics in

patient population (SR, paAF and peAF) need to be known. For this purpose, we employed FSK as a direct activator of adenylyl cyclase to evoke maximum increases in cAMP. There is evidence that FSK does not lose is property to interact with adenylyl cyclase even in diseased cells, since in trabeculae from both SR and peAF patients 10 µM FSK was always able to increase force at high levels (Christ et al., 2014).

Therefore, we have investigated whether FSK can be used as an internal control for maximum cAMP accumulation. For this purpose, every experiment was finished by exposing cells to FSK (10µM). With few exceptions, cells showed a further increase with FSK on top of the different agonists, even when pretreated with cilostamide and rolipram (Figure 52). In addition, cAMP in the presence of FSK was independent of the presence of agonists or PDE inhibitors (Figure 52). More importantly, values for cAMP in the presence of FSK did not differ statistically between SR and paAF and peAF, implicating that the ability to generate maximum cAMP levels is unchanged in peAF (Figure 52).
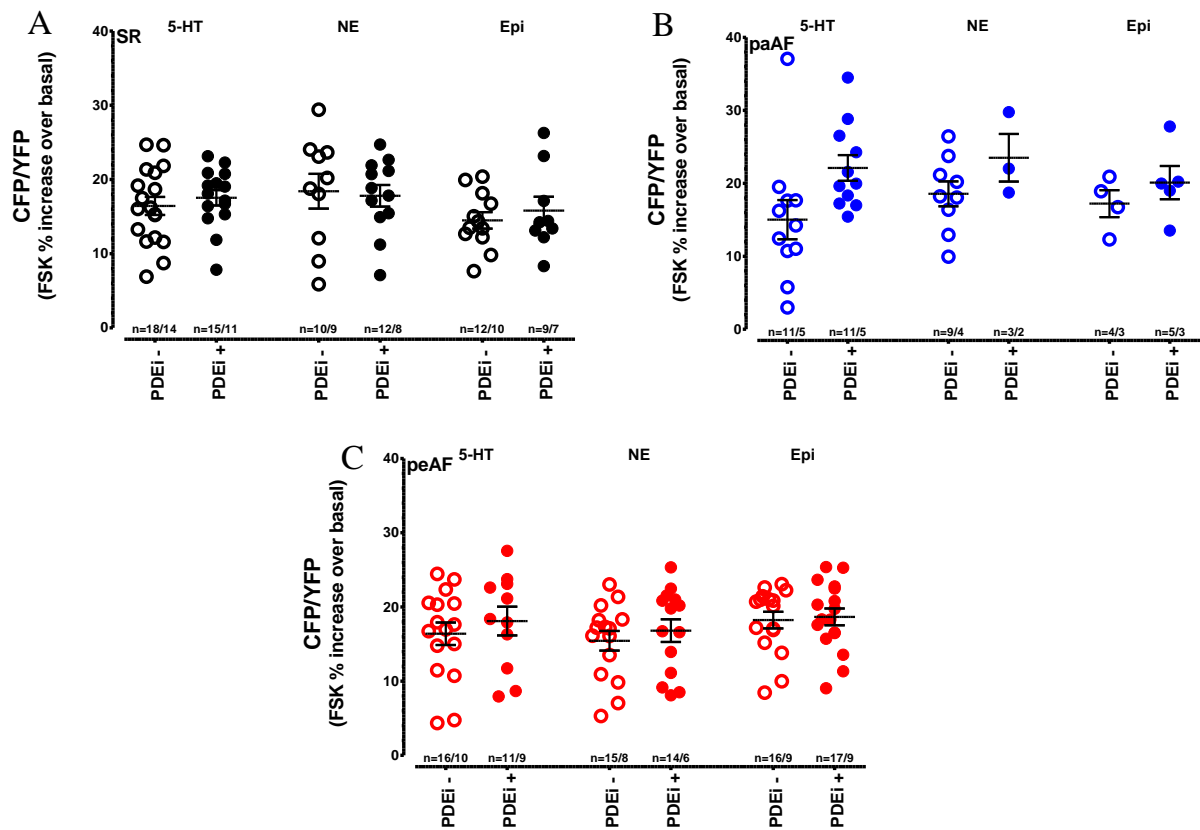
Figure 52: Analysis of FSK responses after application of 5-HT, NE and Epi
The data are shown in the presence and in the absence of PDE3 inhibitor cilostamide (300 nM) together with PDE4 inhibitor rolipram (1 µM) in cells isolated from patients in SR **(A)**, paAF **(B)** and peAF **(C)**. Every circle represents one patient. Empty circles are cells in the absence of PDEi while filled ones in the presence of PDEi. Mean values are calculated per each pathway (5-HT, NE and Epi) and every group (PDEi -; PDEi +). n = number of myocytes/number of patients. The values were not significantly different among groups (one-way ANOVA; followed by Kruskal-Wallis test, based on myocytes).

3.4.3 PDE3 and PDE4 had same impact on basal cAMP in SR, peAF and paAF

As reported before, PDE3 and PDE4 are major regulators of cAMP in HAM (Molina et al., 2012). The application of the PDE4 inhibitor ro 20-1724 10 µM produced a small (~3%) but significant increase in global cAMP, while cilostamide 1 µM, which is the inhibitor of PDE3, increased cAMP 100% more than ro 20-1724 (~6%). The application of the two inhibitors together increased cAMP even further. No data are available for AF (peAF and paAF) (Molina et al. 2012). From the same study no expression data are available, but biochemical data showed a trend to lesser total PDE activity and PDE4 activity in peAF. From our expression data we would expect unchanged activity of PDE3A and PDE4D while expression of PDE4B was increased. However, functional relevance of changes in expression and on global PDE activity are unclear. Therefore, we wanted to investigate, whether contribution of the major players (PDE3 and PDE4) to basal cAMP is different in AF.

For that purpose, we exposed HAMs to both cilostamide (0.3 µM) and rolipram (1 µM) together. Typical time courses of the FRET signals in response to concomitant exposure by rolipram and cilostamide are shown in Figure 53A-C. The signal started to increase just after application of the PDE-inhibitors. Stable steady state was reached within 2 minutes. Each cell responded with an increase in cAMP, but there was a huge variability. The two inhibitors increased cAMP levels by 7 %, 9% and 7.5%, respectively in cells isolated from patients with SR, paAF and peAF (Figure 53D). These results suggested an equal ability of rolipram and cilostamide together to regulate global cAMP among the three groups (SR, paAF and peAF).
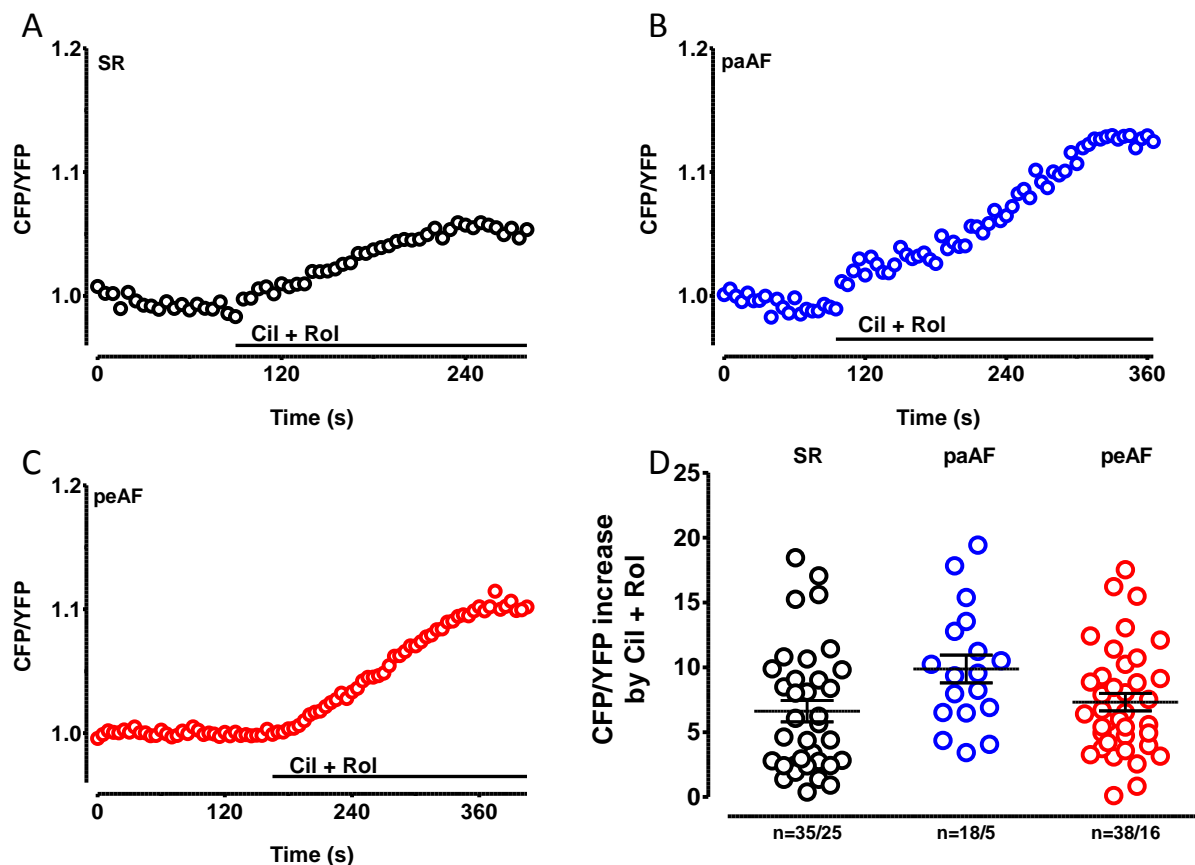
Figure 53: Effects of concomitant inhibition of PDE3 and PDE4 on cAMP in HAM

Time course of the FRET signal indicating change in global cAMP in 3 HAMs from patients with SR (**A**), paAF (**B**) and peAF (**C**) co-exposed to 1 µM rolipram and 300 nM cilostamide. **D**. Depicted are FRET responses to 1 µM rolipram and 300 nM cilostamide in individual myocytes. Each circle represents a single cell, while mean values ± SEM represented with lines, are patients based n = number of myocytes/number of patients. The values were not significantly different between groups (one-way ANOVA; followed by Kruskal-Wallis test, based on myocytes).

3.4.4 Effects of NE on cAMP and their regulation by PDE3 and PDE4 were not changed in peAF and paAF

Equal contribution of PDE3 and PDE4 to regulation of basal cAMP does not exclude the possibility of a different regulation of cAMP among different receptor pathways, such as serotonin receptor or β_1- and β_2-AR.

Myocytes were exposed to only one high concentration (100 µM) of NE (Figure 54) to get maximum β_1-AR stimulation. At the end of each experiment 10 µM FSK was added in the presence of NE to measure maximum cAMP generation. Typical time courses of the FRET signals are shown in figures 54A-C. NE (100 µM) increased cytosolic cAMP levels and FSK (10 µM) increased cAMP further in SR, paAF and peAF (figure 54D). The effects of NE on cAMP were not different among the three groups, demonstrating intact ability of β_1-AR to evoke cAMP even in diseased myocytes from patients with paAF and peAF.
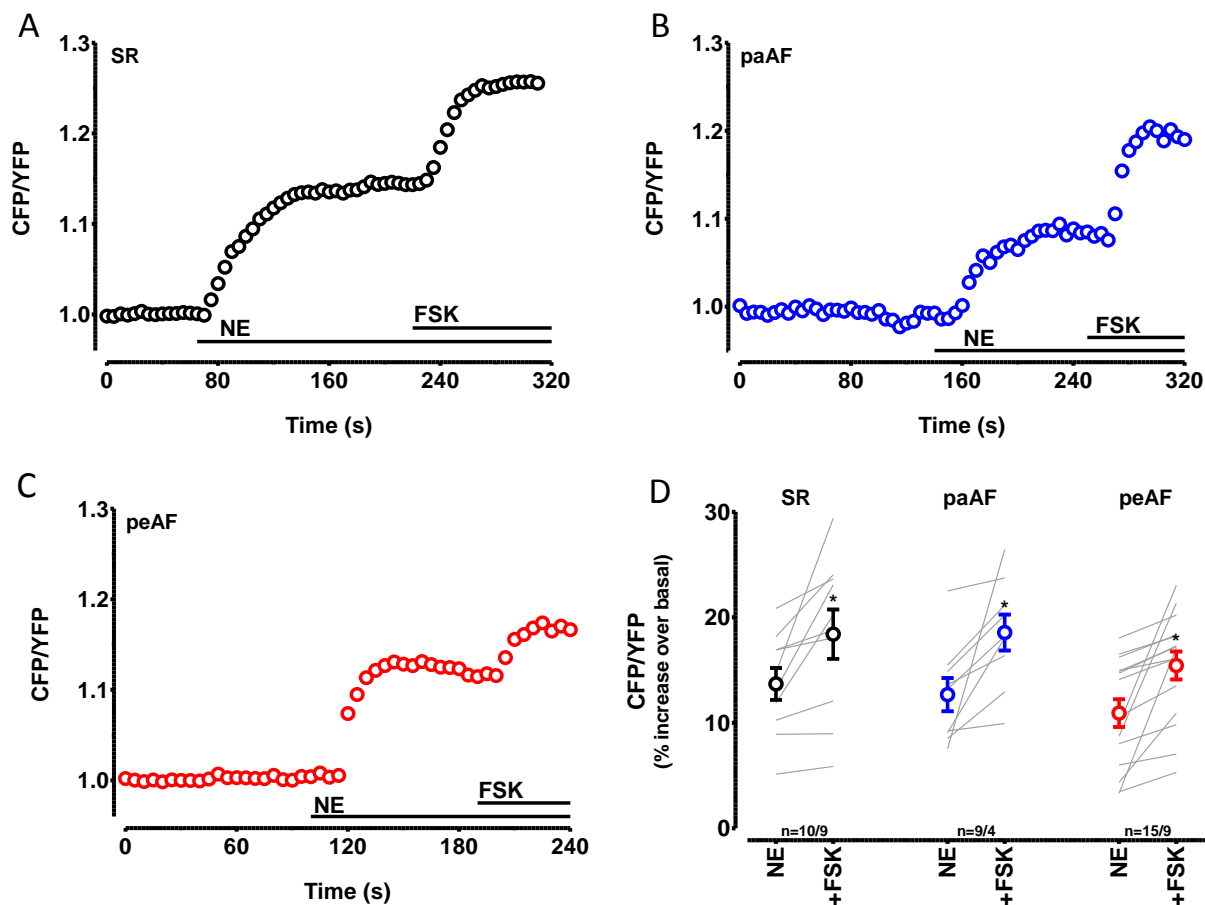
Figure 54: Effects of NE and FSK in the presence of NE on cAMP in HAM
Representative time course of the FRET signal indicating change in global cAMP in 3 HAMs from patients with SR **(A)**, paAF **(B)** and peAF **(C)** exposed to 100 µM NE and in the continuous presence of NE to 10 µM forskolin (FSK). All experiments were performed in the presence of ICI118,551, which is a blocker of β_2-AR. Each line connects data for responses calculated from the myocyte of an individual patient. Summary of the results in panel **D**. Depicted are FRET responses to both NE and FSK in the presence of NE (+FSK) in individual myocytes. Mean values ± SEM are indicated by the circles. n = number of myocytes/number of patients. *p < 0.05 FSK *vs.* NE (paired t-test). Values for NE and FSK were not significantly different between groups (one-way ANOVA; followed by Kruskal-Wallis test, based on myocytes).

Subsequently, we measured cAMP increases by NE in the concomitant presence of cilostamide (Cil, 300 nM) and rolipram (Rol, 1 µM) in HAM from the three groups of patients. Typical time courses are shown in figures 55A-C. As can be appreciated from the dot plots graph, rolipram and cilostamide increased cAMP and NE increased the signal further (Figure 55D). In SR the increase by NE alone was not larger than in the presence of cilostamide and rolipram (Figure 56). However, in peAF there were significant higher cAMP levels in the presence of cilostamide and rolipram and NE than with NE alone (data normalized to FSK, Figure 56). A tendency to a bigger participation of PDE3 and PDE4 could be observed also in myocytes coming from patients in paAF (Figure 56).

Figure 55: Effects of concomitant inhibition of PDE3 and PDE4, NE and FSK on cAMP in HAM
Representative time course of the FRET signal indicating change in global cAMP in 3 HAMs from patients in SR **(A)**, paAF **(B)** and in peAF **(C)** exposed to 300 nM cilostamide and 1 µM rolipram (Cil + Rol). All the experiments were performed in the presence of ICI118.551. Each line connects data for responses calculated from cells of an individual patient. Summary of the results in the panel **D**. Depicted are FRET responses to Cil + Rol, to 100 µM NE and to 10 µM FSK in the presence of Cil + Rol and 100 µM NE (+FSK) in individual myocytes. Mean values ± SEM are indicated by the circles. n = number of myocytes/number of patients. *p < 0.05 NE *vs.* the corresponding values for Cil + Rol alone and FSK *vs.* the corresponding values for Cil + Rol alone. (one-way ANOVA followed by Kruskal-Wallis test; myocytes based). ANOVA test failed in paAF, because of low cell number. # indicates paired t-test for +NE vs. C+R and +FSK vs. C+R in paAF.

Figure 56: Effects of NE in the presence and in the absence of PDE3 and PDE4 inhibitors on cAMP in HAM

Analysis of NE responses expressed as % of FSK-effect in the absence and in the presence of PDE inhibitors (0.3 µM cilostamide and 1 µM rolipram, -PDEi, +PDEi), indicating single values cells based and mean values ± SEM patients based. n = number of myocytes/number of patients. [#]$p < 0.05$ *vs.* respective values for -PDEi (one-way ANOVA followed by Kruskal-Wallis test; patients based).

3.4.5 Effects of Epi on cAMP and their regulation by PDE3 and PDE4 were not changed in peAF and paAF

From our epinephrine data, the increase of incidence of arrhythmias after application of the PDE-inhibitors was 3 fold higher in SR than in peAF (Figure 49). We decided to investigate whether the lower increase in arrhythmias after application of PDEs inhibitors was due to cAMP dysregulation in diseased cells.

As for NE, myocytes were first exposed to high concentration (100 µM) of Epi alone (Figure 57) to get maximum β_2-AR stimulation. At the end of each experiment 10 µM FSK was added in the presence of Epi to evoke maximum cAMP generation. Typical time courses of the FRET signals are shown in Figure 56A-C. 100 µM Epi increased cytosolic cAMP levels and FSK (10 µM) was able to enhance cAMP levels even further in SR, paAF and peAF (figure 57D). The effects of NE on cAMP were not different among the three groups, demonstrating intact ability of β_2-AR to evoke cAMP even in diseased myocytes from patients with paAF and peAF.

Afterwards, we measured cAMP levels under the co-exposure of cilostamide (Cil, 300 nM) and rolipram (Rol, 1 µM) in HAMs from the three groups of patients. Typical time courses are shown in figures 57A-C. As can be appreciated from the dot plots graph, rolipram and cilostamide increased cAMP and Epi increased the signal further (Figure 58D). The increase by Epi alone was not larger than in the presence of cilostamide and rolipram in SR, peAF and paAF (Figure 59). A tendency to a greater impact of PDE3 and PDE4 could be observed in myocytes isolated from patients in paAF (Figure 59).

Figure 57: Effects of Epi and FSK in the presence of Epi on cAMP in HAM
Time course of the FRET signal indicating change in global cAMP in 3 HAMs from patients with SR (**A**), paAF (**B**) and peAF (**C**) exposed to 100 µM Epi and in the continuous presence of Epi to 10 µM forskolin (FSK). All experiments were performed in the presence of CGP20712A, which is a blocker of β_1-adrenergic receptor. Each line connects data for responses calculated from the myocyte of an individual patient. Summary of the results in panel **D**. Depicted are FRET responses to Epi (+Epi) both Epi and forskolin in the presence of Epi (+FSK) in individual myocytes. Mean values ± SEM are indicated by the circles. n = number of myocytes/number of patients. *$p < 0.05$ FSK *vs.* Epi (paired t-test). Values for Epi and FSK were not significantly different between groups (one-way ANOVA; followed by Kruskal-Wallis test, based on myocytes).
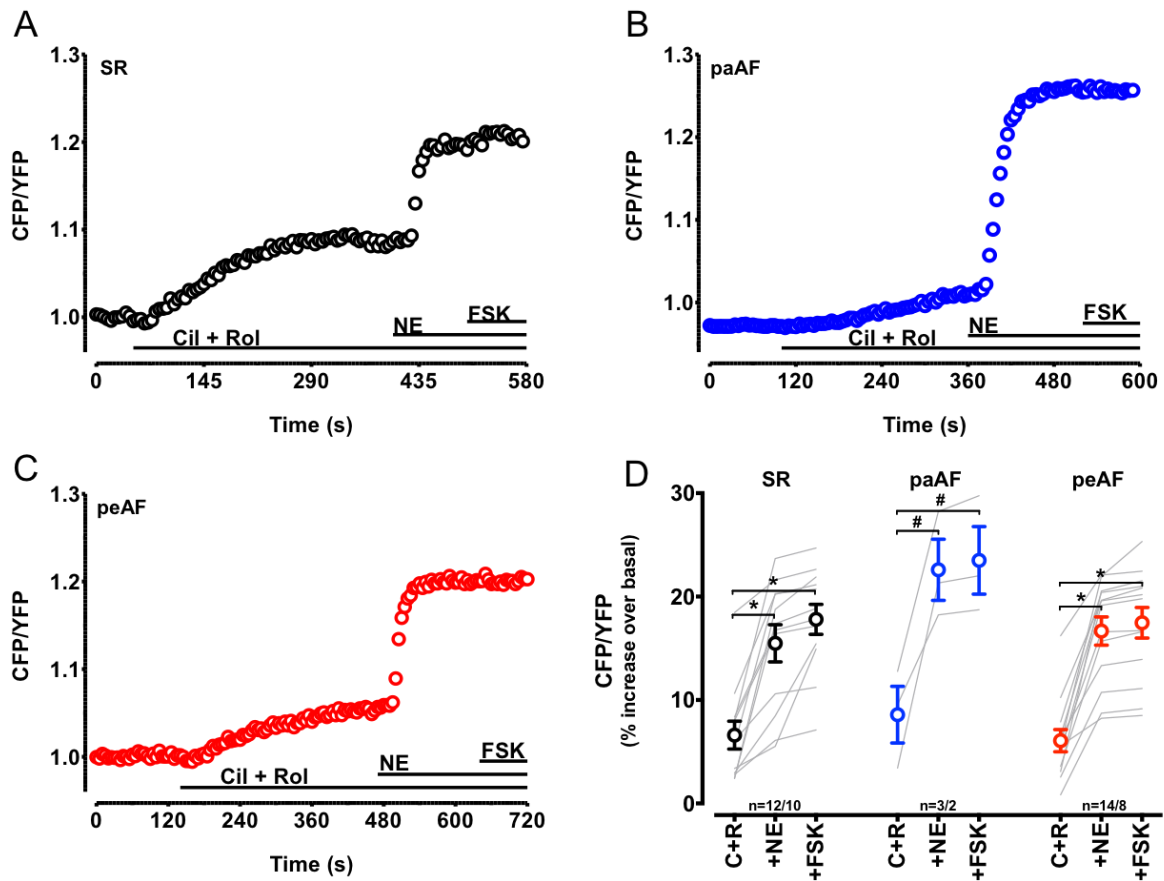
Figure 58: Effects of concomitant inhibition of PDE3 and PDE4, on Epi and FSK induced cAMP in HAM

Time course of the FRET signal indicating change in global cAMP in 3 HAMs from patients in SR (**A**), paAF (**B**) and in peAF (**C**) exposed to 300 nM cilostamide and 1 µM rolipram (Cil + Rol). All the experiments were performed in the presence of CGP20712A. Each line connects data for responses calculated from cells of an individual patient. Summary of the results in the panel **D**. Depicted are FRET responses to Cil + Rol, to 100 µM Epi (+Epi) and to 10 µM forskolin in the presence of Cil + Rol and 100 µM Epi (+FSK) in individual myocytes. Mean values ± SEM are indicated by the circles. n = number of myocytes/number of patients. *p < 0.05 Epi vs. the corresponding values for Cil + Rol alone. Each value was not significantly different between groups (one-way ANOVA followed by Kruskal-Wallis test; myocytes based).
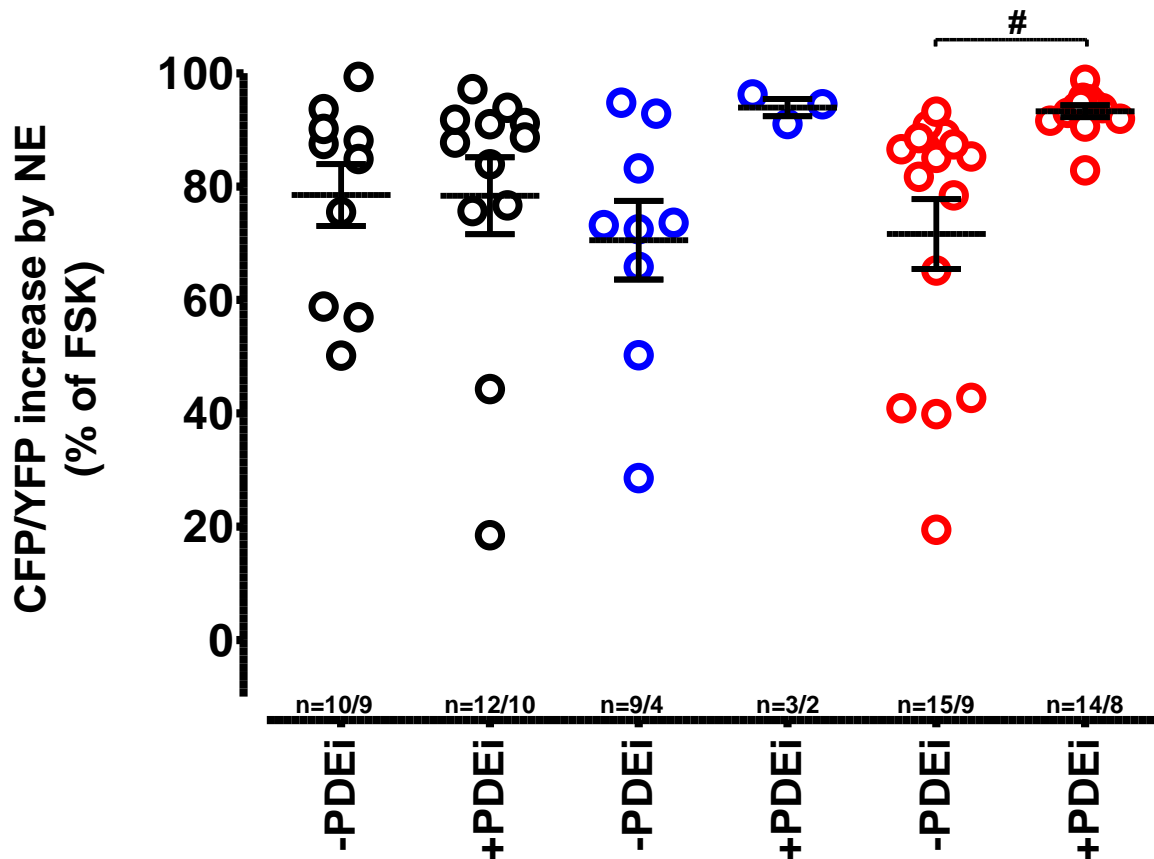
Figure 59: Effects of Epi in the presence and in the absence of PDE3 and PDE4 inhibitors on cAMP in HAM

Analysis of Epi responses in the absence and in the presence of PDE inhibitors (0.3 µM cilostamide and 1 µM rolipram, -PDEi, +PDEi), indicating single values cells based and mean values ± SEM patients based. n = number of myocytes/number of patients. (one-way ANOVA followed by Kruskal-Wallis test; patients based).

3.4.6 5-HT-induced cAMP increases were decreased by PDE3 and PDE4 in peAF

From results obtained wit NE and Epi we have to expect intact ability of β_1-and β_2-AR to increase cAMP. Since inotropic actions of 5-HT are blunted in peAF, we wanted to investigate whether cAMP increases by 5-HT are diminished in peAF

The first step was to explore 5-HT effects on cAMP in SR. Myocytes were exposed to a single high concentration (100 µM) of 5-HT (Figure 60).
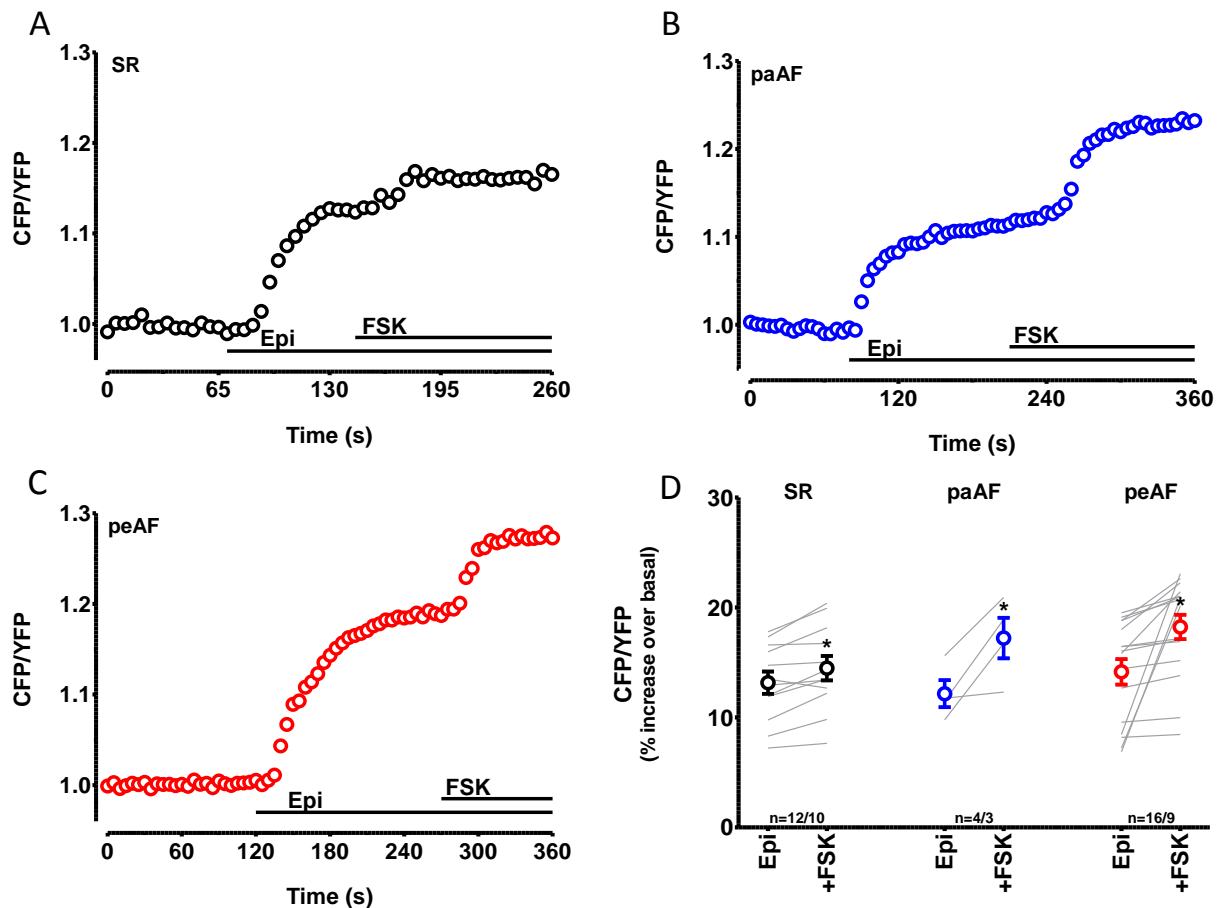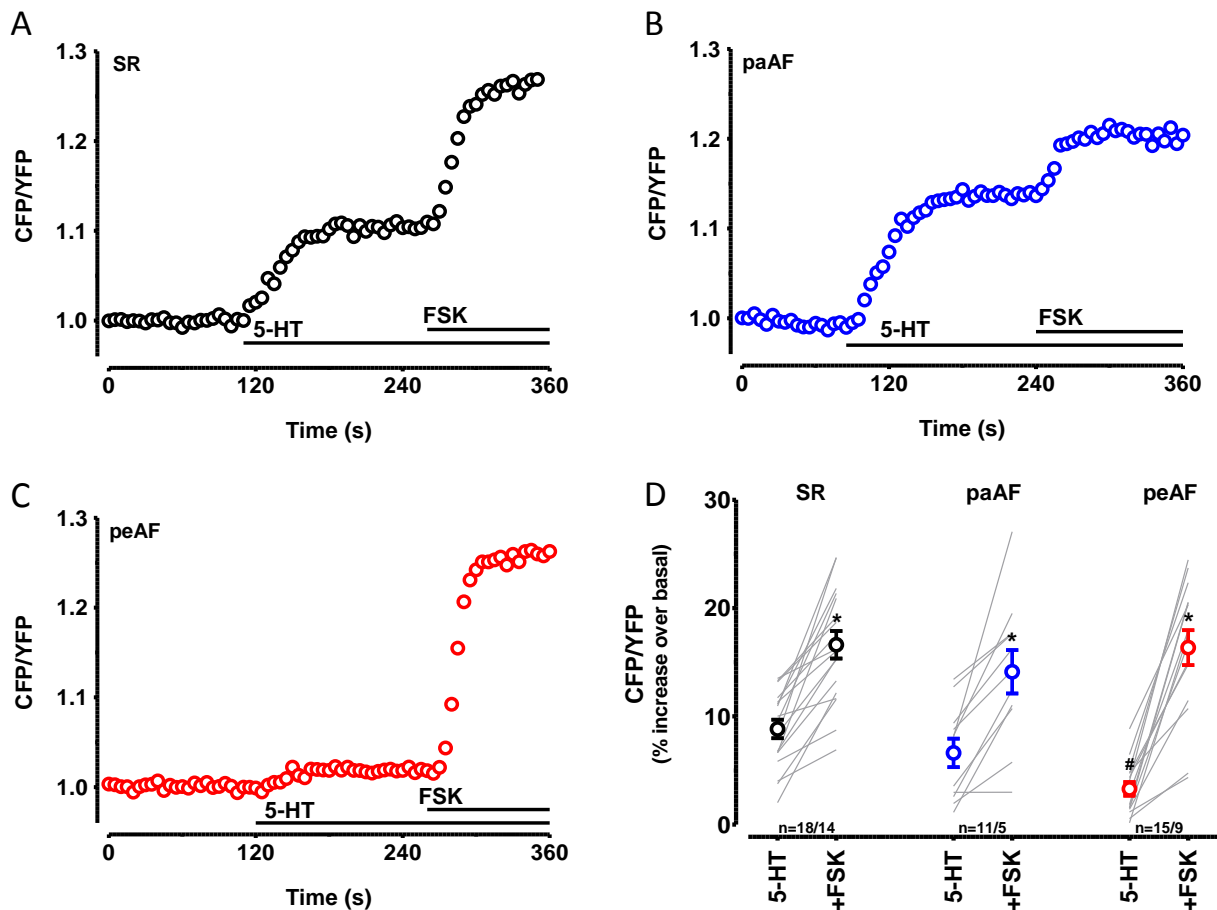
Figure 60: Effects of 5-HT and FSK in the presence of 5-HT on cAMP in HAM
Time course of the FRET signal indicating change in global cAMP in 3 HAMs from patients with SR
(**A**), paAF (**B**) and peAF (**C**) exposed to 100 µM 5-HT and in the continuous presence of 5-HT to 10
µM forskolin (FSK). Each line connects data for responses calculated from the myocyte of an individual
patient. Summary of the results in panel **D**. Depicted are FRET responses to both 5-HT and FSK in the
presence of 5-HT (+FSK) in individual myocytes. Mean values ± SEM are indicated by the circles. n =
number of myocytes/number of patients. *p < 0.05 *vs.* respective 5-HT (paired t-test)(; #p < 0.05 *vs.* 5-
HT in SR one-way ANOVA; followed by Kruskal-Wallis test, based on myocytes). Values for FSK
were not significantly different between groups (one-way ANOVA; followed by Kruskal-Wallis test,
based on myocytes).

At the end of each experiment 10 µM FSK was added in the presence of 5-HT to measure maximum

cAMP generation. Typical time courses of the FRET signals are shown in Figures 60A-C. 5-HT (100

µM) increased cytosolic cAMP levels and FSK (10 µM) increased cAMP further in SR, paAF and peAF.

However, cAMP levels after 5-HT alone were 63% smaller (significantly lower: p value = 0.0007) in

peAF than in SR or paAF (Figure 60D), suggesting either a diminished ability of the 5-HT4 receptor to

activate adenylyl cyclase or an increased susceptibility of 5-HT-evoked signals to PDE3 and PDE4.

To test this hypothesis, we measured cAMP levels under the exposure to concomitant cilostamide (Cil,

0.3 µM) + rolipram (Rol, 1 µM) in HAMs from the three groups of patients. Typical time courses are

shown in Figures 61A-C. Interestingly, the relative increase of cytosolic cAMP caused by the two PDE-

inhibitors was not larger in peAF than in SR or paAF (Figure 61D), not supporting the hypothesis that

a higher PDE activity *per se* might reduce the cAMP increase under 5-HT4 receptor stimulation in peAF. The magnitude of the 5-HT induced cAMP levels in peAF was increased in the presence of cilostamide and rolipram and was no longer smaller than in SR and paAF (Figures 62). Therefore, there are profound differences in PDE3 and PDE4 contribution to regulate 5-HT-evoked cAMP in peAF.
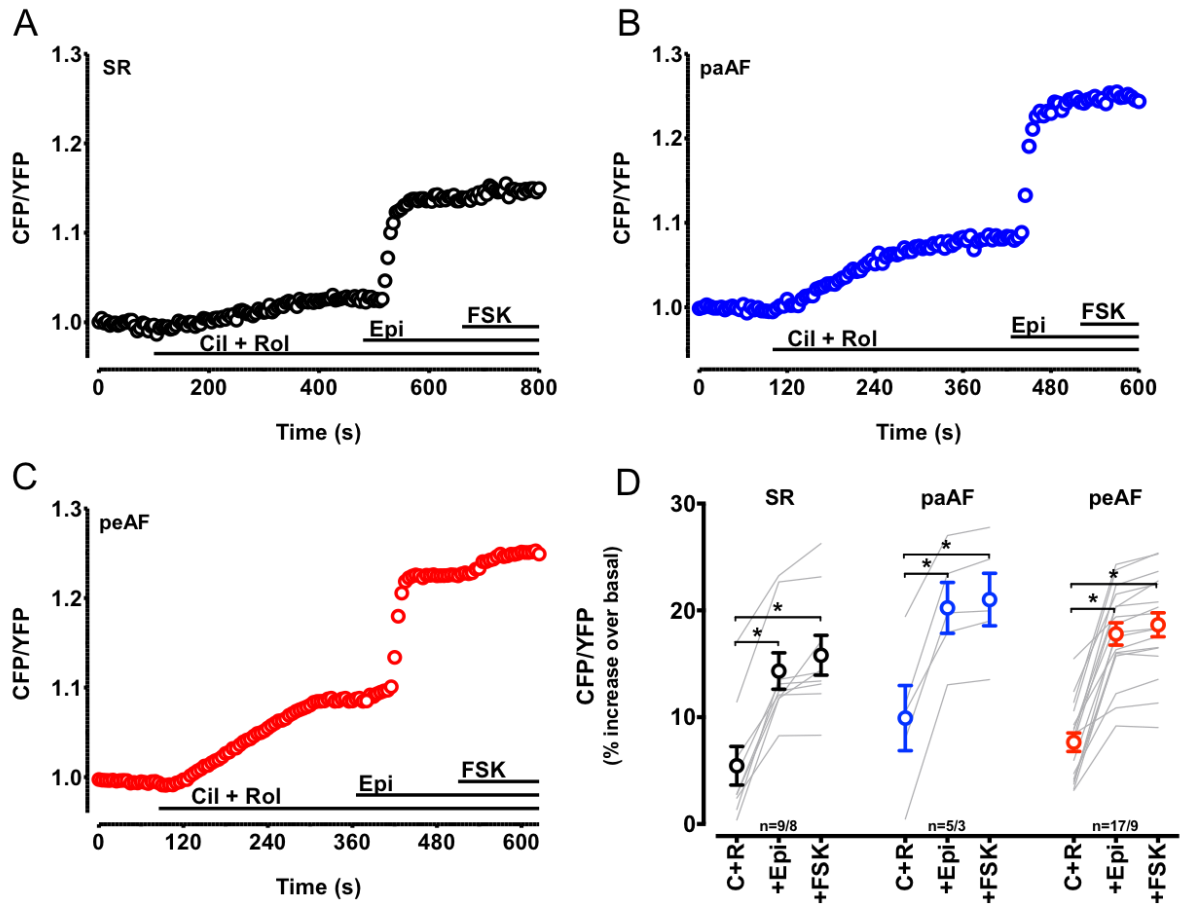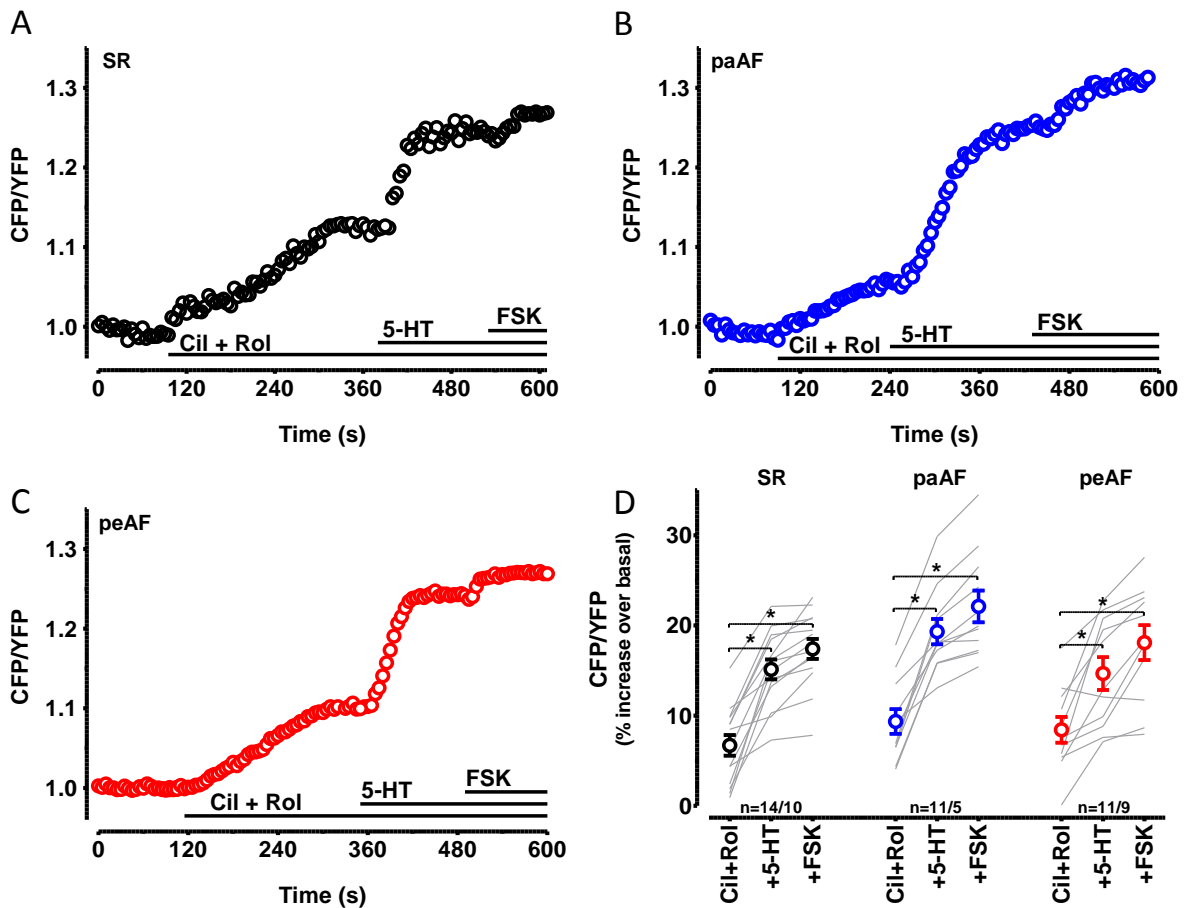

Figure 61: Effects of concomitant inhibition of PDE3 and PDE4, 5-HT and FSK on cAMP in HAM
Time course of the FRET signal indicating change in global cAMP in 3 HAMs from patients in SR **(A)**, paAF **(B)** and in peAF **(C)** exposed to 0.3 µM cilostamide and 1 µM rolipram (Cil + Rol). Each line connects data for responses calculated from cells of an individual patient. Summary of the results in the panel **D**. Depicted are FRET responses to Cil + Rol, to 100 µM 5-HT (+5-HT) and to 10 µM forskolin in the presence of Cil + Rol and 100 µM 5-HT (+FSK) in individual myocytes. Mean values ± SEM are indicated by the circles. n = number of myocytes/number of patients. [#]$p < 0.05$ *vs.* the corresponding values for Cil + Rol alone. Values for FSK in the presence of Cil + Rol and 5-HT were not significantly different between groups (one-way ANOVA followed by Kruskal-Wallis test; myocytes based).
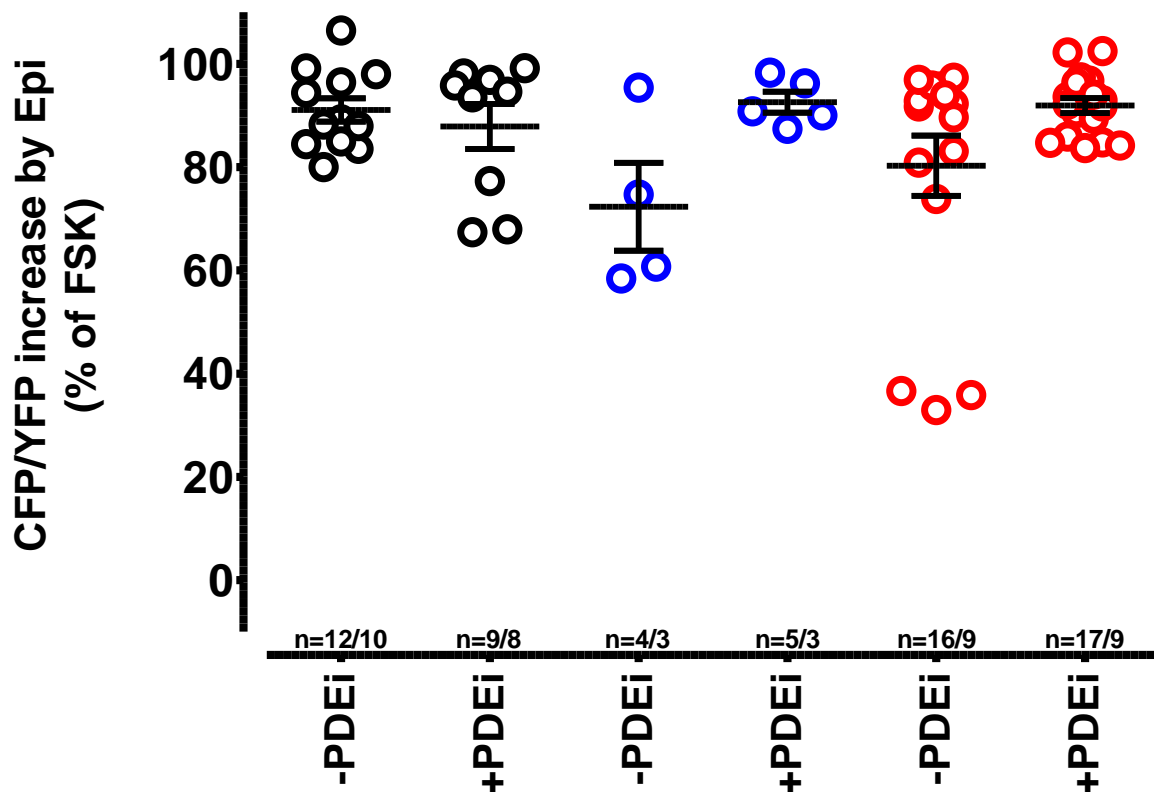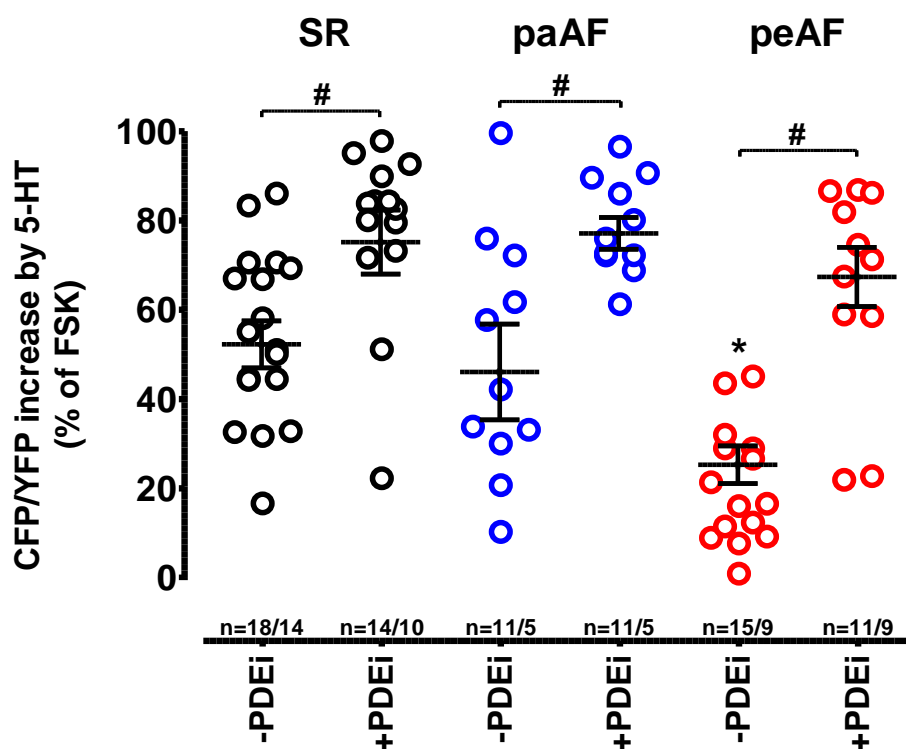
Figure 62: Effects of 5-HT in the presence and in the absence of PDE3 and PDE4 inhibitors on cAMP in HAM

Analysis of 5-HT responses in the absence and in the presence of PDE inhibitors (0.3 µM cilostamide and 1 µM rolipram, -PDEi, +PDEi), indicating single values cells based and mean values ± SEM patients based. n = number of myocytes/number of patients. $*p < 0.05$ *vs.* –PDEi in SR; $\#p < 0.05$ *vs.* respective values for -PDEi (one-way ANOVA followed by Kruskal-Wallis test; patients based).

3.5 Analysis by a mixed model

In the sections above we have separately analyzed experimental data patients classified as SR, paAF and peAF. In a next step we have used a mixed model to adjust not only for effects by experimental conditions but also by clinical variables. Work was done by Dr. Geelhoed Bastiaan (Department of General and Interventional Cardiology, University Heart Center, Hamburg, Germany) in a model, able to calculate both univariate statistics and multivariate statistics.

Effect of experimental conditions

For univariate analysis data were normalized to the average effect of all the conditions, which was 13.3% increase in FRET. From the univariate analysis, we could appreciate a significant smaller effect of 5-HT and Cil+Rol compared to the estimated average measurements value (Figure 63).

74
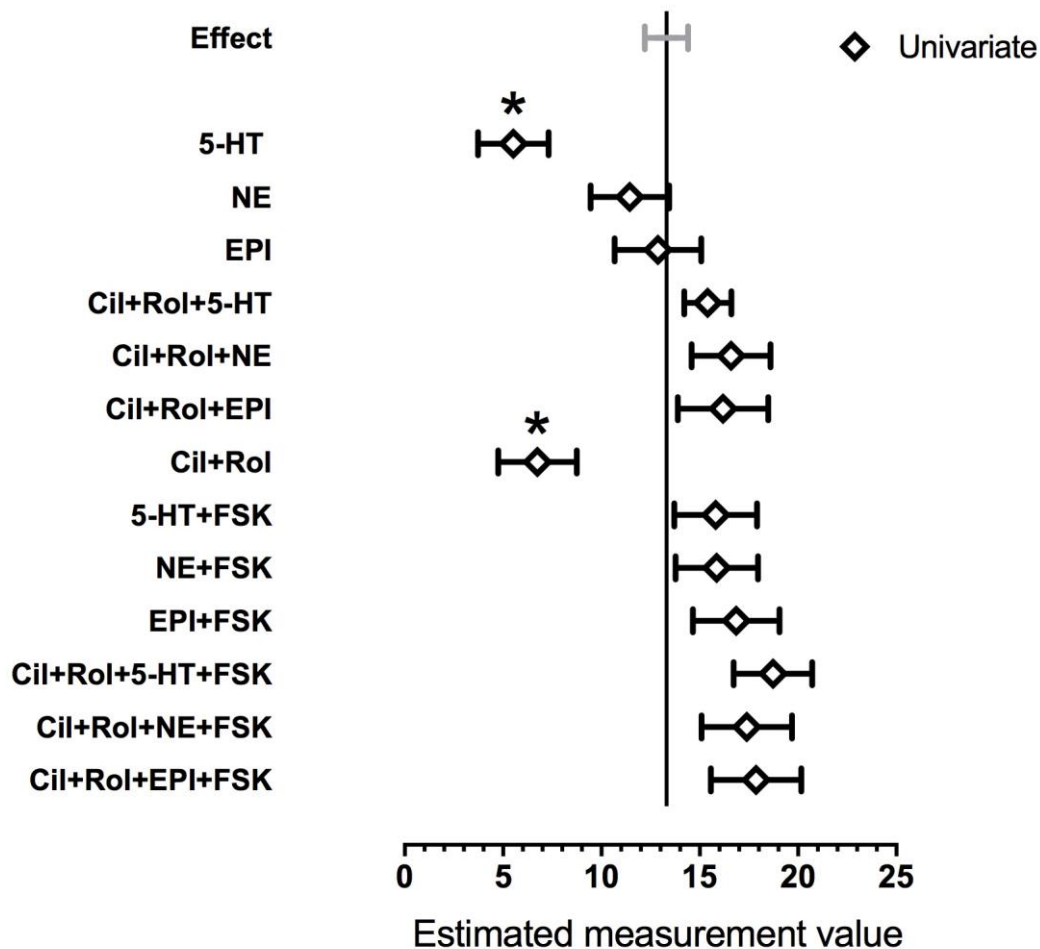
Figure 63: Impact of experimental condition on cAMP increase (univariate analysis)
Effect of different experimental conditions on global cAMP concentrations in HAM as measured by FRET. The average effect amounted to 13.3% increase in FRET signal (shown as vertical line). The statistics were run in a univariate model. Empty rhombus represents average of univariate data per condition. Standard deviation was symmetrically calculated. The more the value is departed from the reference the higher is the impact of the experimental condition on the general outcome. *$p < 0.05$ *vs.* estimated measurement value. Data are mean values ± SEM.

Effects of clinical variables

The variability of FRET data may result from different clinical conditions of patients. In order to investigate how our experimental results were affected by those clinical data, we decided to check their impact on the estimated measurement value by a univariate test.

As shown, estimated effect size of impact by clinical variables are all close to the average (Figure 64). The surgical procedure mitral valve replacement (Mitralklappenersatz, MKE) shifts values to the left despite did not yet reach statistical significance (SEM crossing mean value).

75
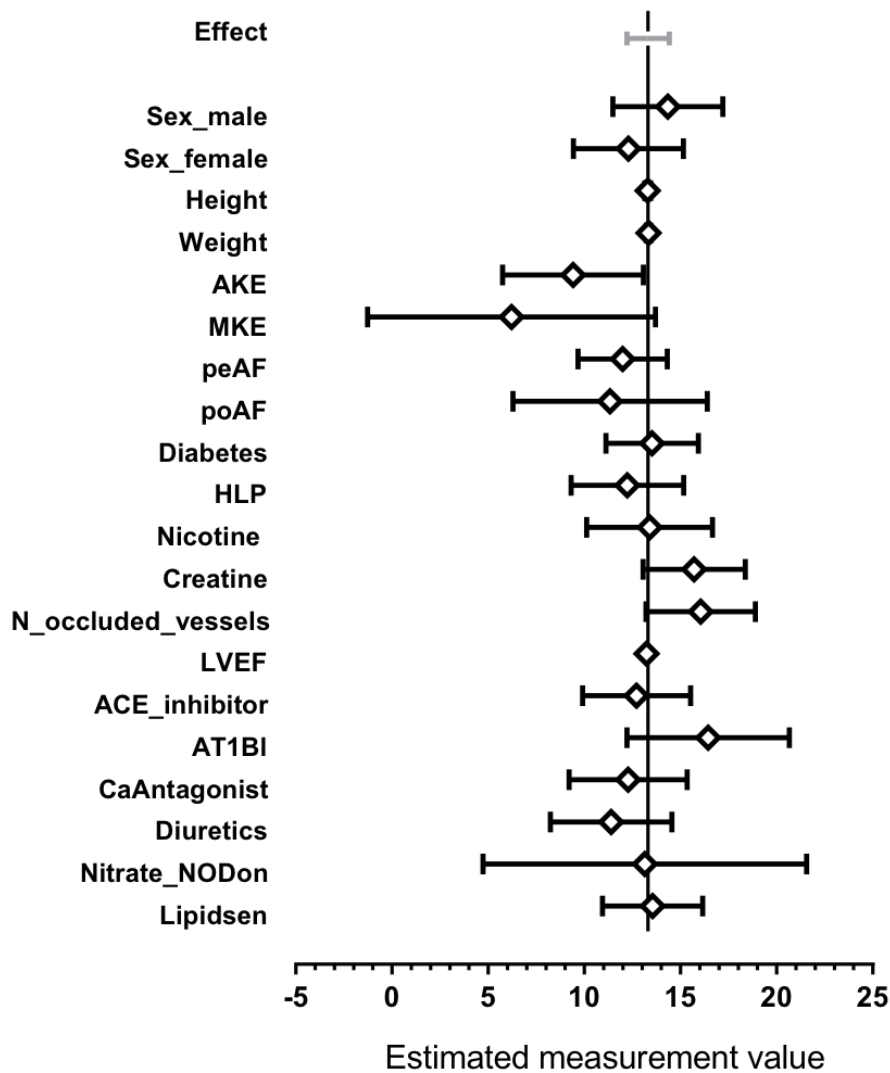
Figure 64: Impact of clinical variables on cAMP increase (univariate analysis)
Analysis of estimated impact of clinical variables to the estimated measurement value (13.3 % of FRET). The statistics were run in a univariate model. Empty rhombus represents average of univariate data per condition. Standard deviation was symmetrically calculated. The more the value is departed from the reference the higher is the impact on the general outcome. No parameter reached statistical significance. Data are mean values ± SEM.

Interaction with paAF and peAF

Subsequently, we analyzed putative interactions between the experimental conditions described in Figure 63 and the clinical condition AF. Analysis were run separately for paAF and peAF.

Data points for an interaction with paAF showed values mostly located around the estimated measurement value (Figure 65). A seen also in Figure 63, 5-HT and Cil+Rol effect values in the multivariate are slightly shifted to left from the general effect suggesting a small impact of paAF, to the smaller effect size by 5-HT in peAF. Shift for Cil+Rol hard to explain. It should be noted that both shifts did not reach the level of significance.
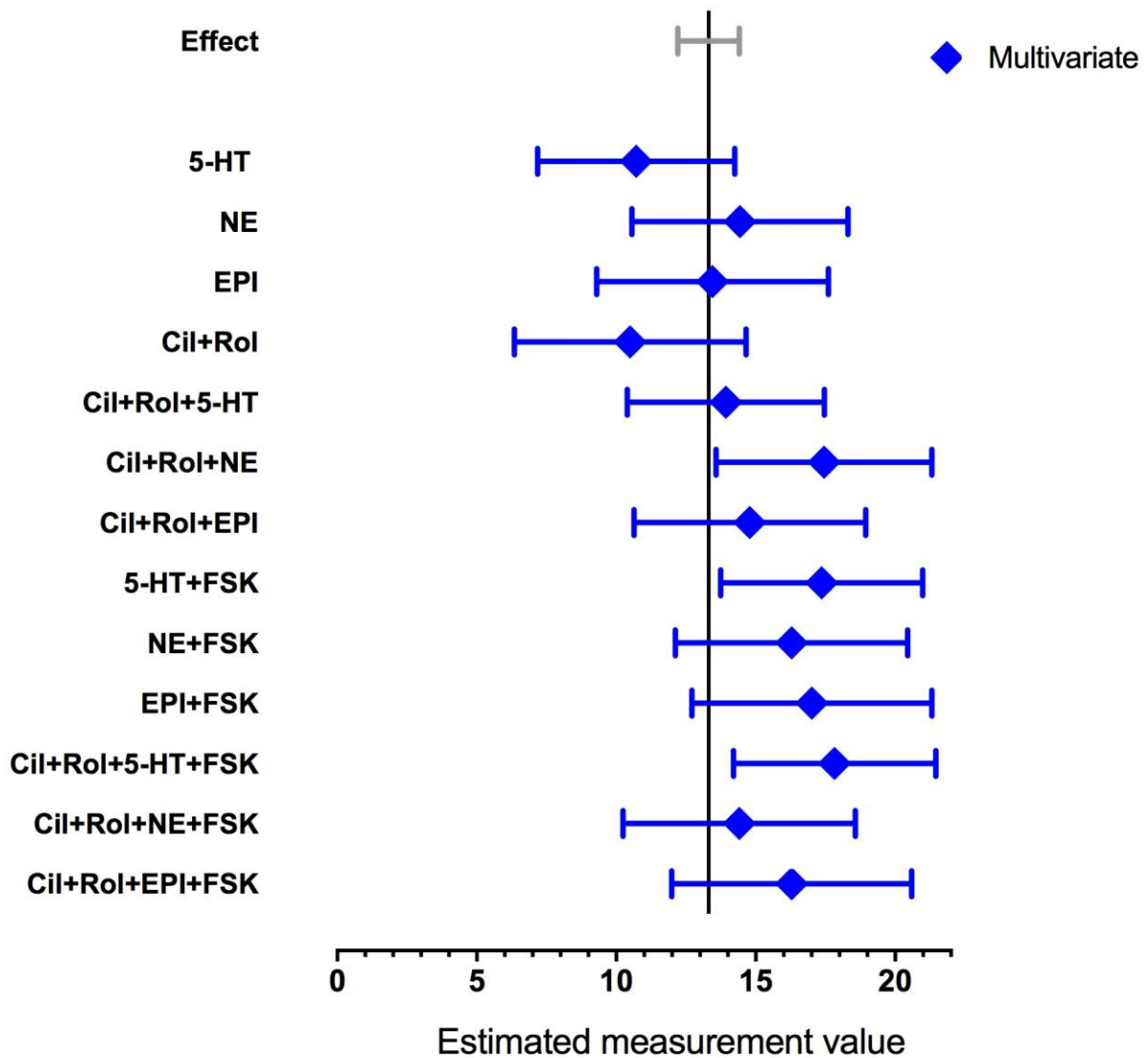
Figure 65: Interaction of experimental conditions and paAF

Analysis of FRET experiments conditions effects in paAF on cAMP compared to the estimated measurement value (13.313). The statistics were run in a multivariate model. Filled rhombus represents multivariate data for interaction with paAF. Standard deviation was symmetrically calculated. The more the value is departed from the reference the higher is the impact on the general outcome. Data are mean values ± SEM.

Also most of data points for interaction with peAF showed values located around the estimated measurement value, with the exception of 5-HT (Figure 66). 5-HT value was significantly smaller than the estimated measurement value in the multivariate model interacting with peAF (Figure 66), indicating that there is a strong interaction between peAF and 5-HT effects on cAMP.
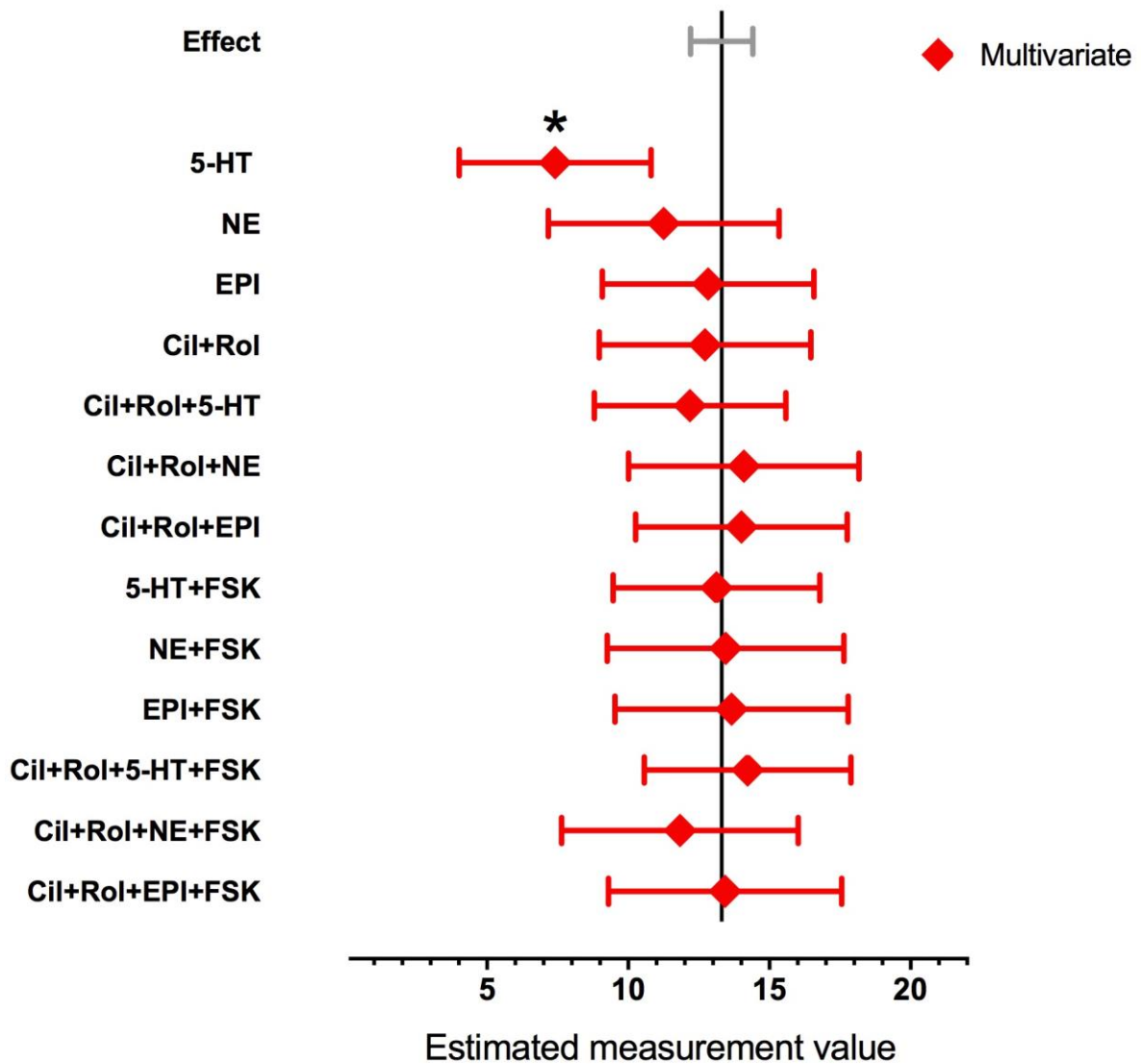
Figure 66: Interaction of experimental conditions with peAF

Analysis of FRET experiments conditions effects in peAF on cAMP compared to the estimated measurement value (13.3%). The statistics were run in a multivariate model. Filled rhombus represents multivariate for interaction with ECG in peAF. Standard deviation was symmetrically calculated. The more the value is departed from the reference the higher is the impact on the general outcome. Data are mean values ± SEM.

4. Discussion

4.1 Expression or activity of PDE in AF

With about 50% of total PDE activity PDE3 is assumed to be the key player in cAMP hydrolysis in human atrium. Any other PDE isoform contributes to a much lesser extent. The next most important PDE is PDE4 with 15% contribution to total PDE activity (Molina et al., 2012). Using an antibody provided by Dr. Chen Yan (University of Rochester, NY, USA), Roszmaritza et al. found three bands of PDE3A (Rozmaritsa et al., 2014). Here we found only two bands (Figure 37). Difference may relate to different antibodies preparations, since antibodies were a gift of the same researcher. It remains unclear whether different lots were used. Rosmaritza et al. reported almost identical expression PDE3A in AF and SR. We could confirm these results (Figure 37). Collectively our results and the results of Roszmaritza claim against relevant changes in PDE3A expression in peAF.

For detection of PDE4B and PDE4D we used an antibody preparation provided by Dr. Marco Conti (University of California, San Francisco, USA). So far there are no reports about PDE4 expression in human AF. There is a trend to decreased hydrolytic activity of total PDE and PDE4 in AF vs. SR (Molina et al., 2012). Comparison of PDE4 activity in AF vs. SR was done by defining PDE4 activity as rolipram-sensitive enzymatic activity (Molina et al., 2012). Subtype-selective expression of PDE4B vs. PDE4D was measured from immunoprecipitated pellets in SR only. PDE4D showed a five time higher activity than PDE4B, indicating PDE4D the more relevant subtype in human atrium (Molina et al., 2012). Here, we saw a tendency to a lower protein expression of PDE4D in peAF (Figure 38), fitting nicely the reported trend to lower PDE4 activity by Molina et al. (Molina et al., 2012). From the WB results, presented in our study we cannot compare PDE4B vs. PDE4D within the groups (SR and AF). In peAF PDE4B expression was two times higher than in SR (Figure 39). However, functional relevance of this change is unclear, since at least in SR total PDE4B contributes to total PDE4 activity only 10%, meaning ~1.5% of total PDE activity. It seems unlikely that the observed doubling of very low expression of PDE4B in peAF should have a substantial impact on global cAMP regulation.

4.2 Physiological relevance of PDE4 in SR and AF

4.2.1 Effect of PDE4 on basal I_{CaL}

We could not find an increase in I_{Ca} by inhibition of PDE4 with 10 µM rolipram in SR (Figure 40). This finding argues against relevant contribution of PDE4 to regulation of Ca-channel activity in human atrium in SR. Moreover, rolipram was not able to increase I_{Ca} in peAF, making contribution of PDE4 to reduced I_{Ca} in peAF unlikely (Figure 41). Our findings are in line with recent data published by Berk et al. but are at variance to Molina et al. where Ro 20-1724, another inhibitor of PDE4, was used. In that study Ro 20-1724 increased I_{Ca} by about 60% over control when measured under steady state control conditions (Molina et al., 2012). Concentrations of 300 nM gave maximum effects. Taken in to account

an IC_{50} value of Ro 20-17242 of about 2 µM the findings of Molina et al. suggest that a 15% inhibition of activity of PDE4 (about 2.3% of total PDE activity) should increase I_{Ca}. This would implicate a high level of compartmentation in PDE activity. No data about Ro 20-1724 are available in AF. However, it should be noted that results with Ro 20-1724 could not be confirmed by others (Berk et al., 2016). The reason for the discrepancy remains unclear.

4.2.2 Effect of PDE4 on NE and Epi activated I_{Ca}

From earlier work it is known that non-selective inhibition of PDEs by IBMX increase I_{Ca} in the absence of 5-HT but do not potentiate maximum 5-HT effects (both in SR and AF) (Berk et al., 2016). One possible explanation could be that at high agonist concentration Ca^{2+} channels may reach a maximum conductivity that cannot be increased further. Therefore, we used such concentrations of NE and Epi that increases I_{Ca} by about 50% (Figure 40, 41). However, we could not detect any hint that pre-treatment by rolipram (10 µM) increased effects of NE and Epi (both 1 µM) in SR and AF (Figure 40, 41). Our findings are hard to compare to results by Molina et al. because of methodological differences. They measured effects of Ro 20-1724 (10 µM) on β-AR stimulation not under steady state conditions. For β-AR stimulation they used 100 nM isoprenaline. From such a concentration we would expect almost maximum effects (Galindo TA et al., 2009). However, exposure to isoprenaline was stopped before I_{Ca} had increased completely. Recovery time (reaching control values before Iso) was taken as a read-out (Molina et al., 2012). In line with Berk et al. maximum peak effects were not significantly larger in the presence of PDE inhibitors, but reversal to basal values were much slower (increase in recovery time). This study provides the first data on PDE4-effects on I_{Ca} evoked by β-AR stimulation in human atrial cardiomyocytes under steady state conditions with catecholamine concentrations giving half maximum effects (Figure 40, 41).

The small or even absent impact of PDE4 to regulation of I_{Ca} response by submaximal catecholamine concentrations could be a peculiarity of the atrium. From animal studies (animal model: rat) it is known that rolipram potentiated I_{Ca} responses to 1 µM NE on I_{Ca} in ventricular but not in atrial cardiomyocytes (Christ et al., 2009) (Figure 67).
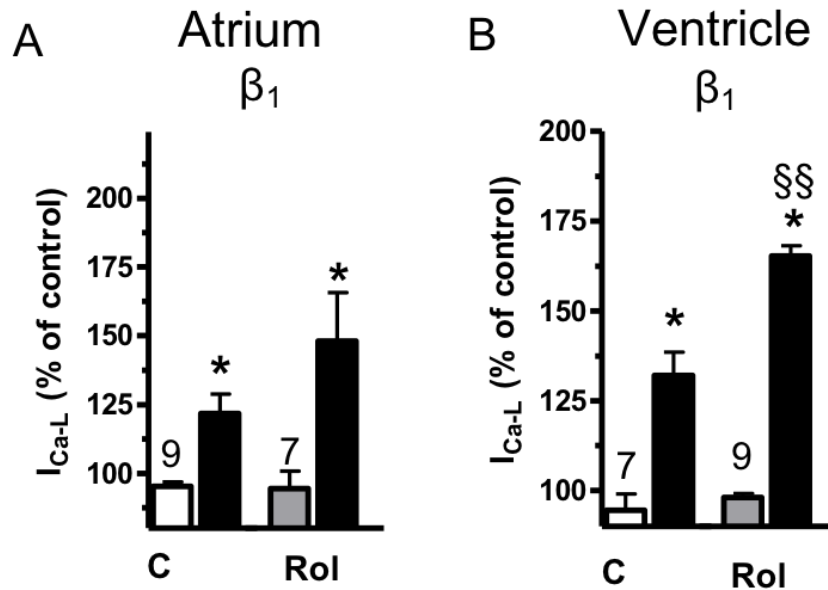
Figure 67: Effects of rolipram on $I_{Ca,L}$ responses to 1 µM NE

$I_{Ca,L}$ was measured in myocytes isolated from rat atrium **(A)** and rat ventricle **(B)**. "C" indicates control condition (no PDE inhibitor), white column is the baseline and the black one refers to the current under stimulation of β_1-AR with 1 µM NE. "Rol" indicates rolipram treated cells, in grey column effect of rolipram alone and the black one in the concomitant presence of 1 µM rolipram and 1 µM NE. *p < 0.05 *vs.* "C" or "Rol". §§p < 0.005 *vs.* 1 µM NE in the absence of Rol (black column of group C). (Christ et al., 2009).

4.2.3 Effect of PDE4 on basal contractility

In our work we saw a small but significant increase in force by 10 µM rolipram in SR, paAF and peAF (Figure 42). As in the study of Molina et al. there is no overt positive inotropy with 10 µM rolipram. Positive inotropy can be detected only when TMC were used for normalization to compensate for the notorious run down of force over time. Obviously more than 50% inhibition of PDE4 is needed to unmask a marginal impact on basal force by PDE4, since 1 µM rolipram was ineffective (Berk et al., 2016).

4.2.4 Effect of PDE4 β-AR induced inotropy

Rolipram (10 µM) does not increase sensitivity for β_1-AR evoked positive inotropy in SR (Figure 43). This finding is in line with earlier work (Engel A., 2013). However, these data were obtained with only 1 µM rolipram in order to avoid concomitant inhibition of PDE3, because of only moderate selectivity of rolipram for PDE4 over PDE3. As discussed in section Methods, rolipram at 1 µM inhibits PDE4 by about 50% in experiments by Berk et al (2016). From the present study we have to assume a more complete (around 90%) inhibition of PDE4. Rolipram 10 µM inhibits PDE3 of about 2-3%. PDE3-inhibition shifts the concentration-response curve for NE inotropy to the left. Absence of shift by 10 µM rolipram argues against relevant inhibition of PDE3 by 10 µM rolipram in our experiments. The same holds true for paAF and peAF. The absence of PDE4 contribution to regulate β_1-AR evoked positive inotropy in SR precludes any interpretation of contractility data whether PDE4 activity is decreased in

peAF and in paAF. Our findings in SR are in strong contrast to rats, where even low concentrations of rolipram (1 µM) induces a leftward shift of the concentration response-curve for the positive inotropic effect of NE, with even larger shift in atrium compared to ventricles (Christ et al., 2009).

The absence of sensitization for β_1-AR evoked positive inotropy from rolipram is somewhat unexpected (Figure 43). From the work of Molina et al., no concentration-response curves for NE induced inotropy are available. There is however a hint to putative interaction between isoprenaline and rolipram from this study. Rolipram was ineffective under basal condition (no isoprenaline) but increased force in the presence of low concentrations of isoprenaline (10 nM). However, from an increase of force at a single concentration of isoprenaline it cannot be concluded to sensitization for β_1-AR evoked positive inotropy. We have therefore tried to model how inhibition of PDE4 could increase submaximal isoprenaline effects without changing EC_{50}.:

1. Increase in basal force by PDE4 inhibition is a hypothesis. Nevertheless, to achieve a 10 % increase in force at 10 nM isoprenaline, it would be required an increase in the starting point (basal force) of 30% that is not realistic (absence of positive inotropic effect by rolipram 10 µM, as seen in Figure 42 and by Molina et al.).
2. Increase in steepness of the curve is another possibility but would imply that effects of lower concentrations are attenuated (not realistic, when compared to Figure 42).
3. Increase in steepness only in the upper part of the curve would nicely fit to the experimental data and would imply higher contribution of PDE to hydrolysis of cAMP at higher agonist concentration (Figure 68).

Effects of PDE on catecholamine induced inotropy can differ between β_1-AR and β_2-AR stimulation. For instance, in human failing ventricles inhibition of PDE3 caused greater potentiation of the positive inotropic effects by β_2-AR stimulation with Epi than by β_1-AR stimulation with NE (Molenaar et al., 2013). Therefore, we measured effects of 10 µM rolipram also on β_2-AR stimulation evoked inotropy by Epi. However as seen for β_1-AR stimulation by NE there was no sensitization by 10 µM rolipram for Epi-induced inotropy (Figure 47).

Theoretical curve
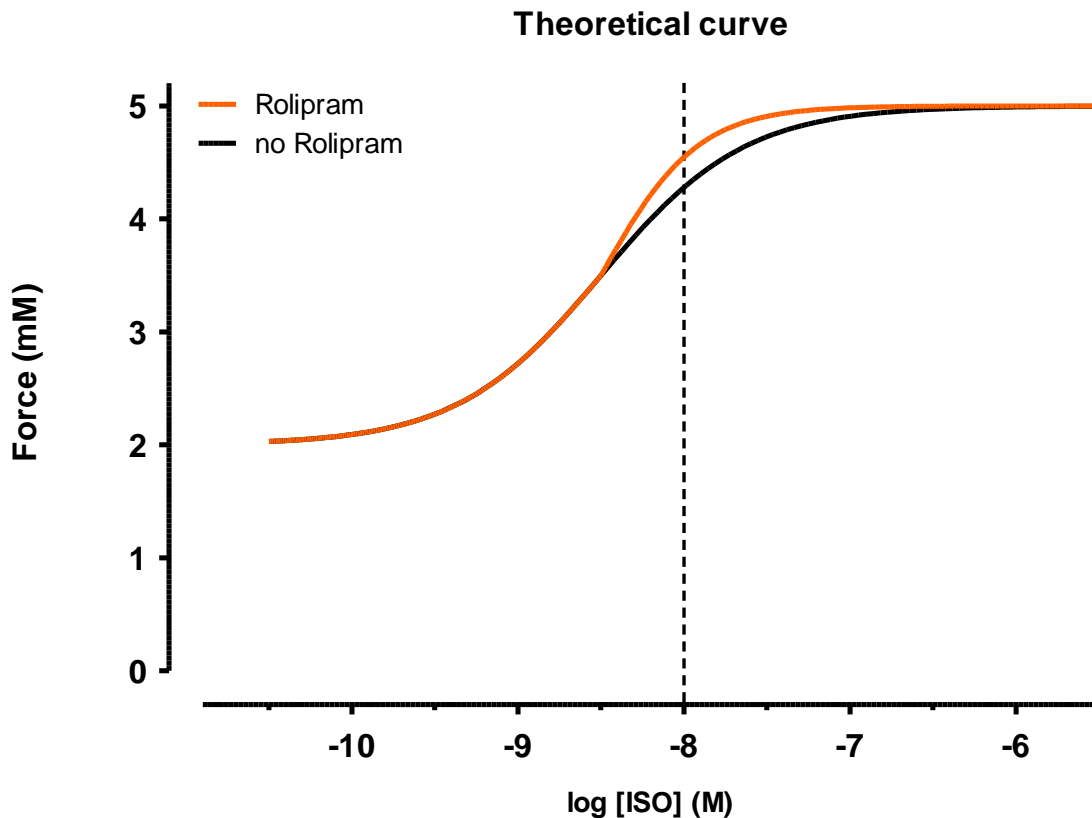
Figure 68. Modelling of PDE4 inhibition over ISO increase in inotropy
Simulation of force increase over increasing concentration of ISO in the presence and in the absence of
10 µM rolipram. In the presence of rolipram the concentration response curve appears to increase in
steepness only in the upper part (ISO concentration higher than 10 nM). The curve was calculated from
concentration-response curve for NE (Christ et al., 2014) assuming a 30 fold lower IC_{50} for isoprenaline
than for NE (Galindo TA et al., 2009).

4.2.5 Effect of PDE4 on β-AR induced arrhythmias

Rolipram (10 µM) did not modify inotropy evoked by $β_1$-AR stimulation by NE or by $β_2$-AR stimulation
by Epi (Figure 43, 47). In contrast it clearly increased arrhythmias in SR but not in peAF (Figure 45,
49). In paAF potentiation of NE-induced arrhythmias by 10 µM rolipram was not larger than in SR
(Figure 45).

Potentiation of both $β_1$-AR and $β_2$-AR induced arrhythmias by PDE4-inhibition was described in SR by
Molina et al (Molina et al., 2012). No data are given for AF. In that study surprisingly even very low
concentration of rolipram (0.1 µM) were effective to induce arrhythmias (Molina et al., 2012). As
discussed in the sub-chapter 4.2.4, 0.1 µM rolipram should not block more than 10% of PDE4. This may
imply the existence of highly compartmented cAMP pools relevant for arrhythmias induction.
Therefore, we replicated experiments with 0.1 µM rolipram. There was a trend for higher incidence of
arrhythmias in the presence of 0.1 µM rolipram than in control. In our experiments, 10 µM rolipram is
needed to evoke a relevant number of arrhythmias. Reasons for that discrepancy to Molina et al about

arrhythmias by 0.1 µM rolipram remains unclear. It should be anyway noted that L-type Ca^{2+}-channels are not critically involved in catecholamine-induced arrhythmias facilitated, since 10 µM rolipram had no effect on basal I_{Ca} and on catecholamine increased I_{Ca}.

From the interpretation that reduced PDE4 activity predisposes to AF, it should be expected a smaller contribution of PDE4 to electrical stability in paAF and peAF. In fact, 10 µM rolipram has lost its ability to facilitate catecholamine-induced arrhythmias (Figure 45, 49). However, catecholamine-induced arrhythmias are vanished in peAF even in the absence of PDE4 inhibitor, making interpretation difficult (Christ et al., 2014). From the finding that in peAF even a combination of cilostamide and rolipram has lost its ability to potentiate arrhythmias evoked by 5-HT (Berk et al., 2016), we can speculate that a more general remodeling take place in peAF reducing arrhythmias. As shown before in computer model calculations larger inward rectifier potassium currents (I_{k1}) in peAF could protect against arrhythmias (Koivumäki et al., 2014). In conclusion our results in peAF do not allow a clear judgement whether PDE4 contribution to electrical stability is reduced.

Our findings about loss of catecholamine-induced arrhythmias in peAF fits nicely earlier data (Christ et al., 2014). However, in the present study basal and maximum force was not different between SR and AF. Absence of contractile dysfunction is completely unexpected and in strong contrast to earlier work (Schotten et al., 2011; Christ et al., 2014; Berk et al., 2016). Reasons remain unclear. Correct classification as peAF vs. paAF could be an issue. However, misclassification seems unlikely because of the difference in arrhythmias between SR and AF. We cannot rule out that majority of peAF tissue may have undergone early remodeling with loss of arrhythmias and preserved contractility. Further studies are needed to clarify that issue.

4.3 Physiological relevance of concomitant inhibition of PDE3 and PDE4 on cAMP in AF

In peAF 5-HT-induced inotropy is lost, while indirect evidence from Ca^{2+} current measurements suggests intact cAMP delivery by 5-HT receptors (Christ et al., 2014). The blunted inotropic response upon 5-HT in peAF can be restored by concomitant inhibition of PDE3 and PDE4 (Berk et al., 2016). These findings suggest different contribution of PDE3 and PDE4 to the regulation of 5-HT effects in peAF vs. SR. Functional studies were done with 300 nM cilostamide and 1 µM rolipram to avoid non-selective PDE4 inhibition by cilostamide and more importantly block of PDE3 by rolipram (sub-chapters 2.8.5, 2.8.6). In order to compare directly FRET-data to functional data we used identical concentrations as used in the study of Berk et al. However, it should be taken in to account that 1 µM rolipram inhibits PDE4 by only about 50%.

4.3.1 What is the functional relevance of cAMP produced by rolipram and cilostamide alone?

Concomitant inhibition of PDE3 and PDE4 (300 nM cilostamide and 1 µM rolipram) increases cAMP in SR (Figure 53) to ~60% and to ~80% of maximum effects of NE/Epi (Figure 54, 57) and 5-HT (Figure 60), respectively. In contrast, the increase in I_{Ca} by non-selective PDE inhibition with IBMX (10 µM) is

clearly less (20%) (Berk et al., 2016). Increase in force by concomitant inhibition of PDE3 and PDE4 (300 nM cilostamide and 1 µM rolipram) is even hard to detect (Berk et al., 2016). From these findings we conclude that, the majority of cAMP evoked by inhibition of PDE3 and PDE4 and monitored by FRET does not reach targets relevant for contractility both in SR and in peAF. This finding illustrates some limitation in globally expressed FRET-sensors. Application of FRET-sensors with restricted expression to the close vicinity of relevant partners of electromechanical coupling should help to clarify that issue.

4.3.2 NE, EPI and 5-HT increases cAMP to the same extent in SR

Increases in cAMP by β_2-AR activation was not smaller than with β_1-AR activation in SR (Figure 54, 57). Since only about 15% of total β-AR population consist to β_2-AR (Kaumann et al., 1996), this finding indicates stronger coupling of β_2-AR than by β_1-AR to adenylyl cyclase. Unclear if β_2-AR changes in peAF. Binding studies for β_1- and by β_2-AR in peAF are not available. From unchanged mRNA expression encoding for β_1- and by β_2-AR in peAF we would not expect a reduction in protein expression for β_1- and by β_2-AR (Grammer et al., 2001). In SR 5-HT receptor density is 10-fold lower than β-AR density (Kaumann et al., 1996). Taken in to account that cAMP responses to 5-HT in SR are not significantly smaller than with NE/EPI (Figure 60), this would imply a 10-fold stronger coupling of 5-HT receptors than β-AR.

4.3.3 Both cAMP and force responses to NE and Epi are preserved in peAF

Increases in cAMP by NE and Epi are preserved in peAF (Figure 54, 57). The same hold true for absolute force increase NE and Epi effects (Christ et al., 2014). However, in earlier studies maximum force in the presence of NE and Epi or Iso is less in peAF than in SR (Schotten et al., 2011). The easiest explanation for that phenomena could be that basal cAMP levels are reduced in peAF and even with equal increase in cAMP absolute maximum levels will still be lower than in SR. This hypothesis cannot be verified by FRET-measurements, because signals cannot be calibrated. Therefore, no information on absolute levels of cAMP are available. Biochemical data argue against relevant reduction of basal cAMP in peAF. Several proteins involved in electro-mechanical coupling show unchanged basal PKA-dependent phosphorylation (Christ et al., 2014). Even increased PKA-dependent phosphorylation of several targets of electro-mechanical coupling was reported (El-Armouche et al., 2006). Other mechanisms than loss of basal cAMP have to be considered to explain reduction in maximum force in the presence of NE and Epi in peAF.

4.3.4 5-HT responses are reduced in peAF

In this study 5-HT effects on cAMP are reduced by about 63% in peAF (Figure 60, 62). The smaller increase in cAMP by 5-HT in peAF cannot be explained by differences in clinical variables other than peAF as shown by multivariate regression analysis (Figure 64, 66). The drastic loss in positive inotropy by 5-HT in peAF is accompanied by an preserved cAMP accumulation close to Ca^{2+} channels   as

concluded from inhibition experiments with 8-Br-cAMPs as a cAMP antagonist (Christ et al., 2014). However, this technique does not allow detection of small changes like in the present work using a FRET sensor. Reason for the reduction in cAMP response by 5-HT in peAF are unclear. However, it should be noted that mRNA expression for 5-HT (but not for β_1- and by β_2-AR) is reduced by about 36% in peAF (Grammer et al., 2001). Therefore, reduction of 5-HT-R could be the reason for the reduced cAMP generation. Binding data are not available at present.

4.3.5 In peAF 5-HT-evoked increases in cAMP, I_{Ca} and force are all reduced, but to a different extent

The 63% reduction of 5-HT evoked increase in cAMP in peAF (Figure 60, 62) is paralleled with a reduction in I_{Ca} response by only 30% (Berk et al., 2016), while inotropic actions are reduced by more than 80% compared to SR (Christ et al., 2014). These findings suggest different sensitivity of partners in electromechanical coupling to cAMP generated by 5-HT in peAF. Alternatively, cAMP could be reduced at different levels within different compartments for I_{Ca} and force.

4.3.6 What is the relevance of 5-HT evoked cAMP potentiated by rolipram and cilostamide in peAF vs. SR?

Concomitant presence of rolipram and cilostamide increases cAMP response to 5-HT in SR and in peAF (Figure 61, 62). However, there are quantitative differences. The reduced cAMP response to 5-HT in peAF can be completely rescued by concomitant presence of rolipram and cilostamide, while in SR increase by rolipram and cilostamide are clearly less, indicating larger reduction of 5-HT effects on cAMP in peAF by PDE3 and PDE4. These findings are in line with contractility data: rolipram and cilostamide tend to increase maximum force in the presence of 5-HT in SR and paAF (not significant) while inotropic effects of 5-HT in peAF are markedly increased (Berk et al., 2016). These findings strongly suggest that maximum inotropic effects of 5-HT are reduced by PDE3 and PDE4 in human atrium. Anyhow, the larger effects of PDE3 and PDE4 on 5-HT-responses in peAF do not result from increased contribution of PDE3 and PDE4 by their self (Figure 53).

More likely cAMP responses to 5-HT in peAF in the absence of inhibition of PDE3 and PDE4 can no longer exceed a critical level necessary to evoke positive inotropy.

4.3.7 FSK response in human atrium myocytes is independent from rhythm, PDE-inhibition and β-AR or 5-HT-R stimulation

5-HT effects on cAMP are reduced in peAF (Figure 60). Increases in cAMP in the presence of FSK and NE or Epi is always larger than in the presence of NE or Epi alone (Figure 54, 57). Increase in cAMP in the presence of NE or Epi is larger in cells pretreated with cilostamide and rolipram (Figure 55, 58). However, cAMP in the presence of FSK did neither depend on rhythm nor on pretreatment by PDE-inhibitors (Figure 52). This finding suggests intact ability of adenylyl cyclase to generate cAMP in

peAF. Therefore, it seems justified to use cAMP values in the presence of FSK as an internal control to normalize PDE inhibitor/agonist effects on cAMP to maximum capacity of an individual cell.

Effect size of cAMP increase by NE, Epi and even more by 5-HT are smaller than by FSK in SR and AF. Inotropic responses to NE, Epi, FSK and 5-HT are equal in size in SR, but reduced for NE, Epi and even more to 5-HT in peAF (Christ et al., 2014), illustrating that small cAMP signals can lose relevance for inotropy in peAF.

4.3.8 Application of a nonlinear regression model to study effects of clinical variables on cAMP responses

We saw reduced cAMP responses to 5-HT in peAF (Figure 60). To investigate whether clinical variables may affect experimental data many studies compare mean values describing clinical characteristics between experimental groups (e. g. SR vs. AF). However, this approach does not allow impact estimation for individual clinical characteristics. Application nonlinear regression model is at present the best method to investigate for impact of clinical characteristics. This approach represents now state of the art in epidemiological and drug treatment studies. Here we have used such a sophisticated approach and could show that the observed changes in cAMP rspeonse to 5-HT in peAF are not because of differences in clinical characteristics than peAF (Figure 63-66).

5. Conclusion and future perspective

There is an evident need to better understand the mechanism underlying initiation, developing and remodeling in AF. Since at present drug treatment of AF has low efficacy and substantial toxicity a deeper understanding of biological processes would lead to the discovery of new targets for drug treatment as well as surgical intervention. This work aimed to elucidate a small piece in the puzzle, whether PDE3 and PDE4 contribute to remodeling of AF.

In the first part of the project we tried to solve the discrepancy between arrhythmia induction and lack of potentiation of positive catecholamine-induced inotropy by PDE4 inhibition. For that purpose, we used a more complete inhibition of PDE4 by 10 µM rolipram compared to lower concentrations used in previous studies. Interestingly, we could not see a shift of the concentration-response curve for NE- and Epi-induced inotropy to the left, neither in SR nor paAF or peAF. However, PDE4 inhibition increased catecholamine-induced arrhythmias in SR and paAF, but not in peAF. This suggests an important contribution of PDE4 in the control of electrical stability, which is lost in peAF.

The second part of the present study aimed to estimate the contribution of PDE3 and PDE4 to cAMP regulation in paAF and peAF under basal conditions and when cAMP delivery is enhanced. Increases in cAMP by β_1- and by β_2-AR stimulation were preserved in peAF while increases after application of 5-HT were reduced in peAF, but not in paAF. Pre-treatment with PDE3 and PDE4 inhibitors succeeded to increase further cAMP levels in the presence of NE and Epi and restore in peAF the diminished response to 5-HT to same levels of catecholamines. In contrast, cAMP increases by inhibition of PDE3 and PDE4 alone were not different between SR and AF. This discrepancy suggests different remodeling of global and receptor-controlled cAMP-pools in AF.

The situation in paAF regarding PDE4-induced arrhythmias and cAMP regulation by 5-HT resembles closely the situation in SR, arguing that paAF may represent a not yet remodeled situation. Our findings does not support the idea that paAF may represent a highly vulnerable transition phase to peAF.

The arrhythmia induction by rolipram in SR and paAF was not accompanied by an increase in I_{Ca} and force. The rescue of 5-HT inotropy in peAF by inhibition of PDE3 and PDE4 was not accompanied by an increase in I_{Ca}. These two findings suggest that cAMP is differently regulated in hypothetical compartments relevant for I_{Ca}, inotropy and arrhythmias.

Here we used globally expressed FRET based cAMP sensors to study impact of PDE3 and PDE4 on regulation of G-protein coupled receptor activation. There is a dissociation between global cAMP measured by FRET and physiological parameters like Ca^{2+} current and force.

Application of FRET-based cAMP sensors locally expressed (Börner S et al., 2011; Schleicher et al.,, 2018) (Figure 69) should allow the study of cAMP localized in different cellular domains such as RyR,

or Ca^{2+}-channels and should give new insights in the remodeling of cAMP regulation by PDE3 and PDE4 in peAF.

Figure 69: Representative HAM after 48 hours of culture and transfected with the plasma membrane cAMP sensor Epac1-camps (pm-E1-camps)

6. Bibliography

Allessie et al. (2001). Pathophysiology and prevention of atrial fibrillation. *Circulation., 103*(5), 769-77.

Allessie et al. (2010). Electropathological substrate of long-standing persistent atrial fibrillation in patients with structural heart disease: longitudinal dissociation. *Circ Arrhythm Electrophysiol., 3*(6), 606-15.

Anderson et al. (2017). Plasma Catecholamine Levels on the Morning of Surgery Predict Post-Operative Atrial Fibrillation. *JACC Clin Electrophysiol., 3*(12), 1456-1465.

Anné et al. (2005). Matrix metalloproteinases and atrial remodeling in patients with mitral valve disease and atrial fibrillation. *Cardiovasc Res., 67*(4), 655-66.

Antzelevitch et al. (2011). Overview of Basic Mechanisms of Cardiac Arrhythmia. *Card Electrophysiol Clin., 3*(1), 23–45.

Arbelo et al. (2014). The atrial fibrillation ablation pilot study: a European Survey on Methodology and results of catheter ablation for atrial fibrillation conducted by the European Heart Rhythm Association. *Eur Heart J., 35*(22), 1466-78.

Börner S et al. (2011). FRET measurements of intracellular cAMP concentrations and cAMP analog permeability in intact cells. *Nat Protoc., 6*(4), 427-38.

Beavo JA. (1995). Cyclic nucleotide phosphodiesterases: functional implications of multiple isoforms. *Physiol Rev., 75*(4), 725-48.

Bender et al. (2006). Cyclic nucleotide phosphodiesterases: molecular regulation to clinical use. *Pharmacol Rev., 58*(3), 488-520.

Benjamin et al. (1994). Independent risk factors for atrial fibrillation in a population-based cohort. The Framingham Heart Study. *JAMA, 271*(11), 840-4.

Berk et al. (2016). In permanent atrial fibrillation, PDE3 reduces force responses to 5-HT, but PDE3 and PDE4 do not cause the blunting of atrial arrhythmias. *Br J Pharmacol., 173*(16), 2478-89.

Bers DM. (2008). Calcium cycling and signaling in cardiac myocytes. *Annu Rev Physiol., 70*, 23-49.

Berthet et al. (1957). The relationship of epinephrine and glucagon to liver phosphorylase. IV. Effect of epinephrine and glucagon on the reactivation of phosphorylase in liver homogenates. *J Biol Chem., 224*(1), 463-75.

Bilski AJ et al. (1983). The pharmacology of a beta 2-selective adrenoceptor antagonist (ICI 118,551). *J Cardiovasc Pharmacol., 5*(3), 430-7.

Calkins et al. (2017). 2017 HRS/EHRA/ECAS/APHRS/SOLAECE expert consensus statement on catheter and surgical ablation of atrial fibrillation. *Heart Rhythm, 14*(10), 275-e444.

Cappato et al. (2010). Updated worldwide survey on the methods, efficacy, and safety of catheter ablation for human atrial fibrillation. *Circ Arrhythm Electrophysiol., 3*(1), 32-8.

Cavanaugh DJ et al. (1963). Disassociation of heart cells by collagenase. *Nature, 200*, 261-2.

Chakir K et al. (2003). The third intracellular loop and the carboxyl terminus of beta2-adrenergic receptor confer spontaneous activity of the receptor. *Mol Pharmacol., 64*(5), 1048-58.

Chimenti et al. (2010). Histological substrate of human atrial fibrillation. *Biomed Pharmacother., 64*(3), 177-83.

Christ et al. (2004). *L-type Ca2+ current downregulation in chronic human atrial fibrillation is associated with increased activity of protein phosphatases* (Vol. 110). Circulation.

Christ et al. (2006). Cilostamide potentiates more the positive inotropic effects of (−)-adrenaline through β2-adrenoceptors than the effects of (−)-noradrenaline through β1-adrenoceptors in human atrial myocardium. *Naunyn Schmiedebergs Arch Pharmacol., 374*(3), 249-53.

Christ et al. (2009). Inotropy and L-type Ca2+ current, activated by beta1- and beta2-adrenoceptors, are differently controlled by phosphodiesterases 3 and 4 in rat heart. *156*(1), 62-83.

Christ et al. (2011). Human atrial β(1L)-adrenoceptor but not β$_3$ -adrenoceptor activation increases force and Ca(2+) current at physiological temperature. *Br J Pharmacol., 162*(4), 823-39.

Christ et al. (2014). Arrhythmias, elicited by catecholamines and serotonin, vanish in human chronic atrial fibrillation. *Proc Natl Acad Sci U S A., 111*(30), 11193-8.

Christ T et al. (2004). An aqueous extract of the marine sponge Ectyoplasia ferox stimulates L-type Ca2+-current by direct interaction with the Cav1.2 subunit. *Naunyn Schmiedebergs Arch Pharmacol., 370*(6), 474-83.

Comtois et al. (2005). Of circles and spirals: bridging the gap between the leading circle and spiral wave concepts of cardiac reentry. *Europace., 2*, 10-20.

Dagres et al. (2009). Complications of atrial fibrillation ablation in a high-volume center in 1,000 procedures: still cause for concern? *J Cardiovasc Electrophysiol., 20*(9), 1014-9.

de Vos et al. (2010). Progression from paroxysmal to persistent atrial fibrillation clinical correlates and prognosis. *J Am Coll Cardiol., 55*(8), 725-31.

Deneke et al. (2015). Silent cerebral events/lesions related to atrial fibrillation ablation: a clinical review. *J Cardiovasc Electrophysiol., 26*(4), 455-463.

Dipilato et al. (2004). Fluorescent indicators of cAMP and Epac activation reveal differential dynamics of cAMP signaling within discrete subcellular compartments. *Proc Natl Acad Sci U S A., 101*(47), 16513-8.

Dobrev et al. (2005). The G protein-gated potassium current I(K,ACh) is constitutively active in patients with chronic atrial fibrillation. *Circulation., 112*(24), 3697-706.

Dooley DJ et al. (1986). CGP 20712 A: a useful tool for quantitating beta 1- and beta 2-adrenoceptors. *Eur J Pharmacol., 130*(1-2), 137-9.

El-Armouche et al. (2006). Molecular determinants of altered Ca2+ handling in human chronic atrial fibrillation. *Circulation., 114*(7), 670-80.

Elkayam et al. (1998). Calcium channel blockers in heart failure. *Cardiology., 89* , 38-46.

El-Sherief et al. (2013). Basics of cardiopulmonary bypass: normal and abnormal postoperative CT appearances. *RadioGrapichs, 33*(1), 63-72.

Engel A. (2013). Die Bedeutung von PDE 3 und PDE 4 für kontraktile Dysfunktion und Arrhythmieneigung bei chronischem Vorhofflimmern des Menschen.

Förster T. (2012). Energy migration and fluorescence. 1946. *J Biomed Opt., 17*(1), 011002.

Fenger-Groen et al. (2019). Depression, antidepressants, and the risk of non-valvular atrial fibrillation: A nationwide Danish matched cohort study. *Eur J Prev Cardiol., 26*(2), 187-195.

Fleming et al. (2008). Milrinone use is associated with postoperative atrial fibrillation after cardiac surgery. *Circulation., 118*(16), 1619-25.

Galindo TA et al. (2009). Ontogenic changes of the control by phosphodiesterase-3 and -4 of 5-HT responses in porcine heart and relevance to human atrial 5-HT(4) receptors. *Br J Pharmacol., 156*(2), 237-49.

Gille E at al. (1985). The affinity of (-)-propranolol for beta 1- and beta 2-adrenoceptors of human heart. Differential antagonism of the positive inotropic effects and adenylate cyclase stimulation by (-)-noradrenaline and (-)-adrenaline. *Naunyn Schmiedebergs Arch Pharmacol., 331*(1), 60-70.

Go et al. (2001). Prevalence of diagnosed atrial fibrillation in adults: national implications for rhythm management and stroke prevention: the AnTicoagulation and Risk Factors in Atrial Fibrillation (ATRIA) Study. *JAMA, 285*(18), 2370-5.

Goldberger et al. (2014). Digitalis use in contemporary clinical practice: refitting the foxglove. *JAMA Intern Med., 174*(1), 151-4.

Goldstein et al. (1991). Diltiazem increases late-onset congestive heart failure in postinfarction patients with early reduction in ejection fraction. The Adverse Experience Committee; and the Multicenter Diltiazem Postinfarction Research Group. *Circulation., 83*(1), 52-60.

Gonzales FD et al. (2011). Ingestion of Japanese plums (Prunus salicina Lindl. cv. Crimson Globe) increases the urinary 6 sulfatoxymelatonin and total antioxidant capacity levels in young, middle-aged and elderly humans: Nutritional and functional characterization of their content. *Journal of food and nutrition research, 50*, 229-236.

Grammer et al. (2001). Atrial L-type Ca2+-channel, beta-adrenorecptor, and 5-hydroxytryptamine type 4 receptor mRNAs in human atrial fibrillation. *Basic Res Cardiol., 96*(1), 82-90.

Greiser et al. (2014). Tachycardia-induced silencing of subcellular Ca2+ signaling in atrial myocytes. *J Clin Invest., 124*(11), 4759–4772.

Haissaguerre et al. (1998). Spontaneous initiation of atrial fibrillation by ectopic beats originating in the pulmonary veins. *N Engl J Med., 339*(10), 659-66.

Hall J et al. (1990). Selective beta 1-adrenoceptor blockade enhances positive inotropic responses to endogenous catecholamines mediated through beta 2-adrenoceptors in human atrial myocardium. *Circ Res., 66*(6), 1610-23.

Hart et al. (2007). Meta-analysis: antithrombotic therapy to prevent stroke in patients who have nonvalvular atrial fibrillation. *Ann Intern Med., 146*(12), 857-67.

Heubach et al. (2002). Physiological antagonism between ventricular beta 1-adrenoceptors and alpha 1-adrenoceptors but no evidence for beta 2- and beta 3-adrenoceptor function in murine heart. *Br J Pharmacol., 136*(2), 217-29.

Hoffmann et al. (2004). Comparative pharmacology of human beta-adrenergic receptor subtypes--characterization of stably transfected receptors in CHO cells. *Naunyn Schmiedebergs Arch Pharmacol., 369*(2), 151-9.

Iwasaki et al. (2011). Atrial fibrillation pathophysiology: implications for management. *Circulation., 124*(20), 2264-74.

January et al. (2014). 2014 AHA/ACC/HRS guideline for the management of patients with atrial fibrillation: executive summary: a report of the American College of Cardiology/American Heart Association Task Force on practice guidelines and the Heart Rhythm Society. *Circulation, 130*(23), 2071-104.

Kalman et al. (1995). Atrial fibrillation after coronary artery bypass grafting is associated with sympathetic activation. *Ann Thorac Surg., 60*(6), 1709-15.

Kaumann AJ. (1994). Do human atrial 5-HT4 receptors mediate arrhythmias? *Trends Pharmacol Sci., 15*(12), 451-5.

Kaumann AJ. (2013). Surprises from a cardiac 5-HT$_4$ TG mouse: spontaneous atrial arrhythmias by endogenous 5-HT of atrial origin? Different mechanism of arrhythmias through 5-HT$_4$ receptors and β-adrenoceptors? *Naunyn Schmiedebergs Arch Pharmacol., 386*(5), 353-6.

Kaumann AJ and Molenaar P. (1997). Modulation of human cardiac function through 4 beta-adrenoceptor populations. *Naunyn Schmiedebergs Arch Pharmacol., 355*(6), 667-81.

Kaumann AJ et al. (1989). A comparison of the effects of adrenaline and noradrenaline on human heart: the role of beta 1- and beta 2-adrenoceptors in the stimulation of adenylate cyclase and contractile force. *Eur Heart J., 10* , 29-37.

Kaumann et al. (1990). A 5-hydroxytryptamine receptor in human atrium. *Br J Pharmacol., 100*(4), 879-85.

Kaumann et al. (1993). Both beta 1- and beta 2-adrenoceptors mediate catecholamine-evoked arrhythmias in isolated human right atrium. *Naunyn Schmiedebergs Arch Pharmacol., 348*(5), 536-40.

Kaumann et al. (1996). Comparison of the densities of 5-HT4 receptors, beta 1- and beta 2-adrenoceptors in human atrium: functional implications. *Naunyn Schmiedebergs Arch Pharmacol., 353*(5), 592-5.

Kaumann et al. (2006). 5-hydroxytryptamine receptors in the human cardiovascular system. *Pharmacol Ther., 111*(3), 674-706.

Kelly Freeman et al. (2012). Clinical Considerations for Roflumilast: A New Treatment for COPD. *Consult Pharm., 27*(3), 189-93.

Koivumäki et al. (2014). In silico screening of the key cellular remodeling targets in chronic atrial fibrillation. *PLoS Comput Biol., 10*(5), e1003620.

Kotecha et al. (2014). Efficacy of β blockers in patients with heart failure plus atrial fibrillation: an individual-patient data meta-analysis. *Lancet., 384*(9961), 2235-43.

Kovács et al. (2004). Mechanism of blebbistatin inhibition of myosin II. *J Biol Chem, 279*(34), 35557-63.

Kraft A. (2019). Phosphodiesterases 4B and 4D Differentially Regulate cAMP Signaling in Calcium Handling Microdomains of Adult Mouse Cardiomyocytes.

Lapi et al. (2015). The use of antidepressants and the risk of chronic atrial fibrillation. *J Clin Pharmacol., 55*(4), 423-30.

Lee CH et al. (2015). Inhaled bronchodilators and the risk of tachyarrhythmias. *Int J Cardiol., 190*, 133-9.

Leroy J et al. (2008). Spatiotemporal dynamics of beta-adrenergic cAMP signals and L-type Ca2+ channel regulation in adult rat ventricular myocytes: role of phosphodiesterases. *Circ Res., 102*(9), 1091-100.

Lim et al. (2007). Ablate and pace strategy for atrial fibrillation: long-term outcome of AIRCRAFT trial. *Europace., 9*(7), 498-505.

Llyod-Jones et al. (2004). Lifetime risk for development of atrial fibrillation: the Framingham Heart Study. *Circulation, 110*(9), 1042-6.

Lohse MJ et al. (2008). Optical techniques to analyze real-time activation and signaling of G-protein-coupled receptors. *Trends Pharmacol Sci., 29*(3), 159-65.

Mika et al. (2013). Differential regulation of cardiac excitation-contraction coupling by cAMP phosphodiesterase subtypes. *Cardiovasc Res., 100*(2), 336-46.

Mironov et al. (2009). Imaging cytoplasmic cAMP in mouse brainstem neurons. *BMC Neurosci., 10*(29).

Miyawaki A. et al. (2003). Visualization of the spatial and temporal dynamics of intracellular signaling. *Dev Cell., 4*(3), 295-305.

Mo et al. (2017). The β3 -adrenoceptor agonist mirabegron increases human atrial force through β1 -adrenoceptors: an indirect mechanism? *Br J Pharmacol., 174*(16), 2706-2715.

Molenaar et al. (2013). PDE3, but not PDE4, reduces β_1 - and β_2 -adrenoceptor-mediated inotropic and lusitropic effects in failing ventricle from metoprolol-treated patients. *169*(3), 528-38.

Molina et al. (2012). Cyclic adenosine monophosphate phosphodiesterase type 4 protects against atrial arrhythmias. *Journal of the American College of Cardiology, 59*(24), 2182-2190.

Murphy et al. (2007). A national survey of the prevalence, incidence, primary care burden and treatment of atrial fibrillation in Scotland. *Heart, 93*(5), 606-12.

Nguyen et al. (2009). Histopathological substrate for chronic atrial fibrillation in humans. *Heart Rhythm., 6*(4), 454-60.

Nikolaev VO et al. (2004). Novel single chain cAMP sensors for receptor-induced signal propagation. *J Biol Chem., 279*(36), 37215-8.

Nikolaev VO et al. (2006). Monitoring of cAMP synthesis and degradation in living cells. *Physiology (Bethesda), 21*, 86-92.

Nikolaev VO et al. (2010). Beta2-adrenergic receptor redistribution in heart failure changes cAMP compartmentation. *Science, 327*(5973), 1653-7.

Oba et al. (2013). Efficacy and safety of roflumilast in patients with chronic obstructive pulmonary disease: a systematic review and meta-analysis. *Ther Adv Respir Dis., 7*(1), 13-24.

Olesen et al. (2015). Non-vitamin K antagonist oral anticoagulation agents in anticoagulant naïve atrial fibrillation patients: Danish nationwide descriptive data 2011-2013. *Europace., 17*(2), 187-93.

Omori et al.,. (2007). Overview of PDEs and their regulation. *Circ Res., 100*(3), 309-27.

Peng-Sheng Chen et al.,. (2014). Role of the Autonomic Nervous System in Atrial Fibrillation: Pathophysiology and Therapy. *Circ Res., 114*(9), 1500–1515.

Ponikowski et al. (2016). 2016 ESC Guidelines for the diagnosis and treatment of acute and chronic heart failure: The Task Force for the diagnosis and treatment of acute and chronic heart failure of the European Society of Cardiology (ESC). *Eur Heart J., 37*(27), 2129-2200.

Queiroga et al. (2003). Ablate and pace revisited: long term survival and predictors of permanent atrial fibrillation. *Heart., 89*(9), 1035-8.

Rabe et al.,. (2005). Roflumilast--an oral anti-inflammatory treatment for chronic obstructive pulmonary disease: a randomised controlled trial. *Lancet., 366*(9485), 563-71.

Rehmann H. et al. (2003). Communication between the regulatory and the catalytic region of the cAMP-responsive guanine nucleotide exchange factor Epac. *J Biol Chem., 278*(26), 23508-14.

Rochais et al. (2006). A specific pattern of phosphodiesterases controls the cAMP signals generated by different Gs-coupled receptors in adult rat ventricular myocytes. *Circ Res., 98*(8), 1081-8.

Rooij J. et al. (1998). Epac is a Rap1 guanine-nucleotide-exchange factor directly activated by cyclic AMP. *Nature, 396*(6710), 474-7.

Rozmaritsa et al. (2014). Attenuated response of L-type calcium current to nitric oxide in atrial fibrillation. *Cardiovasc Res., 101*(3), 533-42.

Salpeter et al. (2004). Cardiovascular effects of beta-agonists in patients with asthma and COPD: a meta-analysis. *Chest., 125*(6), 2309-21.

Sanders L. and Kaumann AJ. (1992). A 5-HT4-like receptor in human left atrium. *Naunyn Schmiedebergs Arch Pharmacol., 345*(4), 382-6.

Sanders L. et al. (1995). Sensitization of human atrial 5-HT4 receptors by chronic beta-blocker treatment. *Circulation., 92*(9), 2526-39.

Sarkar M. and Prabhu V. (2017). Basics of cardiopulmonary bypass. *Indian J Anaesth., 61*(9), 760–767.

Schleicher et al.,. (2018). Using cAMP Sensors to Study Cardiac Nanodomains. *J Cardiovasc Dev Dis., 5*(1).

Schmidt et al. (2015). Upregulation of K(2P)3.1 K+ Current Causes Action Potential Shortening in Patients With Chronic Atrial Fibrillation. *Circulation., 132*(2), 82-92.

Schotten et al. (2011). Pathophysiological mechanisms of atrial fibrillation: a translational appraisal. *Physiol Rev., 91*(1), 265-325.

Schreck et al. (1997). Emergency management of atrial fibrillation and flutter: intravenous diltiazem versus intravenous digoxin. *Ann Emerg Med., 29*(1), 135-40.

Segal et al. (2000). The evidence regarding the drugs used for ventricular rate control. *J Fam Pract., 49*(1), 47-59.

Spach et al. (1994). Initiating reentry: the role of nonuniform anisotropy in small circuits. *J Cardiovasc Electrophysiol., 5*(2), 182-209.

Sprenger JU et al. (2012). FRET microscopy for real-time monitoring of signaling events in live cells using unimolecular biosensors. *J Vis Exp., 20*(66), e4081.

Sudo et al. (2000). Potent effects of novel anti-platelet aggregatory cilostamide analogues on recombinant cyclic nucleotide phosphodiesterase isozyme activity. *Biochem Pharmacol., 59*(4), 347-56.

Tisdale et al. (1998). A randomized, double-blind comparison of intravenous diltiazem and digoxin for atrial fibrillation after coronary artery bypass surgery. *Am Heart J., 135*(5 Pt 1), 739-47.

Ulimoen et al. (2013). Comparison of four single-drug regimens on ventricular rate and arrhythmia-related symptoms in patients with permanent atrial fibrillation. *Am J Cardiol., 111*(2), 225-30.

Van Wagoner et al. (1999). Atrial L-type Ca^{2+} currents and human atrial fibrillation. *Circ Res., 85*(5), 428-36.

Vargas et al. (2006). Phosphodiesterase PDE3 blunts the positive inotropic and cyclic AMP enhancing effects of CGP12177 but not of noradrenaline in rat ventricle. *Br J Pharmacol., 147*(2), 158-63.

Voigt et al. (2012). Enhanced sarcoplasmic reticulum Ca^{2+} leak and increased Na^+-Ca^{2+} exchanger function underlie delayed afterdepolarizations in patients with chronic atrial fibrillation. *Circulation., 125*(17), 2059-70.

Voigt et al. (2014). Cellular and molecular mechanisms of atrial arrhythmogenesis in patients with paroxysmal atrial fibrillation. *Circulation., 129*(2), 145-156.

Voigt et al. (2015). Methods for isolating atrial cells from large mammals and humans. *J Mol Cell Cardiol., 86*, 187-98.

Workmann et al. (2010). Cardiac adrenergic control and atrial fibrillation. *Naunyn Schmiedebergs Arch Pharmacol., 381*(3), 235-49.

Wynn et al. (2014). Efficacy of catheter ablation for persistent atrial fibrillation: a systematic review and meta-analysis of evidence from randomized and nonrandomized controlled trials. *Circ Arrhythm Electrophysiol., 7*(5), 841-52.

Zhang J. et al. (2002). Creating new fluorescent probes for cell biology. *Nat Rev Mol Cell Biol., 3*(12), 906-18.

Zoni Berisso et al. (2014). Epidemiology of atrial fibrillation: European perspective. *Clin Epidemiol, 6*, 213–220.

Zuo et al. (2018). Cigarette smoke up- regulates PDE3 and PDE4 to decrease cAMP in airway cells. *Br J Pharmacol., 175*(14), 2988–3006.

7. Supplements

7.1 Materials, devices and codes

Tabella 14: Consumable materials

Product	Manufacturer, #
250 mL Vacuum Filtration "rapid"-Filtermax	TPP, 99500
500 mL Vacuum Filtration "rapid"-Filtermax	TPP, 99500
Aspiration pipette 2 mL	Sarstedt, 86.1252.011
Cell culture flask T175	Sarstedt, 83.3911.002
Cell culture flask T80	Nunc, 178905
Cell culture flask T75/T175 for suspension culture	Sarstedt, 83.3911/2.502
Cell culture microplate 96 well µClear black CELLSTAR	Greiner Bio-One, 655090
Cell culture 96- well glass bottom plates	MatTek, p96G- 1.5- 5- F
Cell culture plate 6 / 12 / 24-well	Nunc
Cell scraper	Sarstedt, 83.1830
Cell strainer 30 µm	Sysmex, 04-004-2326
Cryovial CryoPure 1.6 mL	Sarstedt, 72.380
Neubauer counting chamber	Karl-Hecht KG
Pipette tips	Sarstedt
Pipette tips with Biosphere filter	Sarstedt
Reaction tube graduated 15 mL	Sarstedt, 62.554.502
Reaction tubes conical 15 / 50 mL	Sarstedt
Reaction tubes Safe Lock 0.2 – 2 mL	Eppendorf
Round bottom tube 12 mL	Greiner Bio-One, 163160
Serological pipettes 1 / 2 / 5 / 10 / 25 / 50 mL	Sarstedt
Spinner flasks 500 / 1000 mL	Integra Biosciences, 182101 / 182051
Syringe filtration unit Filtropur S 0.2 µm	Sarstedt, 83.1826.001
TissueLyser Steel Beads	QIAGEN, 69989

Tabella 15: Laboratory devices

Product	Manufacturer, #
accu-jet pro	Brand
Beamsplitter DV2	Photometrix
Cell culture incubator	Binder
Cell culture incubators S2020 1.8, HERAcell 240 & 150i	Thermo Fischer Scientific
Cell culture incubators MCO-19M & MCO-20AIC	Sanyo
Centrifuge Fresco 17	Thermo Fisher Scientific
Centrifuges 5415 R & 5810 R	Eppendorf
Centrifuge J-6B	Beckmann
Centrifuges Rotanta/RP & Universal 30 RF	Hettich
ChemiDocTM Touch Imaging System	Bio-Rad Laboratories
Class II Biological Safety Cabinet	Labgard
CO_2 Incubator	Sanyo
Confocal microscope (LSM800, Airyscan)	Zeiss
Confocal microscope Nikon A1	Nikon
Cryopreservation system Asymptote EF600M	Grant Instruments
Electrophoretic Transfer Cell Mini Trans-Blot cell	Bio-Rad Laboratories
Filter Cube 05-EM	Photometrix
Freezer Comfort	Liebherr
Fridge Comfort	Liebherr
Gel electrophoresis cell Mini-PROTEAN 3 Cell	Bio-Rad Laboratories
Gel electrophoresis tank Sub-cell GT	Bio-Rad Laboratories
Inverted microscope IX73	Olympus
ISM831C	Ismatec
LED KL 1600	Schott
LED pE-100 440 nm	CoolLED
Leica DMI3000 B	Leica
Leica TCS SP5	Leica
LX 320A scs	Precisa
Magnetic stirring and heating plate IKA Combimag RET	Janke & Kunkel & Co KG

Magnetic stirring plate Variomag / Cimarec Biosystem Direct	Thermo Scientific
Magnetic stirring plate Variomag / Cimarec Biosystem 4 Direct	Thermo Scientific
Microscope Axioskop 2 with AxioCam Color	Zeiss
Microscope Axiovert 25 with ProgRes Speed XT core 5 camera	Jenoptik
Microscope EVOS FL Cell Imaging System	Thermo Fischer Scientific
my FUGE	Benchmark
optiMOS	Q imaging
Paraffin Dispenser EG 1120	Leica
PCB1000-2	KERN
pH Level 1	inoLab
Pipettes 10 / 100 / 1000 µL	Eppendorf
Pipette controller Accu-jet pro	Brand
Power supply PowerPac Basic	Bio-Rad Laboratories
Precision Advanced Scale	Ohaus
Puller DMZ	Hilgenberg
RCT standard	IKA
Research plus (10 µL - 10 mL)	eppendorf
S88X dual output square pulse stimulator	Grass
Safety workbench HeraSafe	Heraeus
Safety workbench Safe 2020	Thermo Fischer Scientific
Shaker DRS-12	ELMI
SMZ 745T	Nikon
Thermomixer comfort	Eppendorf
TissueLyser	QIAGEN
Vortex-Genie 2	Scientific Industries
Water Bath	Julabo

Tabella 16: Laboratory softwares

Product	Manufacturer, #
Excel 2013	Microsoft
Fiji 1.52e	NIH
Graph Pad Prism 5.0	GraphPad
Image Lab Version 5.2.1	Bio-Rad Laboratories
ImageJ 1.47v	Wayne Rasband
LabChart 5.51	ADInstruments
Mendeley Desktop 1.15.2	Mendeley
Micro-Manager 1.4.5	Open Imaging
PowerPoint 2013	Microsoft
Word 2013	ZEN
ZEN 2.5	Carl Zeiss

Tabella 17: GHS hazard. H-codes

Code	Phrase
H200	Unstable explosive
H201	Explosive; mass explosion hazard
H202	Explosive; severe projection hazard
H203	Explosive; fire, blast or projection hazard
H204	Fire or projection hazard
H205	May mass explode in fire
H206	Fire, blast or projection hazard: increased risk of explosion if desensitizing
H207	Fire or projection hazard: increased risk of explosion if desensitizing agent is
H208	Fire hazard: increased risk of explosion if desensitizing agent is reduced
H220	Extremely flammable gas
H221	Flammable gas
H222	Extremely flammable aerosol

H223	Flammable aerosol
H224	Extremely flammable liquid and vapour
H225	Highly flammable liquid and vapour
H226	Flammable liquid and vapour
H227	Combustible liquid
H228	Flammable solid
H229	Pressurized container: may burst if heated
H230	May react explosively even in the absence of air
H231	May react explosively even in the absence of air at elevated pressure and/or
H232	May ignite spontaneously if exposed to air
H240	Heating may cause an explosion
H241	Heating may cause a fire or explosion
H242	Heating may cause a fire
H250	Catches fire spontaneously if exposed to air
H251	Self-heating; may catch fire
H252	Self-heating in large quantities; may catch fire
H260	In contact with water releases flammable gases which may ignite
H261	In contact with water releases flammable gas
H270	May cause or intensify fire; oxidizer
H271	May cause fire or explosion; strong oxidizer
H272	May intensify fire; oxidizer
H280	Contains gas under pressure; may explode if heated
H281	Contains refrigerated gas; may cause cryogenic burns or injury
H290	May be corrosive to metals

H311	Toxic in contact with skin
H312	Harmful in contact with skin
H313	May be harmful in contact with skin
H314	Causes severe skin burns and eye damage
H315	Causes skin irritation
H316	Causes mild skin irritation
H317	May cause an allergic skin reaction
	Causes serious eye damage
H319	Causes serious eye irritation
H320	Causes eye irritation
H330	Fatal if inhaled
H331	Toxic if inhaled
H332	Harmful if inhaled
H333	May be harmful if inhaled
H334	May cause allergy or asthma symptoms or breathing difficulties if inhaled
H335	May cause respiratory irritation
H336	May cause drowsiness or dizziness
H340	May cause genetic defects
H341	Suspected of causing genetic defects
H350	May cause cancer
H351	Suspected of causing cancer
H360	May damage fertility or the unborn child
H361	Suspected of damaging fertility or the unborn child
H361d	Suspected of damaging the unborn child

H361e	May damage the unborn child
H361f	Suspected of damaging fertility
H361g	May damage fertility
H362	May cause harm to breast-fed children
H370	Causes damage to organs
H371	May cause damage to organs
H372	Causes damage to organs through prolonged or repeated exposure
H373	May cause damage to organs through prolonged or repeated exposure
H300+H310	Fatal if swallowed or in contact with skin
H300+H330	Fatal if swallowed or if inhaled
H310+H330	Fatal in contact with skin or if inhaled
H300+H310+H330	Fatal if swallowed, in contact with skin or if inhaled
H301+H311	Toxic if swallowed or in contact with skin
H301+H331	Toxic if swallowed or if inhaled
H311+H331	Toxic in contact with skin or if inhaled
H301+H311+H331	Toxic if swallowed, in contact with skin or if inhaled
H302+H312	Harmful if swallowed or in contact with skin
H302+H332	Harmful if swallowed or if inhaled
H312+H332	Harmful in contact with skin or if inhaled
H302+H312+H332	Harmful if swallowed, in contact with skin or if inhaled
H303+H313	May be harmful if swallowed or in contact with skin
H303+H333	May be harmful if swallowed or if inhaled
H313+H333	May be harmful in contact with skin or if inhaled
H303+H313+H333	May be harmful if swallowed, in contact with skin or if inhaled

Code	Phrase
H315+H320	Causes skin and eye irritation
H400	Very toxic to aquatic life
H401	Toxic to aquatic life
H402	Harmful to aquatic life
H410	Very toxic to aquatic life with long-lasting effects
H411	Toxic to aquatic life with long-lasting effects
H412	Harmful to aquatic life with long-lasting effects
H413	May cause long-lasting harmful effects to aquatic life
H420	Harms public health and the environment by destroying ozone in the upper
H433	Harmful to terrestrial vertebrates

Tabella 18: GHS hazard. P-codes

Code	Phrase
P101	If medical advice is needed, have product container or label at hand
P102	Keep out of reach of children
P103	Read label before use
P201	Obtain special instructions before use
P202	Do not handle until all safety precautions have been read and understood
P210	Keep away from heat, hot surfaces, sparks, open flames and other ignition
P211	Do not spray on an open flame or other ignition source
P220	Keep/Store away from clothing/…/combustible materials
P221	Take any precaution to avoid mixing with combustibles
P222	Do not allow contact with air
P223	Do not allow contact with water
P230	Keep wetted with …
P231	Handle under inert gas

P232	Protect from moisture
P233	Keep container tightly closed
P234	Keep only in original container
P235	Keep cool
P240	Ground/bond container and receiving equipment
P241	Use explosion-proof electrical/ventilating/lighting/…/equipment
P242	Use only non-sparking tools
P243	Take precautionary measures against static discharge
P244	Keep valves and fittings free from oil and grease
P250	Do not subject to grinding/shock/…/friction
P251	Do not pierce or burn, even after use
P260	Do not breathe dust/fumes/gas/mist/vapours/spray
P261	Avoid breathing dust/fumes/gas/mist/vapours/spray
P262	Do not get in eyes, on skin, or on clothing
P263	Avoid contact during pregnancy/while nursing
P264	Wash … thoroughly after handling
P270	Do not eat, drink or smoke when using this product
P271	Use only outdoors or in a well-ventilated area
P272	Contaminated work clothing should not be allowed out of the workplace
P273	Avoid release to the environment
P280	Wear protective gloves/protective clothing/eye protection/face protection
P282	Wear cold insulating gloves/face shield/eye protection
P283	Wear fire/flame resistant/retardant clothing
P284	[In case of inadequate ventilation] wear respiratory protection
P301	IF SWALLOWED
P302	IF ON SKIN
P303	IF ON SKIN (or hair)

P304	IF INHALED
P305	IF IN EYES
P306	IF ON CLOTHING
P308	If exposed or concerned
P310	Immediately call a POISON CENTER/doctor/…
P311	Call a POISON CENTER/ doctor/…
P312	Call a POISON CENTER/ doctor/…/if you feel unwell
P313	Get medical advice/attention
P314	Get medical advice/attention if you feel unwell
P315	Get immediate medical advice/attention
P320	Specific treatment is urgent (see … on this label)
P321	Specific treatment (see … on this label)
P330	Rinse mouth
P331	Do NOT induce vomiting
P332	If skin irritation occurs:
P333	If skin irritation or a rash occurs:
P334	Immerse in cool water/wrap in wet bandages
P335	Brush off loose particles from skin
P336	Thaw frosted parts with lukewarm water. Do not rub affected areas
P337	If eye irritation persists:
P338	Remove contact lenses if present and easy to do. Continue rinsing.
P340	Remove person to fresh air and keep comfortable for breathing.
P342	If experiencing respiratory symptoms:
P351	Rinse cautiously with water for several minutes
P352	Wash with plenty of water/…
P353	Rinse skin with water/shower
P360	Rinse immediately contaminated clothing and skin with plenty of water

P361	Take off immediately all contaminated clothing
P362	Take off contaminated clothing
P363	Wash contaminated clothing before reuse
P364	And wash it before reuse
P370	In case of fire:
P371	In case of major fire and large quantities:
P372	Explosion risk in case of fire
P373	DO NOT fight fire when fire reaches explosives
P374	Fight fire with normal precautions from a reasonable distance
P375	Fight fire remotely due to the risk of explosion
P376	Stop leak if safe to do so
P377	Leaking gas fire – do not extinguish unless leak can be stopped safely
P378	Use … to extinguish
P380	Evacuate area
P381	Eliminate all ignition sources if safe to do so
P391	Collect spillage
P301+310	IF SWALLOWED: Immediately call a POISON CENTER/doctor/…
P301+312	IF SWALLOWED: Call a POISON CENTER/doctor/…/if you feel unwell
P301+330+331	IF SWALLOWED: Rinse mouth. Do NOT induce vomiting
P302+334	IF ON SKIN: Immerse in cool water/wrap in wet bandages
P302+352	IF ON SKIN: Wash with plenty of water/…
P303+361+353	IF ON SKIN (or hair): Take off immediately all contaminated clothing. Rinse
P304+312	IF INHALED: Call a POISON CENTER or doctor/physician if you feel
P304+340	IF INHALED: Remove person to fresh air and keep comfortable for
P305+351+338	IF IN EYES: Rinse cautiously with water for several minutes. Remove
P306+360	IF ON CLOTHING: Rinse immediately contaminated clothing and skin with
P308+311	If exposed or concerned: Call a POISON CENTER/ doctor/…

P308+313	If exposed: Call a POISON CENTER or doctor/physician
P332+313	If skin irritation occurs: Get medical advice/attention
P333+313	If skin irritation or a rash occurs: Get medical advice/attention
P335+334	Brush off loose particles from skin. Immerse in cool water/wrap in wet
P337+313	If eye irritation persists get medical advice/attention
P342+311	If experiencing respiratory symptoms: Call a POISON CENTER/doctor/…
P361+364	Take off immediately all contaminated clothing and wash it before reuse
P362+364	Take off contaminated clothing and wash it before reuse
P370+376	In case of fire: Stop leak if safe to do so
P370+378	In case of fire: Use … to extinguish
P370+380	In case of fire: Evacuate area
P370+380+375	In case of fire: Evacuate area. Fight fire remotely due to the risk of explosion
P371+380+375	In case of major fire and large quantities: Evacuate area. Fight fire remotely
P401	Store …
P402	Store in a dry place
P403	Store in a well-ventilated place
P404	Store in a closed container
P405	Store locked up
P406	Store in a corrosive resistant/… container with a resistant inner liner
P407	Maintain air gap between stacks/pallets
P410	Protect from sunlight
P411	Store at temperatures not exceeding … °C/… °F
P412	Do not expose to temperatures exceeding 50 °C/122 °F
P413	Store bulk masses greater than … kg/… lbs at temperatures not exceeding …
P420	Store away from other materials
P422	Store contents under …
P402+404	Store in a dry place. Store in a closed container

P403+233	Store in a well-ventilated place. Keep container tightly closed
P403+235	Store in a well-ventilated place. Keep cool
P410+403	Protect from sunlight. Store in a well-ventilated place
P410+412	Protect from sunlight. Do not expose to temperatures exceeding 50 °C/122 °F
P411+235	Store at temperatures not exceeding … °C/… °F. Keep cool
P501	Dispose of contents/container to …
P502	Refer to manufacturer/supplier for information on recovery/recycling

7.2 List of abbreviations

A	
α-AR	Alpha -adrenergic receptor
AC	Adenylyl cyclase
ACE	Angiotensin converting enzyme
AE	Adverse event
AF	Atrial fibrillation
AHA/ACC/HRS	American Heart Association/American College of Cardiology/Heart Rhythm Society
AKAP	A-kinase anchoring proteins
AP	Action potential
APD	Action potential duration
AT1	Angiotensin II receptor antagonist
ATP	Adenosine triphosphate
AV	Atrioventricular
B	
β_1-AR	Beta 1-adrenergic receptor
β_2-AR	Beta 2-adrenergic receptor
BSA	Bovine serum albumin
C	
cAMP	Cyclic adenosine monophosphate
cDNA	Complementary DNA

CFP	Cyan fluorescent protein
CI	Confident interval
Cil	Cilostamide
CM	Cardiomyocyte
CNBD	Cyclic Nucleotide-Binding Domain
COPD	Chronic obstructive pulmonary disease
CPB	Cardiopulmonary bypass
CRC	Concentration response curve
Ctrl	Control
CV	Conduction velocity
D	
Da	Dalton
DA	Dopamine
DAD	Delayed afterdepolarization
DC	Cardioversion
dia	Diameter
DNA	Deoxyribonucleic acid
E	
EAD	Early afterdepolarization
ECC	Excitation-contraction coupling
ECFP	Enhanced cyan fluorescent protein
ECG	Electrocardiograph
EC-50	Effective concentration 50%
EDTA	Ethylenediaminetetraacetic acid
Epi	Epinephrine
ERP	Effective refractory period
F	
FBS	Fetal bovine serum
FRET	Förster resonance energy transfer or fluorescence resonance energy transfer
FSK	Forskolin

G	
GPCR	G-proteins coupled receptor
Gs	G-proteins
H	
h	Hour
HAM	Human atrium myocyte
HR	Hazard ratio
Hz	Herz
I	
IBMX	3-isobutyl-1-methylxanthine
I_{CaL}	Calcium L-type current
ICUE1	indicator of cAMP using Epac 1
I_f	Pacemaker current
I_{k1}	Inward rectifier K^+ current
ISO	Isoprenaline
I_{ti}	Transient inward current
IVC	Inferior vena cava
L	
LA	Left atrium
LABA	Long-acting inhaled β agonist
LAMA	Long-acting inhaled muscarinic antagonist
LTCC	Voltage-dependent L-type calcium channel
LVEF	Left ventricular ejection fraction
M	
μg	Microgram
μL	Microliter
μm	Micrometre
MEM	Minimum essential medium
mg	Milligram
min	Minutes

mL	Millilitre
mm	Millimetre
MOI	Multiplicity of infection
mRNA	Messenger RNA
N	
NA	Noradrenaline
NC	Nitrocellulose
NE	Norepinephrine
NOAC	Non-vitamin K antagonist oral anticoagulant
P	
paAF	Paroxysmal atrial fibrillation
PBS	Phosphate-buffered saline
PCR	Polymerase chain reaction
PDE	Phosphodiesterase
PDEi	PDE inhibitor
peAF	Persistent atrial fibrillation
PKA	Protein kinase A
PLB	Phospholamban
pm	plasma membrane
PV	Pulmonary vein
PVDF	Polyvinylidene fluoride
Q	
Q1-4	Quartile 1-4
R	
RA	Right atrium
RAPGEF3	Rap Guanine Nucleotide Exchange Factor 3
Ref	Referent
RNA	Ribonucleic acid
Rol	Rolipram
RP	Refractory period

RR	Relative risk
RT	Room temperature
RT-PCR	Real time - PCR
RyR2	Ryanodine receptor 2
S	
SDS	Sodium dodecyl sulfate
SEM	Standard error of the mean
Sr	Sarcoplasmic reticulum
SR	Sinus rhythm
SVC	Superior vena cava
T	
TnI	Troponin I
TnT	Troponin T
TnC	Troponin C
TPER	Tissue Protein Extraction Reagent
TBS	Tris-buffered saline
TMC	Time matched control
U	
U	Unit
UKE	University Medical Center Hamburg Eppendorf
V	
VKA	Vitamin K antagonist
W	
WB	Western blot
WL	Wavelength
Y	
YFP	Yellow fluorescent protein
Others	
5-HT	Serotonin
$5\text{-}HT_4\text{-}R$	Serotonin receptor

| °C | Degree Celsius |

8. Abstract

Atrial fibrillation (AF) is a complex and multifactorial disease and the most common sustained cardiac arrhythmia in humans. Although the disease has been studied for many years, yet exhaustive treatments ensuring eradication of AF does not exist. According with the present literature, AF may be caused by two events: automaticity and/or re-entry. While re-entry is a macro phenomenon happening at the level of tissues connections, automaticity refers to the cellular mechanisms behind ectopic firing. In this thesis we focused indeed on the PKA/cAMP activation pathway and how it changes in cells and tissues isolated from patients in persistent AF (peAF) and paroxysmal AF (paAF).

All the experiments were performed in human atrial trabeculae and myocytes isolated from patients in sinus rhythm (SR), paAF and peAF. L-type Ca^{2+} current ($I_{Ca,L}$) was measured in human atrial myocytes by patch clamp in whole-cell configuration; contractile force and arrhythmias were measured in human atrial trabeculae at 1 Hz each at 37°C; cAMP was recorded in human atrial cells by application of FRET (Fluorescence resonance energy transfer), after previous transfection of the cells with adenovirus encoding for Epac1-camps. In every experimental approach we apply G-proteins coupled receptors agonists norepinephrine (NE), epinephrine (Epi) and serotonin (5-HT) in the presence and in the absence of inhibitors of phosphodiesterases 3 and 4 (PDE3 and PDE4).

PDE4B was higher expressed in peAF. However, selective inhibition of PDE4 by 10 μM rolipram did not increase $I_{Ca,L}$ neither in the absence nor in the presence of submaximum concentrations of NE or Epi in both SR and peAF. Furthermore, PDE4 inhibition did not shift the concentration response curve (CRC) for the positive inotropic effect of catecholamines to the left in SR as well as paAF and peAF. However, inhibition of PDE4 increased arrhythmias in SR and paAF but not in peAF. In peAF, increases in cAMP by $β_1$- and by $β_2$-AR stimulation are as high as in SR while increases after application of 5-HT are significantly smaller in peAF. Pre-treatment with PDE3 and PDE4 inhibitors succeeded to increase further cAMP levels in the presence of NE and Epi and restore the diminished response to 5-HT to same levels of catecholamines in peAF. In contrast, cAMP increases by inhibition of PDE3 and PDE4 alone were not different between SR and AF.

The arrhythmia induction by rolipram in SR and paAF was not accompanied by an increase in I_{Ca} and force. The rescue of 5-HT inotropy in peAF by inhibition of PDE3 and PDE4 was not accompanied by an increase in I_{Ca} and arrhythmias. These findings suggest that cAMP is differently regulated in hypothetical compartments relevant for I_{Ca}, inotropy and arrhythmias.
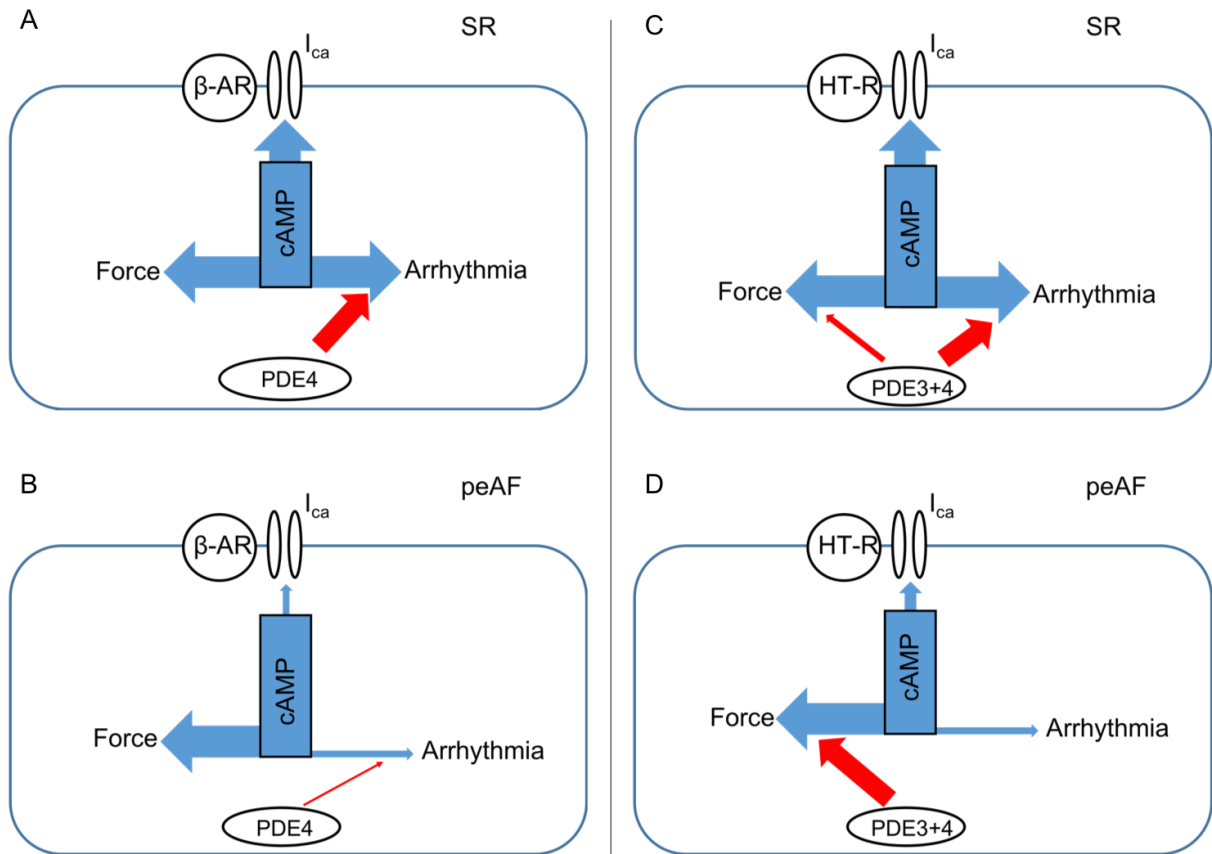
Figure 70: Graphical abstract
Activation of G-protein coupled receptors increases cAMP concentration differently pooled in cardiomyocytes. cAMP is globally located as well as located at the level of Force, Arrythmia and Ca^{2+}-channels. PDE3 and PDE4 differently control cAMP pools in cardiomyocytes. **A)** Cardiomyocyte in SR under stimulation of β-AR: PDE4 controls arrhythmia. **B)** Cardiomyocyte in peAF under stimulation of β-AR: PDE4 does not contribute recovering arrhythmia. **C)** Cardiomyocyte in SR under stimulation of HT-R: PDE3+4 slightly control force and significantly impact on arrhythmia. **D)** Cardiomyocyte in peAF under stimulation of HT-R: PDE3+4 strongly control force but do not regulate arrhythmia. In all schemes I_{Ca} is not moderated by PDE3 and/or PDE4.

9. Zusammenfassung

Vorhofflimmern (atrail fibrillation, AF) is eine komplexe und multifaktorielle Erkrankung, gleichzeitig die häufigste Herzrhythmusstörung des Menschen. Obgleich über viele Jahre Gegenstand intensiver Forschung, existiert bislang keine kausale Therapie. Nach aktueller Literaturlage kann AF entweder durch erhöhte Automatizität und/oder durch re-entry hervorgerufen werden. Während sich re-entry als Makro-Phänomen auf Gewebeebene abspielt ist erhöhte Impulsbildung ein zellulärer Mechanismus. In dieser Arbeit untersuchten wir in wie weit Aktivierung des PKA/cAMP Signalweges Zellen und Gewebe von Patienten im persistierenden AF (peAF) und paroxysmalen AF (paAF) beeinflusst.

Alle Experimente wurden in menschlichen Vorhoftrabekeln und Vorhofmyozyten von Patienten im Sinusrhythmus (SR), paAF und peAF ausgeführt. L-Typ Ca^{2+} Ströme in menschlichen Vorhofmyozyten wurden mittels patch clamp in der whole-cell Konfiguration, Kraft und Arrhythmien wurden in intakten menschlichen Vorhoftrabekeln bei 1 Hz jeweils bei 37 °C. CAMP wurde in menschlichen Vorhofzellen durch FRET, nach Transfektion der Zellen mit einem Adenovirus, codierend für den Sensor epac1-camps. In allen experimentellen Ansätzen wurden Agonisten von G-proteins gekoppelten Rezeptoren (Noradrenalin, Adrenalin und Serotonin) in Abwesenheit oder Anwesenheit von Hemmstoffen der Phosphodiesterase (PDE)3 bzw. 4.

Im peAF war die Expression der PDE4B höher. Allerdings erhöht die selektive Hemmung von PDE4 durch 10 µM Rolipram nicht den I_{Ca} weder in Abwesenheit noch in Anwesenheit submaximaler Konzentrationen von Noradrenalin oder Adrenalin, weder im Sinusrhythmus noch im peAF. Darüber hinaus führt Hemmung der PDE4 nicht zu einer Linksverschiebung der Konzentrations-Wirkungs-Kurve für den positiv inotropen Effekt der Katcecholamine. Hemmung der PDE4 verstärkt Arrhythmien im Sinusrhythmus und im paAF, aber nicht im peAF. Im peAF, nicht aber im paAF sind die cAMP Antworten durch Serotonin reduziert. Hemmung von PDE3 und PDE4 kann die reduzierte cAMP Antwort im peAF wiederherstellen. Dabei ist der Effekt einer Hemmung von PDE3 und PDE4 alleine im peAF nicht größer als im SR.

Die Arrhytmieinduktion durch Rolipram im SR war nicht von einem Anstieg des I_{Ca} und der Kraft begleitet. Das gleiche trifft zu für die die Wiederherstellung der 5-HT induzierten Inotropie durch Hemmung von PDE3 und PDE4 im peAF.

Die Ergebnisse lassen vermuten, dass im menschlichen Vorhof cAMP unterschiedlich reguliert wird für bislang hypothetische Kompartmente, relevant für I_{Ca}, Kraft und Arrhythmien.
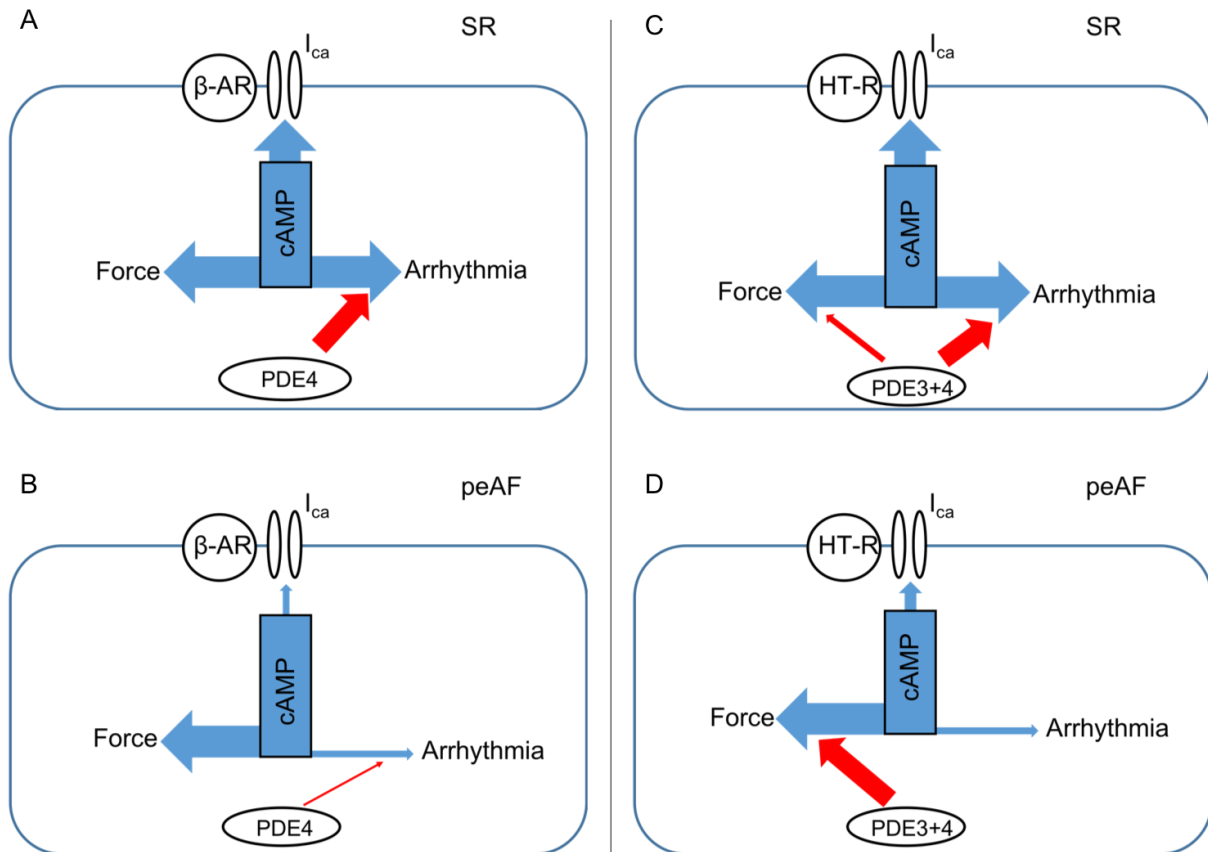
Abbildung 70: Graphischer Abstrakt

Aktivierung von G-Protein gekoppelten Rezeptoren erhöht die cAMP Konzentration in verschiedenen Pools von Kardiomyozyten. CAMP verteilt sich in globale Pools und solche relevant für Ca^{2+}-Kanäle, Kraft und Arrhythmien. PDE3 and PDE4 kontrollieren unterschiedliche pools von cAMP in Kardiomyozyten. **A)** Kardiomyozyten im SR nach Stimulation von β-AR: PDE4 begrenzt Arrhythmien, nicht jedoch die Kraft. **B)** Kardiomyozyten in peAF nach Stimulation von β-AR: keine Kontrolle von Arrhythmien durch PDE4. **C)** Kardiomyozyte im SR nach Stimulation von HT-R: PDE3+PDE4 kontrollieren Kraft und Arrhythmien. **D)** Kardiomyozyte im peAF nach stimulation von HT-R: PDE3+PDE4 haben eine großen Einfluß auf die Kraft aber nicht mehr auf Arrhythmien. . In allen Schemata hat PDE3 und/oder PDE keinen Einfluss auf die Rezeptor-vermittelten I_{Ca} Antworten.

10. Acknowledgments

Finally the biggest thank is for my supervisor Dr. Torsten Christ. He was able to guide me throughout my three years and half of PhD wisely and with competence. He really believed in my capacities in both bad and good times. He taught me to be tireless and to look always to the bright side.

I really appreciate the help of Dr. Geelhoed Bastiaan from the Department of General and Interventional Cardiology, in analyzing the FRET data in a mix model.

"Oh, I always let you down
You're shattered on the ground
But still I find you there
Next to me"
(Imagine Dragons – Next to me)

11. CV

Birth Place: Ivrea (Torino), Italy
Date of birth: 12/03/1989
Nationality: Italian
Address: Bahrenfelder Steindamm 109b, Hamburg, Germany
Mobile: +49 157 38702513
E-mail: dolcebernardo@gmail.com
Skype: bernardodolce
European driving license

Career highlights and aspirations

Marie Curie PhD student with a background in biology. Specializing mostly in cardiovascular pharmacology, live cell imaging and electrophysiology but with an interest also in learning new techniques. First author paper submitted and co-author publication. Lab tutoring.
My next goal would be to spend my acquired knowledge still in basic research.

Core competences

Cardiovascular pharmacology; Live cell imaging; FRET; Electrophysiology; Patch Clamp; Human cardiomyocytes; Human iPS Cells; Team working; Leadership skills.

WORK EXPERIENCE

From March 2018 to present ● Collaboration within my PhD at the Institute of Experimental Cardiovascular Research at Universitätsklinikum Hamburg Eppendorf, Germany.
To address the objectives of my PhD project, we established a collaboration with Dr. Cristina Molina in the research group of Prof. Viacheslav O. Nikolaev.
I am performing FRET experiments.

From May 2017 to July 2017 ● Visiting PhD fellow at the pharmaceutical company Acesion Pharma, University of Copenhagen, Denmark.
I mostly used manual and automated patch clamp on HEK cells. We performed cloning to mutate the binding site of the channels.
Supervisor: Prof. Bo Hjorth Bentzen.

From March 2016 to present ● Marie Skłodowska-Curie PhD fellow at Universitätsklinikum Hamburg Eppendorf, Germany.
Evaluation of PDEs activity on: regulations of I_{CaL}, arrhythmias, force development, cAMP. Evaluation of PDEs and G-coupled receptors expression: proteins levels, proteins localization and co-localization.
My PhD scholarship is an integrated part of AFib-TrainNet (http://afib.ku.dk/). AFib-TrainNet is funded from the Marie Skłodowska-Curie Actions as a European Training Network (ETN).
Supervisors: PD Dr Torsten Christ; Prof. Dr. Thomas Eschenhagen.

EDUCATION AND TRAINING

- ***From October 2012 to May 2015 ● Master of Science (MSc) in Applied Biomolecular Sciences at the University of Perugia, Italy.***
  Master thesis title: "Development of a protocol for the production of Bio-chemicals with high added value from agro-industrial waste."
  Grade 100/110.

- *From October 2008 to October 2012 ● Bachelor of Science (BSc) in Biology at the University of Perugia, Italy.*
  Bachelor thesis title: "Functional role of ion channels in the physiopathology of Glioblastoma". *Grade 96/110.*
- *Simula´s summer school in computational physiology (Oslo – June 2018)*
- *Research leadership, Management and Innovation Workshop (Oslo - February 2018)*
- *PhD summer school: Cardiac electrophysiology – basic and clinical aspects (Copenhagen - June 2017).*
- *Advanced Light Microscopy Workshop at UMIF (Hamburg - January 2017).*
- *Communicating Scientific Research 2016 at Simula Research (Oslo - May and September 2016).*

PUBBLICATIONS, POSTERS, CONGRESSES

Scientific Papers:
- "Impact of phosphodiesterases PDE3 and PDE4 on serotonin receptor 4 mediated increase of cAMP in atrial fibrillation" – Bernardo Dolce, Torsten Christ, Yalin Yaldirim, Herman Reichenspurner, Thomas Eschenhagen, Viacheslav Nikolaev, Alberto J Kaumann, Cristina Molina – Submitted in 2019.
- "A new negative allosteric modulator, AP14145, for the study of small conductance calcium-activated potassium ($K_{Ca}2$) channels" - Simó-Vicens R, Kirchhoff JE, Dolce B, Abildgaard L, Speerschneider T, Sørensen US, Grunnet M, Diness JG, Bentzen BH. British Journal of Pharmacology, 2017.

Posters:
- "Microdomain-specific cAMP regulation in atrial fibrillation" – Deutsche Gesellschaft für Kardiologie (DGK), Mannheim, April 2019.
- "Role of PDE4 for Inotropy and Electrical Stability in Human Atrium" - Cardiac Arrhythmia Symposium, Copenhagen, June 2017.

Congresses:
- DGK Annual Meeting Mannheim, April 2019 (Poster).
- 42nd EWGCCE Meeting, Essen, June 2018 (Talk).
- Cardiac Arrhythmia Symposium, Copenhagen, June 2017 (Poster).
- 40th EWGCCE Meeting, Glasgow, September 2016.

TECHNICAL SKILLS

Imaging techniques: Fluorescence Resonance Energy Transfer (FRET).
Electrophysiology techniques: Patch clamp; Contractility measurements; Automated patch clamp.
Molecular biology techniques: qPCR; cells transfection; Cloning.
Biochemical techniques: Western blot; immunohistochemistry; confocal microscopy.
Cell culture techniques: cells culture techniques on human atrium myocytes and iPS-cells.

LANGUAGE SKILLS

Italian: Mother tongue
English: Fluent
German: Basic (moving from A2 to B1)

COMPUTER SKILLS

Good knowledge of Microsoft Office™ (Word™, Excel™ and PowerPoint™), GraphPad Prism, Adobe Premier and Illustrator, iMovie.

I authorize the treatment of my personal data in according to the law D.lgs. 196 of 30 June 2003

12. Affidavit - Eidesstattliche Versicherung

I hereby expressly declare that I have written the work myself and without outside help, not used sources and tools other than those stated, and individually acknowledged the parts taken literally or in terms of content from the works used according to the edition (edition and year of publication), volume and page of the work used. Furthermore, I declare not to have submitted the dissertation to a subject representative at another university for review or otherwise applied for admission to a doctorate. I consent to my dissertation being examined by the Dean's Office of the Faculty of Medicine using a standard plagiarism detection software.

Signature: ....

Ich versichere ausdrücklich, dass ich die Arbeit selbständig und ohne fremde Hilfe verfasst, andere als die von mir angegebenen Quellen und Hilfsmittel nicht benutzt und die aus den benutzten Werken wörtlich oder inhaltlich entnommenen Stellen einzeln nach Ausgabe (Auflage und Jahr des Erscheinens), Band und Seite des benutzten Werkes kenntlich gemacht habe.

Ferner versichere ich, dass ich die Dissertation bisher nicht einem Fachvertreter an einer anderen Hochschule zur Überprüfung vorgelegt oder mich anderweitig um Zulassung zur Promotion beworben habe.

Ich erkläre mich einverstanden, dass meine Dissertation vom Dekanat der Medizinischen Fakultät mit einer gängigen Software zur Erkennung von Plagiaten überprüft werden kann.

Unterschrift: ....